12-19-2003

An Investigation and Comparison of Accepted Design Methodologies for the Analysis of Laterally Loaded Foundations

Chad Rachel
University of New Orleans

AN INVESTIGATION AND COMPARISON OF ACCEPTED DESIGN METHODOLOGIES FOR THE ANALYSIS OF LATERALLY LOADED FOUNDATIONS

A Thesis

Submitted to the Graduate Faculty of the
University of New Orleans
in partial fulfillment of the
requirements for the degree of

Master of Science
in
The Department of Civil Engineering

by

Chad M. Rachel

B.S., University of New Orleans, 2000

December 2003

ACKNOWLEDGEMENT

I would like to express my sincere gratitude to Dr. John B. Grieshaber for his assistance, guidance, and instruction during my graduate studies at the University of New Orleans. Thank you to Dr. Kenneth McManis and Dr. Mysore S. Nataraj for taking the time to serve on my thesis committee. I would like to thank the New Orleans District of the U.S. Army Corps of Engineers for financing my graduate education. I would like to thank Mr. Shung Kwok Chiu, Mr. Richard Pinner, and the other senior engineers of Structure Foundations, New Orleans District for providing me with geotechnical knowledge and guidance. I would like to thank Ms. Sandra Brown of the New Orleans District Library for assisting me in locating references for this thesis. I would like to thank the geotechnical staff at Virginia Tech for the valuable geotechnical knowledge that they provided to me. I offer thanks to my parents, who instilled good educational values in me, which was instrumental in the pursuit of advanced studies. Finally, and above all, I would like to thank my wife Cathy, and children Sebastian and Sydney, for their love, support, encouragement, and sacrifice.

TABLE OF CONTENTS

ABSTRACT

Single piles and pile groups are frequently subjected to high lateral forces. The safety and functionality of many structures depends on the ability of the supporting pile foundation to resist the resulting lateral forces. In the analysis and design of laterally loaded piles, two criterions usually govern. First, the deflection at the working load should not be so excessive as to impair the proper function of the supporting member. Second, the ultimate strength of the pile should be high enough to take the load imposed on it under the worst loading condition. Typically, pile length, pile section, soil type, and pile restraint dictate the analysis.

This paper presents different methods, specifically Broms' method and the p-y method, for both the analysis and design of laterally loaded single piles. Both linear and nonlinear analyses are considered. The measured results of several full-scale field tests performed by Lymon Reese are compared to computed results using Broms' method of analysis and the p-y method of analysis. Observations are made as to the correlation between the results and recommendations are made as to the applicability of the accepted methods for the analysis and design of laterally loaded piles.

INTRODUCTION

It is well known that pile foundations are subjected to vertical loading. In addition to being subjected to vertical loads, single piles and pile groups are often subjected to high lateral loads. These loads may be forces of nature such as wave or wind loads, man made loads such as mooring loads, or by lateral earth pressures. For example, structures constructed for offshore use are subjected to static and cyclic lateral loads caused by waves and wind. The safety and functionality of these structures depends on the ability of the supporting pile foundation to resist the resulting lateral loads.

Pile supported retaining walls, abutments, sector gates, or lock structures frequently resist high lateral loads. These lateral loads may be caused be lateral earth pressures acting on a retaining structure, by differential fluid pressures acting on a sector gate or lock structure, or by horizontal thrust loads acting on abutments of bridges.

In the analysis and design of laterally loaded piles, three criterions usually govern. First, the deflection at the working load should not be so excessive as to impair the proper function of the supporting member. Second, the ultimate strength of the pile should be high enough to take the load imposed on it under the worst loading condition (Broms, 1964b). And third, the load carrying capacity of the soil should not be exceeded, allowing the pile to rotate freely.

This paper presents different methods for both the analysis and design of laterally loaded single piles. The methods are presented in such a way as to guide the reader from the original concepts and theories of the laterally loaded foundation, to the more state-of-the-art approaches. Although each of the methods presented are well accepted in literature and have been used extensively to analyze the problem of the laterally loaded foundation, each does not provide the same information. While some methods provide information such as ultimate soil capacity and bending moments in the pile, others provide information such as lateral deflections and bending moments in the pile. It is well known that the problem of the laterally loaded pile is a soil-structure interaction type problem. Because of this, information on the lateral deflection of the pile is needed for an adequate analysis or design.

This paper considers both linear and nonlinear analyses of single piles. Pile groups and effects of pile spacing are beyond the scope of this paper, and will not be considered. The measured results of several full-scale field tests performed in stiff clay formations and sand formations are compared to computed results using Broms' linear approach and the nonlinear p-y criteria developed by Reese and Matlock. Only methodologies that consider the lateral deflection of the pile are included in the comparisons. Observations and recommendations are made as to the correlation between the results and the applicability and limits of the methodologies.

Additionally, a computer software program known as FB-Pier, developed by the University of Florida, is used to perform a series of sensitivity analyses. The analyses are performed assuming various soil and pile scenarios. The effects of varying each

parameter independently is studied and the observations are reported.

In addition to this thesis being written to fulfill the requirements of the Master of Science Degree, the contents of the thesis will be used to assist the New Orleans District of the U.S. Army Corps of Engineers. The New Orleans District is currently in a transition period of adapting the p-y methodologies. Previously, the New Orleans District designed for lateral loads on pile foundation by using either a conservative linear subgrade modulus method of analysis or by using battered piles. Several of the recent projects assigned to the New Orleans District, such as the IHNC Lock Replacement and the Harvey Canal Sector Gate Structure require a large footprint and large diameter piles. It is realized that the methods used in past designs will not be cost effective for this type of project. The author's intent is for the findings reported in this paper to be used as a reference for future designs of laterally loaded foundations by the New Orleans District.

I. THEORY OF BEAM ON ELASTIC FOUNDATION

The analysis of bending of beams on an elastic foundation was developed on the assumption that the reaction forces of the foundation are proportional at every point to the deflection of the beam at that point, and independent of the pressure or deflection occurring in other parts of the foundation. This assumption was first introduced by E. Winkler in 1867 (Hetenyi, 1942). Its application to soil foundations should be regarded only as a practical approximation. It is perhaps the simplest approximation that can be made regarding the nature of a supporting elastic media.

However, its drawback is that the soil is not treated as a continuum, but rather as a series of discrete resistances. The physical properties of soil are obviously of a much more complex nature than that which could be accurately represented by such a simple mathematical relationship as the one assumed by Winkler (Hetenyi, 1942).

Consider a straight beam supported along its entire length by an elastic medium and subjected to vertical forces acting in the principle plane of the symmetrical cross-section. The beam will deflect producing continuously distributed reaction forces in the supporting media. The intensity of these reaction forces, p, at any point is proportional to the deflection of the beam, y, at that point. Or, $p = ky$, where k is the proportionality constant (Hetenyi, 1942).

The elasticity of the material assumed by this relationship can be characterized by a force distributed over a unit area causing a unit deflection. The constant of the supporting material, k_0, in units of lb/in^3, is called the modulus of subgrade reaction and thus k, in units of lb/in^2, will be simply k_0 multiplied by the width of the beam, b, or $k = k_0 b$. By considering the equilibrium of the element in Fig. (1-1), and summing the forces in the vertical direction, Hetenyi (1942) presents

$$Q - (Q + dQ) + kydx - qdx = 0,$$

or $$\frac{dQ}{dx} = ky - q \qquad (1\text{-}1).$$

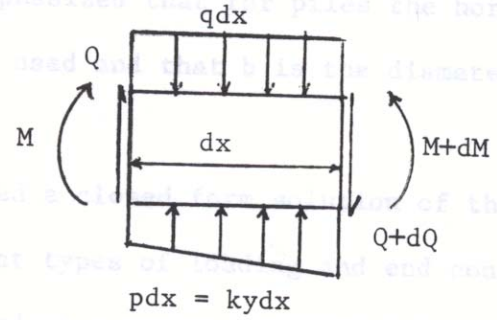

Fig. (1-1)
Equilibrium Forces on an Element
(Hetenyi, 1942)

Making use of the relationship $Q = dM/dx$, we can write (Hetenyi, 1942),

$$\frac{dQ}{dx} = \frac{d^2M}{dx^2} = ky - q \qquad (1\text{-}2).$$

Using the known differential equation of a beam in bending, $EI\left(\frac{d^2y}{dx^2}\right) = -M$, and differentiating it twice, we obtain (Hetenyi, 1942)

$$EI\frac{d^4y}{dx^4} = -\frac{d^2M}{dx^2} \quad (1\text{-}3).$$

Substituting (1-3) into (1-2), we get (Hetenyi, 1942)

$$EI\frac{d^4y}{dx^4} = -ky + q \quad (1\text{-}4).$$

Equation (1-4) is the differential equation for the deflection curve of a beam supported on an elastic foundation. For unloaded parts where $q = 0$, we get (Hetenyi, 1942)

$$EI\frac{d^4y}{dx^4} = -ky \quad (1\text{-}5).$$

If an axial force, P_x, is introduced, then the differential equation will be (Hetenyi, 1942)

$$EI\frac{d^4y}{dx^4} + ky + P_x\frac{d^2y}{dx^2} = 0 \quad (1\text{-}6).$$

It should be emphasized that for piles, the horizontal modulus of subgrade reaction is used and that b is the diameter of the pile for a circular section.

Hetenyi (1942) presented a closed form solution of this differential equation for different types of loading and end conditions. Two such solutions, with a load or a moment concentrated at the end, Figs. (1-2) and (1-3) are presented here. They are of direct interest to pile problems and will be used later by Broms.

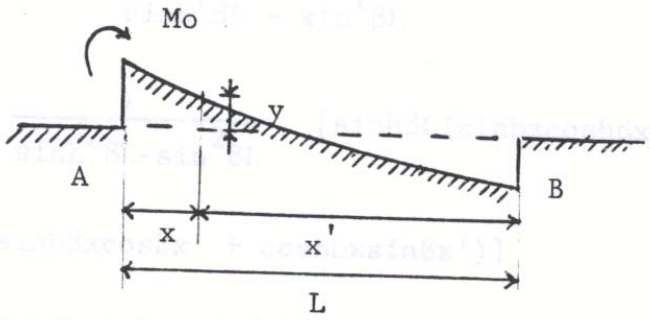

Fig. (1-2)
Beam with Concentrated Moment at End
(Hetenyi, 1942)

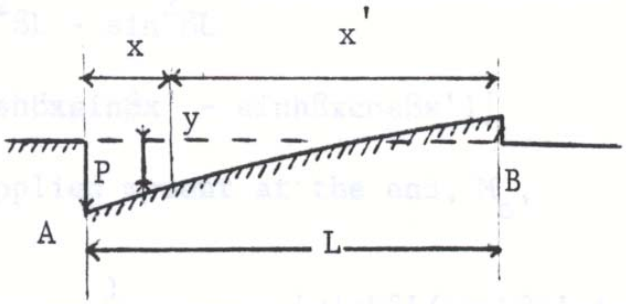

Fig. (1-3)
Beam with Concentrated Force at End
(Hetenyi, 1942)

For a beam with a free end and a concentrated load, p, at one end (Hetenyi, 1942):

$$y(x) = \frac{2p\beta}{k} \frac{\sinh \beta L \cos \beta x \cosh \beta x' - \sin \beta L \cosh \beta x \cos \beta x'}{\sinh^2 \beta L - \sin^2 \beta L} \tag{1-7}$$

$$\theta(x) = \frac{2p\beta^2}{k} \frac{1}{\sinh^2 \beta L - \sin^2 \beta L} [\sinh \beta L(\sin \beta x \cosh \beta x' + \cos \beta x \sinh \beta x') \tag{1-8}$$
$$+ \sin \beta L(\sinh \beta x \cos \beta x' + \cosh \beta x \sin \beta x')]$$

$$M(x) = -\frac{p}{\beta}\frac{\sinh \beta L \sin \beta x \sinh \beta x' - \sin \beta L \sinh \beta x \sin \beta x'}{\sinh^2 \beta L - \sin^2 \beta L} \tag{1-9}$$

$$Q(x) = -p\frac{1}{\sinh^2 \beta L - \sin^2 \beta L}[\sinh \beta L(\cos \beta x \sinh \beta x' - \sin \beta x \cosh \beta x') \tag{1-10}.$$
$$-\sin \beta L(\cosh \beta x \sin \beta x' - \sinh \beta x \cos \beta x')]$$

For the case of an applied moment at the end , M_0, (Hetenyi, 1942)

$$y(x) = \frac{2M_0\beta^2}{k}\frac{1}{\sinh^2 \beta L - \sin^2 \beta L}[\sinh \beta L(\cosh \beta x' \sin \beta x - \sinh \beta x' \cos \beta x) \tag{1-11}$$
$$+\sin \beta L(\sinh \beta x \cos \beta x' - \cosh \beta x \sin \beta x')]$$

$$\theta(x) = \frac{4M_0\beta^3}{k}\frac{\sinh \beta L \cosh \beta x' \cos \beta x + \sin \beta L \cosh \beta x \cos \beta x'}{\sinh^2 \beta L - \sin^2 \beta L} \tag{1-12}$$

$$M(x) = \frac{M_0}{\sinh^2 \beta L - \sin^2 \beta L}[\sinh \beta L(\sinh \beta x' \cos \beta x + \cosh \beta x' \sin \beta x) \tag{1-13}$$
$$-\sin \beta L(\sinh \beta x \cos \beta x' + \cosh \beta x \sin \beta x')]$$

$$Q(x) = 2M_0\beta\frac{\sinh \beta L \sinh \beta x' \sin \beta x + \sin \beta L \sinh \beta x \sin \beta x'}{\sinh^2 \beta L - \sin^2 \beta L} \tag{1-14}$$

where $y(x)$, $\theta(x)$, $M(x)$, and $Q(x)$ are the displacement, slope, moment, and shear at x, respectively, and $\beta = \sqrt[4]{\frac{k}{4EI}}$

where k is the Modulus of Subgrade Reaction in units of lb/in^2 , and EI is the flexural rigidity of the beam.

The differential equation will be used later, with p-y curves, as input data representing the nonlinear relationship between soil reaction and pile deflection to solve for deflection and bending moments along the pile length. In the solution of the

differential equation, appropriate boundary conditions must be selected at the top of the pile to insure that the equations of equilibrium and compatibility are satisfied at the interface between the pile and the superstructure. The selection of the boundary conditions is a simple problem in some instances, for example, where the superstructure is simply a continuation of the pile. However, in other instances, it may be necessary to iterate between solutions for the piles and for the superstructure in order to obtain a correct solution. Such iterations may be required because the soil behavior is usually nonlinear (Reese, 1974).

II. ULTIMATE LATERAL RESISTANCE OF PILES

The calculation of the ultimate lateral resistance and lateral deflection, at working loads of single piles driven in cohesive and cohesionless soil, is considered here based on simplified assumptions of ultimate soil resistance. Both free and fixed headed piles have been considered. These methods were used by engineers before the development of p-y curves.

The ultimate lateral resistance and working load deflections of single piles depends on the dimensions, strength, and flexibility of the individual pile, and on the deformation characteristics of the soil surrounding the loaded pile. The ultimate lateral resistance of a laterally loaded pile will be governed by either the ultimate lateral resistance of the surrounding soil or by the yield or ultimate moment resistance of the pile section. Lateral deflections at working loads have been calculated using the concept of subgrade reaction taking into account edge effects both at the ground surface and at the bottom of each individual pile.

1. General Background

The simplest and direct method of estimating the ultimate lateral resistance of a pile is to consider the statics of the problem. For a laterally loaded pile, passive and active earth pressures will develop. Assuming a general distribution shown in Fig. (2-1), the pile will

rotate around a point at a depth Z_r. The ultimate load and moment, H_u and M_u, to cause failure could be calculated by performing the following integration (Poulous, H. G., and Davis, E. H.):

$$H_u = \int_0^{Z_r} p_u dz - \int_{Z_r}^{L} p_u dz \tag{2-1}$$

$$M_u = H_u e = -\int_0^{Z_r} p_u dz dz + \int_{Z_r}^{L} p_u dz dz \tag{2-2}$$

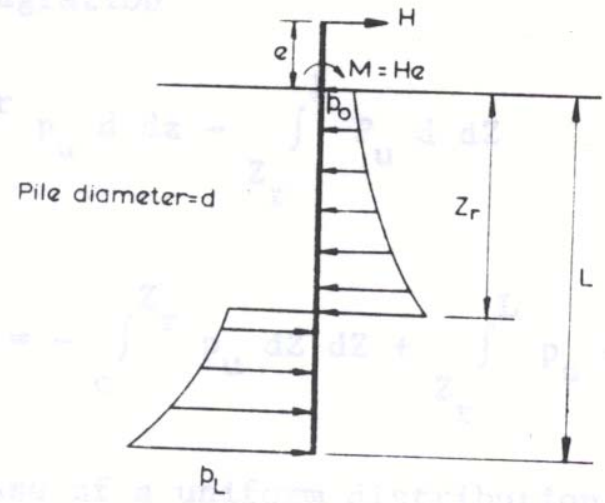

Fig. (2-1)
Unrestrained Laterally-Loaded Pile
(Poulous, H. G., and Davis, E. H.)

In the case of a uniform distribution of soil resistance with depth along the whole length of the pile, that is, $p_0 = p_L = p_u$, the above equations yield the following solutions for the depth of rotation, Z_r, and the ultimate lateral load, H_u (Poulous, H. G., and Davis, E. H.):

$$Z_r = \tfrac{1}{2}\left(\frac{H_u}{p_u d} + L\right) \tag{2-3}$$

$$\frac{M_u}{p_u dL^2} = \frac{H_u e}{p_u dL^2} = \tfrac{1}{4}\left[1 - \left(\frac{2H_u}{p_u dL}\right) - \left(\frac{M_u}{p_u dL}\right)^2\right] \tag{2-4}$$

$$\frac{H_u}{p_u dL} = \sqrt{\left(1 + \frac{2e}{L}\right)^2 + 1} - \left(1 + \frac{2e}{L}\right) \tag{2-5}$$

$\frac{H_u}{p_u dL}$ is plotted against $\frac{e}{L}$ in Fig. (2-2).

For the case of a linear variation of soil resistance with depth, from p_0 at the ground surface to p_L at the pile tip, the following equations may be derived (Poulous, H. G., and Davis, E. H.):

$$4\left(\frac{Z_r}{L}\right)^3 + \left[6\left(\frac{Z_r}{L}\right)^2\right]\left[\frac{e}{L} + \frac{p_0}{p_L p_0}\right] + \left(\frac{12 p_0}{p_L p_0}\right)\left(\frac{e}{L}\right)\left(\frac{Z_r}{L}\right) - \left(3\frac{e}{L}\right)\left(\frac{p_0 + p_L}{p_L - p_0}\right) - \left(\frac{2p_L + p_0}{p_L - p_0}\right) = 0 \tag{2-6}$$

and

$$\frac{H_u}{p_u dL} = \left(1 - \frac{p_0}{p_L}\right)\left(\frac{Z_r}{L}\right)^2 + \left(2\frac{p_0}{p_L}\right)\left(\frac{Z_r}{L}\right) - \tfrac{1}{2}\left(1 + \frac{p_0}{p_L}\right) \tag{2-7}$$

$\frac{H_u}{p_u dL}$ is plotted against $\frac{e}{L}$ in Fig. (2-2) for the case of $p_0 = 0$.

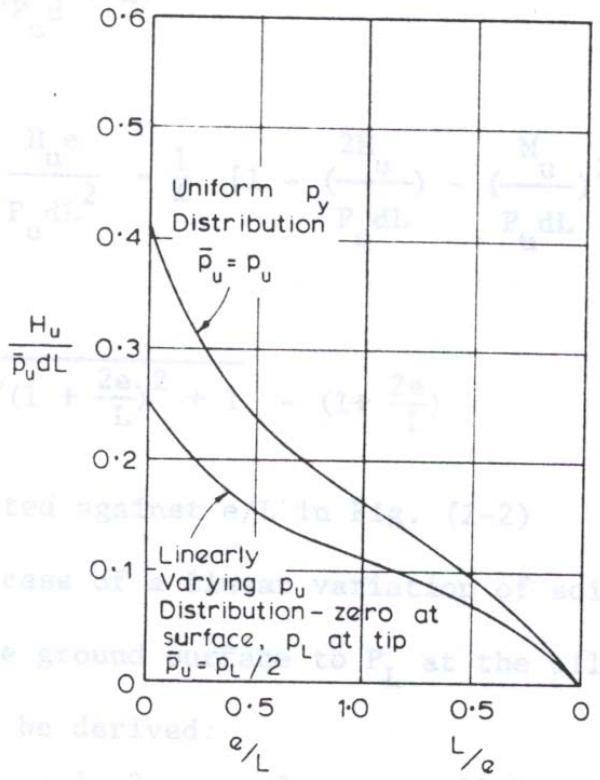

Fig. (2-2)
Ultimate Lateral Resistance of Unrestrained Rigid Piles
(Poulous, H. G., and Davis, E. H.)

For any general distribution of soil resistance with depth, it will be convenient to employ the procedure recommended by Brinch Hansen (1961). In this procedure, the center of rotation is determined by trial and error, such that the resulting moment, taken about the point of application of the load, is zero. When the center of rotation is determined, the ultimate lateral resistance can be obtained from the horizontal equilibrium equation.

This analysis holds true for rigid piles. For non-rigid piles the lesser of either the horizontal load causing failure in the soil along the length of the pile, or the horizontal load causing yielding in the pile section, should be considered. The ultimate soil resistance for a purely cohesive soil p_u is considered generally to increase from the surface down to a depth of about three pile diameters and remain constant for greater depths. The distribution is shown in Fig. (2-10). For a general case of a $c-\phi$ soil, Hansen (1961) expressed the ultimate soil resistance at any depth Z by

$$p_u = qk_q + ck_c \tag{2-8}$$

where q is the vertical overburden pressure, c is the cohesion, and k_q and k_c are factors that are a function of ϕ and $\frac{Z}{d}$. k_q and k_c are plotted in Fig. (2-3) while the limiting values for the ground surface and for an infinite depth are plotted in Fig. (2-4).

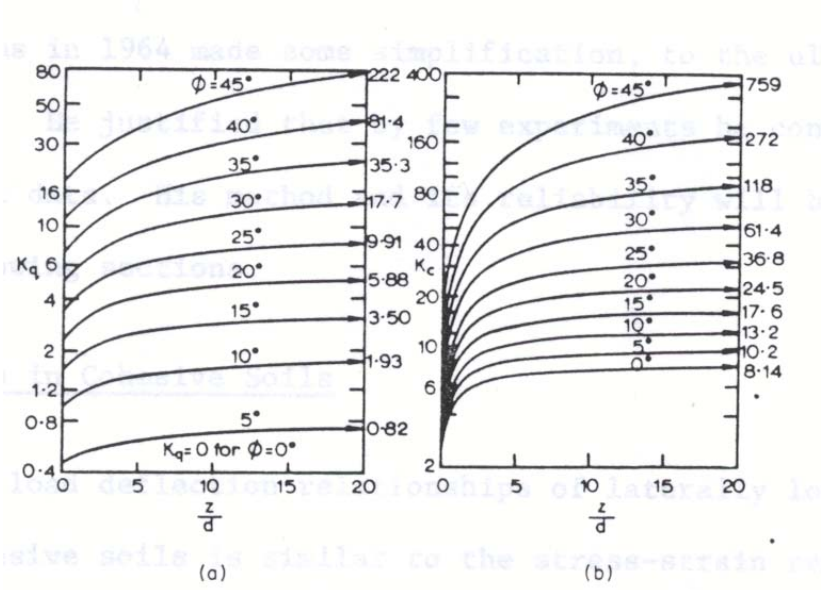

Fig. (2-3)
Lateral Resistance Factors K_q and K_c
(Brinch Hansen, 1961)

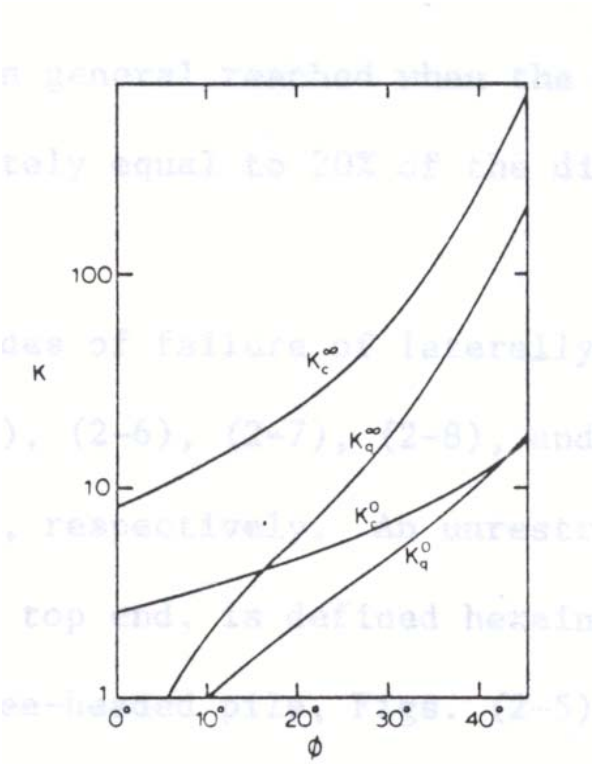

Fig. (2-4)
Lateral Resistance Factors at the Ground Surface (0) and at great depth (∞)
(Brinch Hansen, 1961)

Broms (1964a & 1964b) made some simplification to the ultimate soil resistance. He justified his simplification with several experiments he conducted and with test data. His method and its reliability is the subject of the following sections.

2. Piles in Cohesive Soils

The load deflection relationships of laterally loaded piles driven into cohesive soils are similar to the stress-strain relationships as obtained from consolidated-undrained tests. At loads less than $\frac{1}{2}$ to $\frac{1}{3}$ of the ultimate lateral resistance of the pile, the deflection

increases approximately linear with the applied load. At higher loads, the load-deflection relationships become non-linear and the maximum resistance is, in general, reached when the deflection at the ground surface is approximately equal to 20% of the diameter or side of the pile (Broms, 1964b).

The possible modes of failure of laterally loaded piles are illustrated in Figs. (2-5), (2-6), (2-7), (2-8), and (2-9) for free-headed and restrained piles, respectively. An unrestrained pile, which is free to rotate around its top end, is defined herein as a free-headed pile (Broms, 1964b).

Failure of a free-headed pile, shown in Figs. (2-5) and (2-6), takes place when (a) the maximum bending moment in the pile exceeds the moment causing yielding or failure of the pile section (this takes place when the pile penetration is relatively large), or (b) the resulting lateral earth pressure exceeds the lateral resistance of the supporting soil along the full length of the pile and it rotates as a unit, around a point located at some distance below the ground surface. This takes place when the length of the pile and its penetration lengths are small (Broms, 1964b).

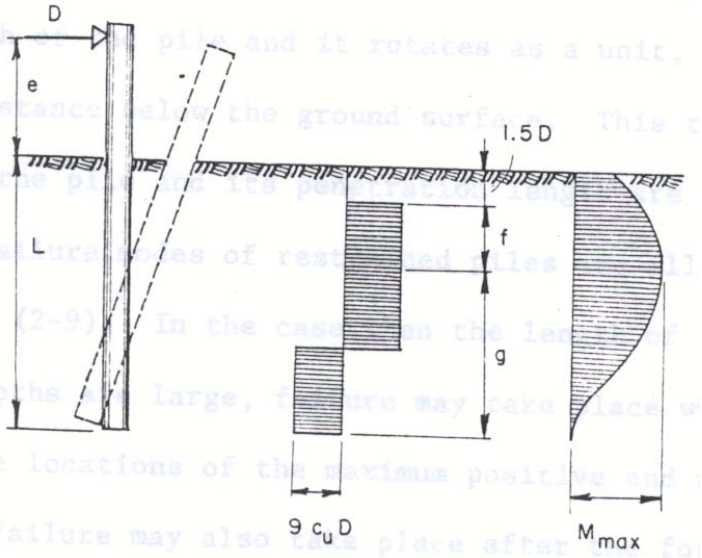

Fig. (2-5)
Deflection, Soil Reaction, and Bending Moment Distribution for a Short, Free-Headed Pile
(Broms, 1964b)

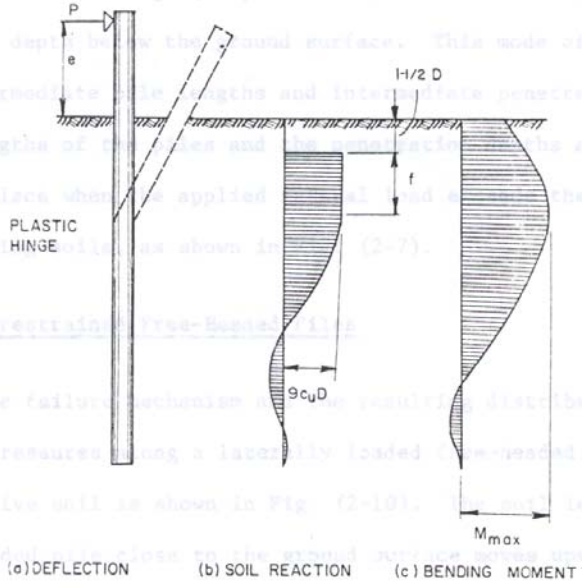

Fig. (2-6)
Deflection, Soil Reaction, and Bending Moment Distribution for a Long, Free-Headed Pile
(Broms, 1964b)

The failure modes of restrained piles are illustrated in Figs. (2-7), (2-8), and (2-9). In the case when the piles and the penetration depths are large, failure may take place when two plastic hinges form at the locations of the maximum positive and negative bending moments. Failure may also take place after the formation of the first plastic hinge at the top end of the pile, if the lateral soil reactions exceed the bearing capacity of the soil along the full length of the pile as shown in Fig. (2-8) and the pile rotates around a point located at some depth below the ground surface. This mode of failure takes place at intermediate pile lengths and intermediate penetration depths. When the lengths of the piles and the penetration depths are small, failure takes place when the applied lateral load exceeds the resistance of the supporting soil, as shown in Fig. (2-7) (Broms, 1964b).

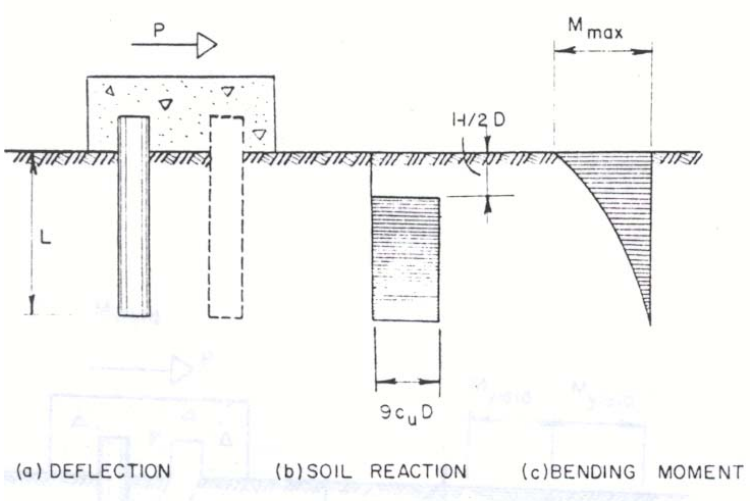

Fig. (2-7)
Deflection, Soil Reaction, and Bending Moment
(Broms, 1964b)

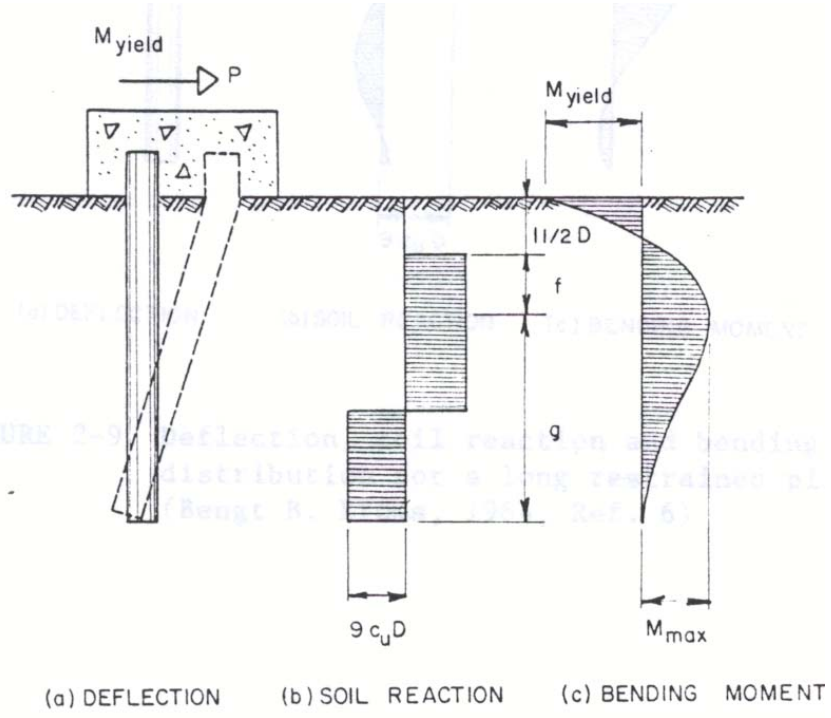

Fig. (2-8)
Deflection, Soil Reaction, and Bending Moment Distribution for a Restrained Pile of Intermediate Length
(Broms, 1964b)

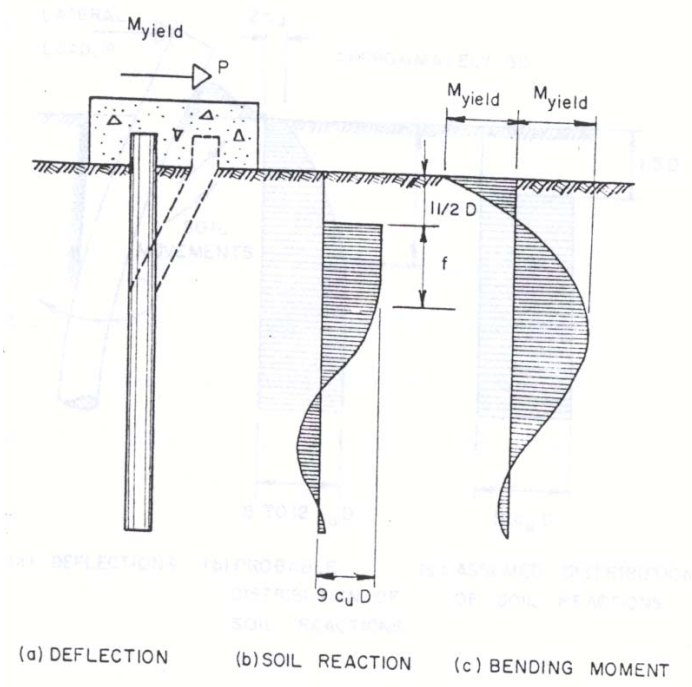

Fig. (2-9)
Deflection, Soil Reaction, and Bending Moment Distribution for a Long Restrained Pile (Broms, 1964b)

a. Unrestrained or Free-Headed Piles

The failure mechanism and the resulting distribution of lateral earth pressures along the laterally loaded free-headed pile driven into a cohesive soil is shown in Fig. (2-10). The soil located in front of the loaded pile close to the ground surface moves upwards in the direction of least resistance, while the soil located at some depth below the ground surface moves in a lateral direction from the front to the back side of the pile. Furthermore, it has been observed that the soil separates from the pile on its backside down to a certain depth below the ground surface (Broms, 1964b).

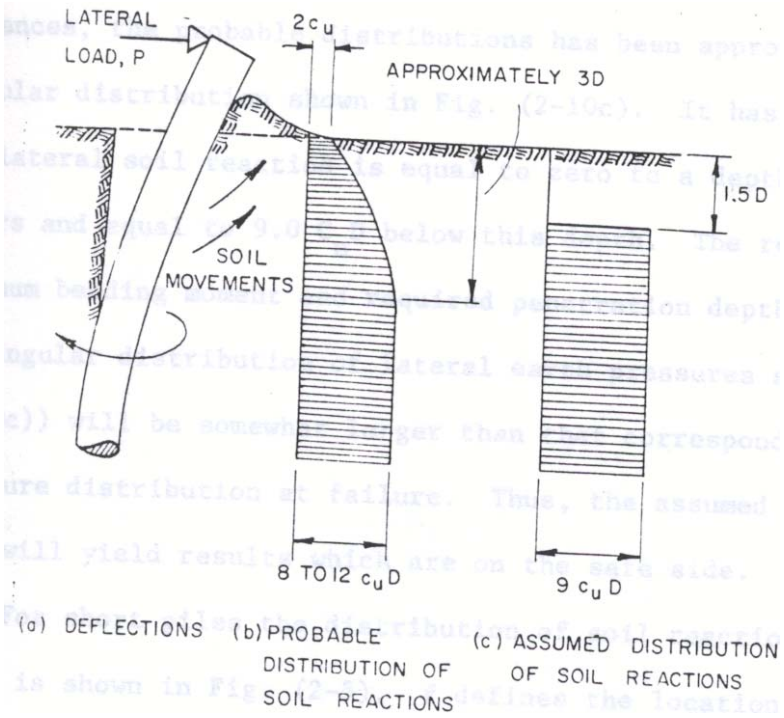

Fig. (2-10)
Distribution of Lateral Earth Pressures
(Broms, 1964b)

The probable distribution of lateral soil reactions is shown in Fig. (2-10b). On the basis of the measured and calculated lateral resistances, the probable distributions have been approximated by the rectangular distribution shown in Fig. (2-10c). It has been assumed that the lateral soil reaction is equal to zero to a depth of 1-½ pile diameters (D) and equal to $9.0c_u D$ below this depth. The resulting calculated maximum bending moment and required penetration depth (assuming the rectangular distribution of lateral earth pressures shown in Fig. (2-10c)) will be somewhat larger than that corresponding to the probable pressure distribution at failure. Thus, the assumed pressure distribution will

yield results that are on the safe side (Broms, 1964b).

For short piles the distribution of soil reaction and bending moments is shown in Fig. (2-5). The distance f defines the location of the maximum moment and since the shear there is zero (Broms, 1964b),

$$f = \frac{H_u}{9c_u D} \tag{2-10}$$

Also, taking moments about the maximum moment location (Broms, 1964b),

$$M_{\max} = H_u\left(e + 1.5D + 0.5f\right) \tag{2-11a}$$

also,

$$M_{\max} = 2.25Dg^2c_u \tag{2-11b}$$

Since $L = 1.5D + f + g$, Eqns. (2-10) and (2-11) can be solved for the ultimate lateral load, H_u. The solution is plotted in Fig. (2-11) in terms of dimensionless parameters L/D and $\frac{P_{ult}}{c_u D^2}$ (where $P_{ult} = H_u$), and applies for short piles in which the yield moment $M_y > M_{\max}$. This inequality should be checked using Eqns. (2-10) and (2-11a).

For long piles, the distribution of soil reaction and bending moment is shown in

Fig. (2-6). Eqn. (2-11b) no longer holds, and H_u is obtained from Eqns. (2-10) and (2-11a) by setting $M_{\max}$ equal to the known value of the yield moment, M_y. This solution is

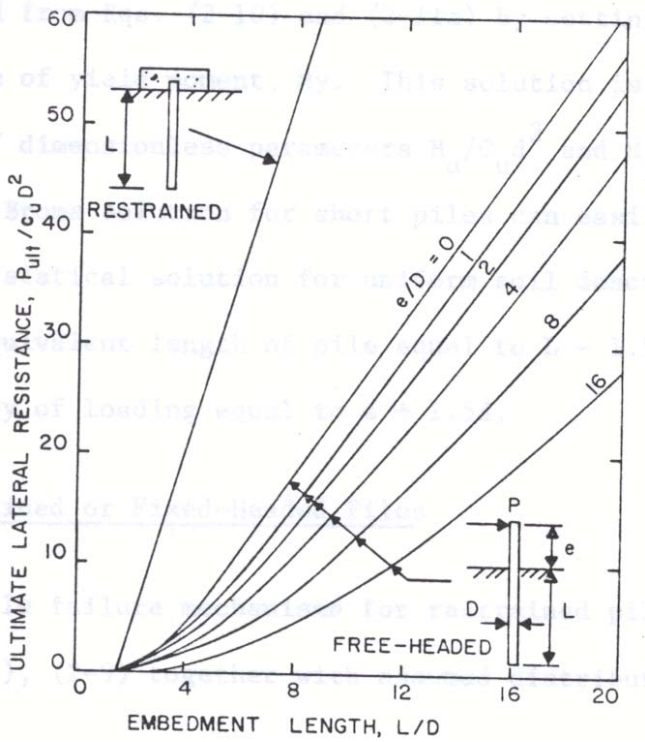

Fig. (2-11)
Ultimate Lateral Resistance for Short Piles in Cohesive Soils
(Broms, 1964b)

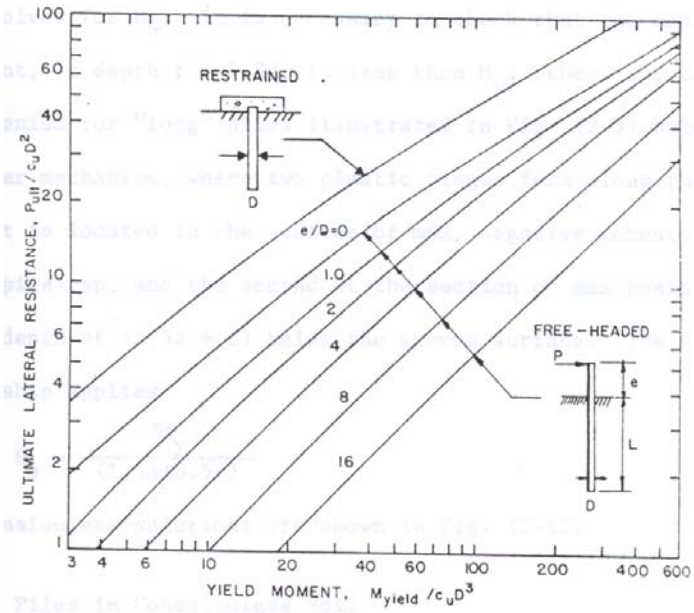

Fig. (2-12)
Ultimate Lateral Resistance for Long Piles in Cohesive Soils
(Broms, 1964b)

plotted in Fig. (2-12) in terms of dimensionless parameters $\frac{M_y}{c_u D^3}$ and $\frac{P_{ult}}{c_u D^2}$ (where $P_{ult} = H_u$). It should be noted that Broms solution for short piles can be recovered from the simple statical solution for uniform soil described previously, by using an equivalent length of pile equal to $L - 1.5D$, and an equivalent eccentricity of loading equal to $e + 1.5D$.

b. Restrained or Fixed-Headed Piles

Possible failure mechanisms for restrained piles are shown in Figs. (2-7), (2-8), and (2-9) together with assumed distribution of soil reaction and moments. For a very short restrained pile, failure takes place when the applied lateral load is equal to the

ultimate lateral resistance of the supporting soil, and the pile moves as a unit in the soil. The following relation holds for short piles (Broms, 1964b):

$$H_u = 9c_u D(L - 1.5D) \tag{2-12}$$

$$M_{\max} = H_u(0.5L + 0.75D) \tag{2-13}$$

Solutions in dimensionless terms are shown in Fig. (2-11).

For intermediate or long piles, failure takes place when the restraining moment at the head of the pile is equal to the ultimate moment resistance of the pile section M_y, and the pile rotates around a point located at some depth below the ground surface. Taking a moment about the ground surface (Broms, 1964b),

$$M_y = 2.25Dg^2c_u - 9c_uDf(1.5D + 0.5f) \tag{2-14}$$

This equation, together with the relationship $L = 1.5D + f + g$, may be solved for H_u. It is necessary to check that the maximum positive moment, at depth $f + 1.5D$, is less than M_y; otherwise, the failure mechanism for long piles shown in Fig. (2-9) holds. For the latter mechanism, where two plastic hinges form along the length of the pile, the first is located in the section of maximum negative moment, at the bottom of the pile cap. The second is located at the section of maximum positive moment at the depth of $f + 1.5D$ below the ground surface. The following relation applies (Broms, 1964b):

$$H_u = \frac{2M_y}{(1.5D + 0.5f)} \tag{2-15}.$$

Dimensionless solutions are shown in Fig. (2-12).

3. Piles in Cohesionless Soil

The possible modes of failure of laterally loaded piles, along with the distribution of soil reaction, are shown in Figs. (2-13), (2-14), (2-16), (2-17), and (2-18) for free-headed and restrained piles driven in cohesionless soils. The mode of failure of a laterally loaded pile driven into a cohesionless soil will depend on the depth of embedment and on the degree of end restraint.

The mechanism of failure and the assumed distribution of soil reaction are shown in Fig. (2-15). The soil located in front of the pile moves in an upward direction, whereas the soil located at the backside of the pile moves downward and fills the void created by the lateral deflection of the pile. However, at relatively large depths, the soil located in front of the pile will move laterally to the backside of the pile instead of upward (Broms, 1964a).

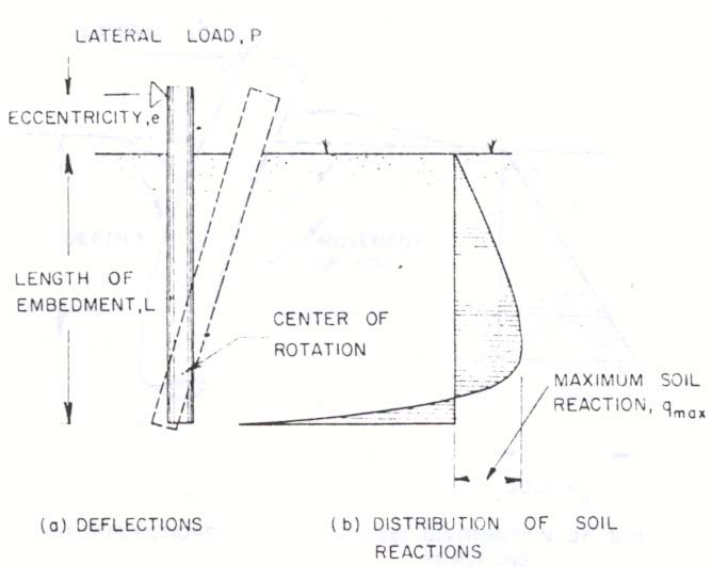

Fig. (2-13)
Failure Mode of a Short, Free-Headed Pile
(Broms, 1964a)

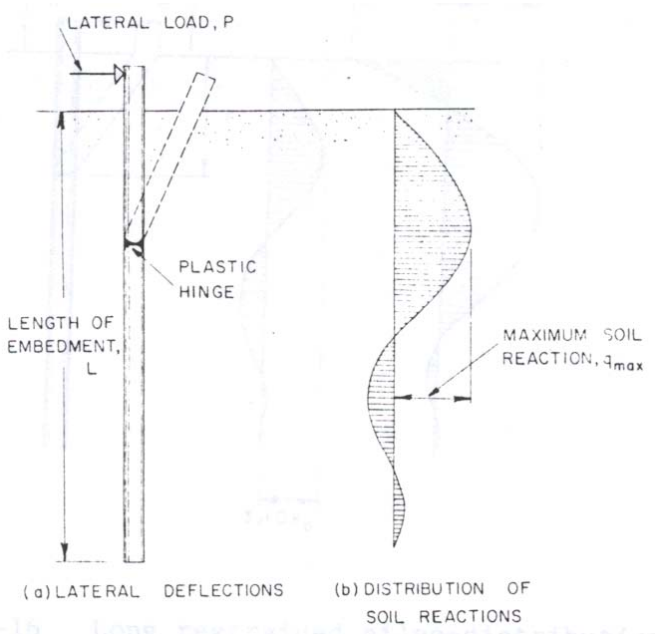

Fig. (2-14)
Failure Mode of a Long, Free-Headed Pile
(Broms, 1964a)

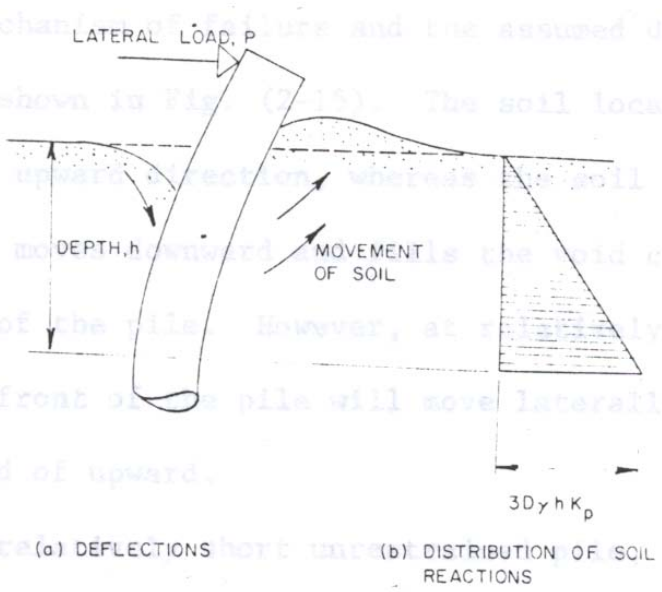

Fig. (2-15)
Assumed Distribution of Soil Reactions
(Broms, 1964a)

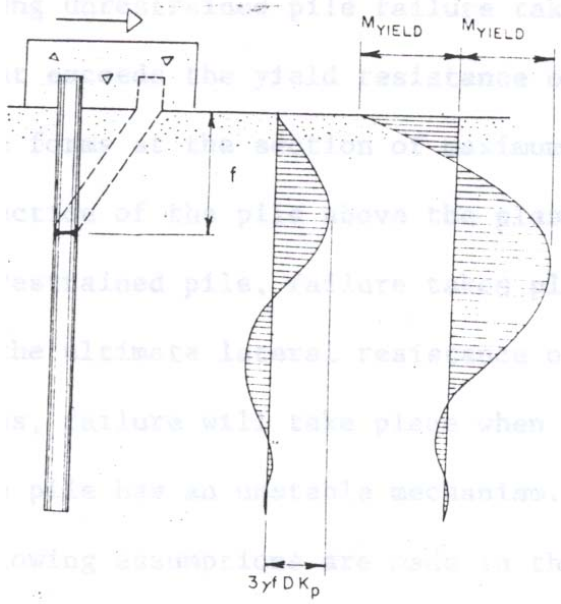

Fig. (2-16)
Distribution of Deflections, Soil Reactions, and Moments for a Long Restrained Pile
(Broms, 1964a)

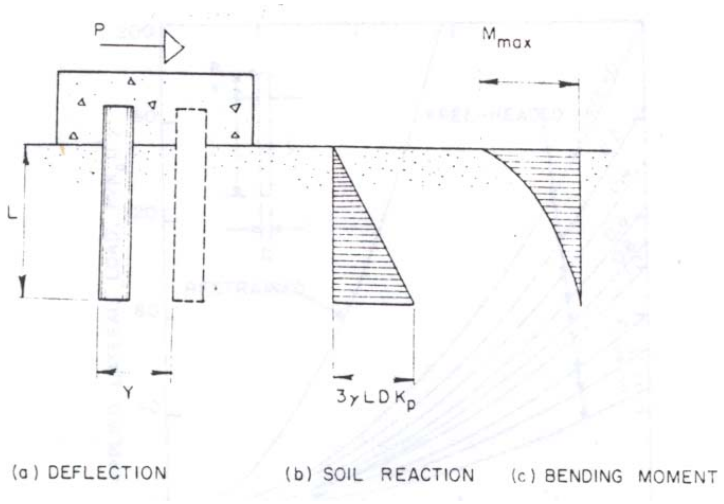

Fig. (2-17)
Distribution of Deflections, Soil Reactions, and Moments for a Short Restrained Pile
(Broms, 1964a)

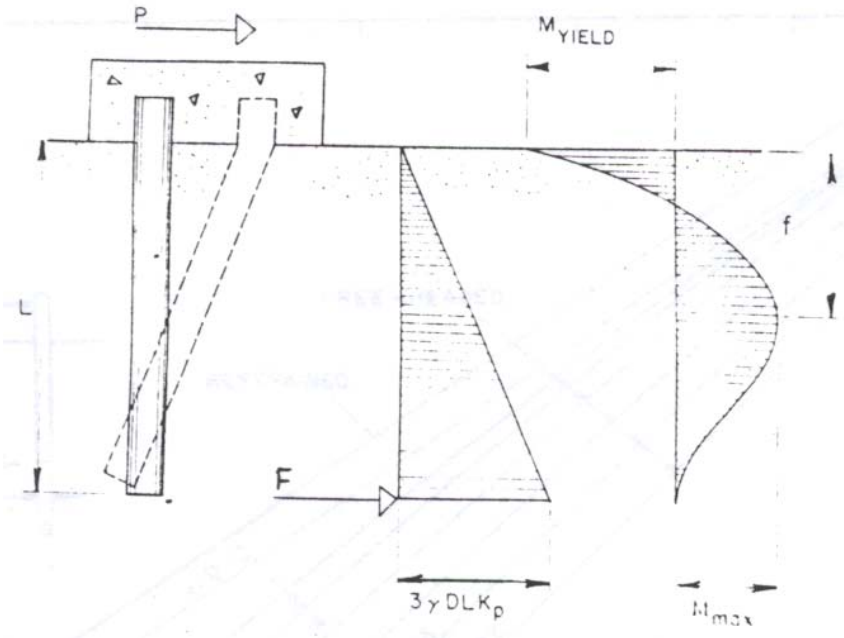

Fig. (2-18)
Distribution of Deflections, Soil Reactions, and Moments for a Pile of Intermediate Length
(Broms, 1964a)

For a relatively short unrestrained pile, failure takes place when the pile rotates as a unit with respect to a point located close to its toe. The negative lateral pressures that develop at the toe, or tip of the laterally loaded pile are large (Broms, 1964a).

For a long unrestrained pile, failure takes place when the maximum bending moment exceeds the yield resistance of the pile section and a plastic hinge forms at the section of the maximum bending moment. The lateral deflection of the pile above the plastic hinge will be large. For a short restrained pile, failure takes place when that load applied is equal to the ultimate lateral resistance of the soil. For intermediate and long piles, failure will take place when one or two plastic hinges form and the pile becomes unstable (Broms, 1964a).

The following assumptions are made in the analysis by Broms (Broms, 1964a):

1. The active earth-pressure acting on the back of the pile is neglected.
2. The distribution of passive pressure along the front of the pile is equal to three times the Rankine passive pressure.
3. The shape of the pile section has no influence on the distribution of the ultimate soil pressure or the ultimate lateral resistance.
4. The full lateral resistance is mobilized at the movement considered.

The simplified assumption of an ultimate soil resistance, p_u, equal to three times the Rankine passive pressure is based on limited empirical evidence from comparisons

between predicted and observed ultimate resistances made by Broms. These comparisons suggest that the assumed factor of 3 may be, in some cases, conservative, as the average ratio of predicted to measured ultimate loads is about 2/3. The distribution of soil resistance is (Broms, 1964a):

$$p_u = 3\sigma_v^{'} K_p \tag{2-16}$$

where

$\sigma_v^{'}$ = effective vertical overburden pressure

$K_p = \left(1+\sin\phi'\right) \Big/ \left(1-\sin\phi'\right)$

$\phi^{'}$ = angle of internal friction (effective stress).

a. Unrestrained or Free-Headed Piles

By taking moments about the toe, the free-headed pile will have an ultimate lateral force given by (Broms, 1964a)

$$H_u = \frac{0.5\gamma D h^3 K_p}{e+L} \tag{2-17}$$

This relationship is plotted in Fig. (2-19) using dimensionless parameters, L/D and $H_u / K_p \gamma D^3$. The maximum moment occurs at a distance f below the surface (Broms, 1964a), where

$$H_u = \tfrac{2}{3}\gamma D K_p f^2 \tag{2-18}.$$

That is, $f = 0.82\sqrt{\dfrac{H_u}{DK_p\gamma}}$.

The maximum moment is (Broms, 1964a)

$$M_{\max} = H_u\left(e + \tfrac{2}{3} f\right) \qquad (2\text{-}19).$$

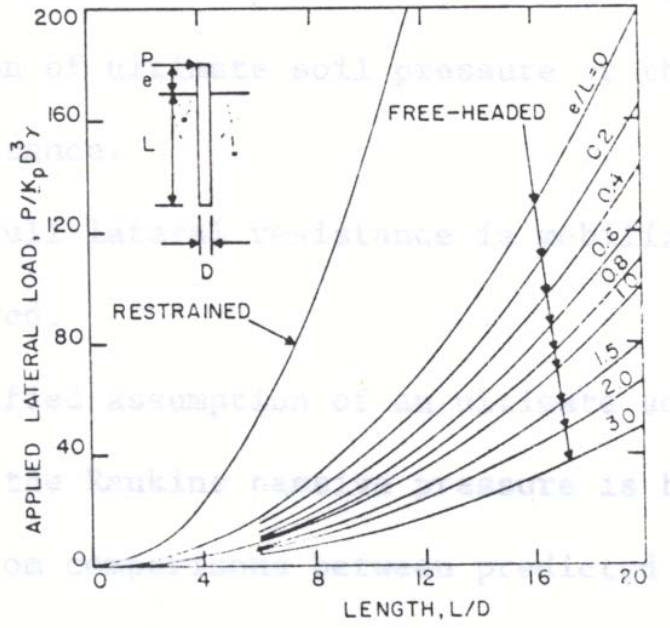

Fig. (2-19)
Ultimate Lateral Resistance for Short Piles
(Broms, 1964a)

If after use of Eqn. (2-17), the calculated value of H_u results in $M_{\max} > M_y$ ($M_{\max}$ from Eqn. (2-19)), then the pile will act as a "long" pile, and H_u may then be calculated from Eqns. (2-18) and (2-19), putting $M_{\max} = M_y$. The solutions for H_u using "long" piles are plotted in Fig. (2-20) in terms of $H_u / K_p \gamma D^3$ and $M_y / D^4 \gamma K_p$.

For short piles, comparisons reveal that Broms' assumptions lead to a higher value of the ultimate load than the general simple analysis. For example, for $L/D = 20$ and $e/L = 0$, Broms' solution gives a load 33% more than that derived from simple

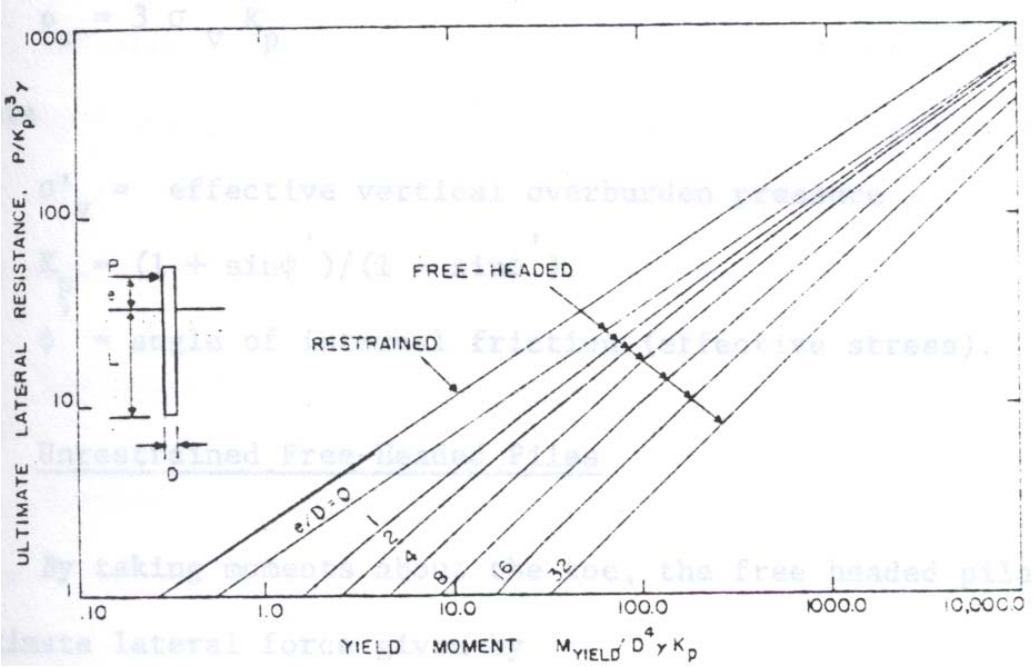

Fig. (2-20)
Ultimate Lateral Resistance for Long Piles
(Broms, 1964a)

statical analysis.

b. Restrained or Fixed-Headed Piles

Similarly for fixed headed piles, the horizontal equilibrium will give (Broms, 1964a)

$$H_u = \tfrac{3}{2}\gamma L^2 D K_p \qquad (2\text{-}20).$$

This solution is plotted in dimensionless form in Fig. (2-19). The maximum moment is (Broms, 1964a)

$$M_{\max} = \tfrac{2}{3} H_u L \qquad (2\text{-}21).$$

If the $M_{\max}$ exceeds M_y, then the failure mode in Fig. (2-18) is relevant. From Fig. (2-18), for horizontal equilibrium:

$$F = \left(\tfrac{3}{2}\gamma D L^2 K_p\right) - H_u \qquad (2\text{-}22).$$

Taking moments about the top of the pile, and substituting for F from Eqn. (2-22),

$$M_y = \left(0.5\gamma D L^3 K_p\right) - H_u L \qquad (2\text{-}23).$$

Hence, H_u may be obtained.

This equation only holds if the maximum moment at depth f is less than M_y, the distance f being calculated from Eqn. (2-18). For the situation shown in Fig. (2-16), where the maximum moment reaches M_y at two locations, it can be found that

$$H_u\left(e + \tfrac{2}{3} f\right) = 2M_y \qquad (2\text{-}24).$$

Dimensionless solutions from this equation are shown in Fig. (2-20).

4. Correlation with Test Results

The ultimate lateral resistances have been compared with some available test data (Broms, 1964a and Broms, 1964b). The average measured ultimate lateral resistances exceeded the calculated resistances by more than 50 percent for cohesionless soil.

However, the measured ultimate lateral resistances of piles tested by Walsenko were found to be only 2/3 of the calculated resistances. These piles were embedded in a fine gravel with a reported angle of internal friction of $\phi = 45°$ as measured by direct shear tests. Frequently it is difficult to measure accurately the shearing strength of gravel by means of direct shear tests. If a value of $\phi = 35°$ is taken as the angle of internal friction, then the average ratio p_{test} / p_{calc} is increased to 1.43, a value that compares well with the remainder of the test data. The conclusion that can be drawn from this comparison is that the ultimate resistance of laterally loaded piles can be estimated conservatively assuming an ultimate lateral soil reaction equal to three times the Rankine lateral earth pressure.

Comparisons have been made by Broms between maximum bending moments calculated from the above approach and values determined experimentally from the available test data. For cohesionless soils, this ratio ranged between 0.54 and 1.61 with an average value of 0.93 (Broms, 1964a). For cohesive soils, the ratio of calculated to observed moment ranged between 0.88 and 1.19, with an average value of 1.06 (Broms, 1964b). While good agreement was obtained, it was pointed out by Broms that the calculated maximum moment is not sensitive to small variations in the assumed soil-resistance distribution.

5. Load-Deflection Prediction

At working loads, the deflection of a single pile or of a pile group can be

considered to increase approximately linearly with the applied loads. Part of the lateral deflection is caused by the shear deformation of the soil at the time of loading and part by consolidation and creep subsequent to loading. The deformation caused by consolidation and creep increases with time.

It will be assumed in the following analysis, that the lateral deflections and distribution of bending moments and shear forces can be calculated at working loads by means of the theory of subgrade reaction. Thus, it will be assumed that the unit soil reaction p (in lb/in) acting on a laterally loaded pile increases in proportion to the lateral deflection y (in inches) expressed by the equation

$$p = K_0 y \tag{2-25}$$

where the coefficient K_0 (in lb/in^2) is defined as the coefficient of subgrade reaction. The numerical value of the coefficient of subgrade reaction varies with the width of the loaded area and the load distribution, as well as with the distance from the ground surface (Broms, 1964b).

It will be assumed that for clay, the modulus is constant with depth and that for granular soils, the modulus increases linearly with depth. For real soils, the relationship between soil pressure p and deflection y is non-linear with the soil pressure reaching a limiting value when the deflection is sufficiently large. The more satisfactory approach to deflection prediction is to perform a non-linear analysis. However, if linear theory is to be

used, it is necessary to choose appropriate secant values of the subgrade modulus. Reese and Matlock argue that the adoption of a linearly increasing modulus of subgrade reaction with depth takes some account of soil yield and nonlinearity, as values of the secant modulus near the top of the pile are likely to be very small, but will increase with depth because of both a higher soil strength and lower levels of deflection. Reese and Matlock's argument is most relevant to piles in sand and soft clay. In some cases, for example, relatively stiff piles in over-consolidated clay at relatively low load levels, the assumption of a constant subgrade modulus with depth may be more appropriate.

Solutions for the simple cases of constant subgrade modulus with depth, and linearly increasing modulus with depth are described below. For horizontal load H applied at ground level to a free-headed or unrestrained pile of length L, the following solutions are given by Hetenyi, and shown before, for horizontal displacement y, slope θ, moment M, and shear Q at a depth z below the surface (Hetenyi, 1964):

$$y = \frac{2H\beta}{K} \cdot k_{yH} \tag{2-26a}$$

$$\theta = \frac{2H\beta^2}{K} \cdot k_{\theta H} \tag{2-26b}$$

$$M = -\frac{H}{\beta} \cdot k_{MH} \tag{2-26c}$$

$$Q = -H \cdot k_{QH} \tag{2-26d}$$

where β, k_{yH}, $k_{\theta H}$, k_{MH}, and k_{QH} are coefficients used with horizontal loads H and

are described previously, and where

$$K = K_h d \tag{2-27}$$

$K_h =$ horizontal subgrade reaction (in lb/in^3)

$d =$ diameter of pile (in inches)

The corresponding expressions for moment loadings M_0 applied at the ground surface are as follows (Hetenyi, 1964):

$$y = \frac{2M_0\beta^2}{K} \cdot k_{yM} \tag{2-28a}$$

$$\theta = \frac{4M_0\beta^3}{K} \cdot k_{\theta M} \tag{2-28b}$$

$$M = M_0 \cdot k_{MM} \tag{2-28c}$$

$$Q = 2M_0\beta \cdot k_{QM} \tag{2-28d}$$

Solutions for the case of a fixed-head or restrained pile may be obtained from the above solutions for a free-head pile by adding to the solutions for horizontal loading H , the solutions for an applied moment of (Hetenyi, 1964)

$$M_0 = -\left(\frac{H}{2\beta}\right)\left[\frac{k_{\theta H}(z=0)}{k_{\theta M}(z=0)}\right] \tag{2-29}$$

This will be the applied moment to produce zero slope at the pile head.

For deflections and rotations at the soil surface, plots are shown in Fig. (2-21).

For a free-headed or unrestrained pile, for constant K_h (Barber, 1953),

deflection $$\rho = \left(\frac{H}{K_h dL} \right) \cdot I_{\rho H} + \left(\frac{M_0}{K_h dL^2} \right) \cdot I_{\rho M} \quad \text{(2-30a)}$$

rotation $$\theta = \left(\frac{H}{K_h dL} \right) \cdot I_{\theta H} + \left(\frac{M_0}{K_h dL^2} \right) \cdot I_{\theta M} \quad \text{(2-30b)}$$

For a fixed-headed pile, which is free to translate but not to rotate (Barber, 1953),

deflection $$\rho = \left(\frac{H}{K_h dL} \right) \cdot I_{\rho F} \quad \text{(2-31)}$$

where

H = applied horizontal force at the ground surface

M_0 = applied moment at the ground surface

d = diameter of the pile

L = length of the pile

$I_{\rho H}$, $I_{\rho M}$, $I_{\theta H}$, $I_{\theta M}$, and $I_{\rho F}$ = deflection and rotation influence factors from Fig. (2-21)

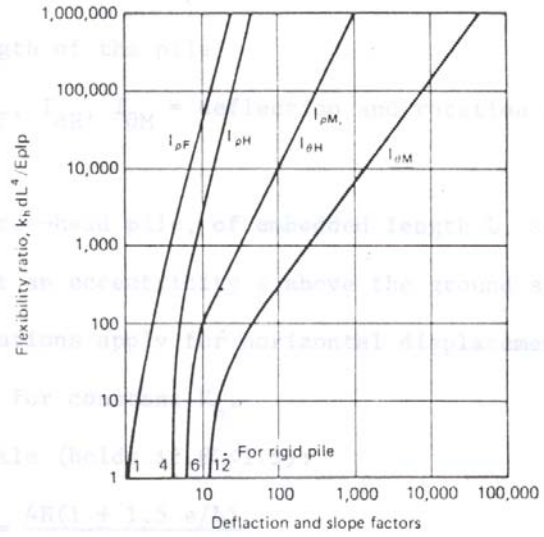

Fig. (2-21)
Top Deflection and Rotation for Lateral Loads on Vertical Piles for Constant k_h
(Barber, 1953)

For a free-headed pile, of embedded length L, subjected to a horizontal load H at an eccentricity e above the ground surface, the following limiting solutions apply for horizontal displacement and rotation at the ground line, for a constant K_h (Broms, 1964b):

1. Rigid pile (holds if $\beta L < 1.5$)

$$\rho = \frac{4H\left(1+1.5\frac{e}{L}\right)}{K_h dL} \tag{2-32a}$$

$$\theta = \frac{6H\left(1+2\frac{e}{L}\right)}{K_h d L^2} \tag{2-32b}$$

2. Infinitely long pile (holds if $\beta L > 2.5$)

$$\rho = \frac{2H\beta(e\beta+1)}{K_h d} \tag{2-33a}$$

$$\theta = \frac{2H\beta^2(1+2e\beta)}{K_h d} \tag{2-33b}$$

For a fixed-headed pile, the limiting solutions are (Broms, 1964b):

1. Rigid pile (holds if $\beta L < 0.5$)

$$\rho = \frac{H}{K_h d L} \tag{2-34}$$

2. Infinitely long pile (holds if $\beta L > 1.5$)

$$\rho = \frac{H\beta}{K_h d} \tag{2-35}$$

For linearly varying K_h with depth, Terzaghi expressed the variation as follows (Broms, 1964a):

$$K_h = n_h\left(\frac{z}{d}\right) \tag{2-36}$$

where

$n_h =$ coefficient of subgrade reaction at a depth of unity below the ground surface

(units of $force/length^3$)

z = depth below ground surface

d = pile diameter

No convenient closed form solutions are available for this case, but the following limiting solutions apply for free-headed piles (Broms, 1964a):

1. Rigid pile ($z_{\max} < 2.0$)

$$\rho = \frac{18H\left(1+1.33\frac{e}{L}\right)}{L^2 n_h} \tag{2-37a}$$

$$\theta = \frac{24H\left(1+1.5\frac{e}{L}\right)}{L^3 n_h} \tag{2-37b}$$

2. Infinitely long pile ($z_{\max} > 4.0$)

$$\rho = \frac{2.4H}{(n_h)^{3/5}(EI)^{2/5}} + \frac{1.6He}{(n_h)^{2/5}(EI)^{3/5}} \tag{2-38a}$$

$$\theta = \frac{1.6H}{(n_h)^{2/5}(EI)^{3/5}} + \frac{1.74He}{(n_h)^{1/5}(EI)^{4/5}} \tag{2-38b}$$

For fixed-headed piles (Broms, 1964a):

1. Rigid pile ($z_{\max} < 2.0$)

$$\rho = \frac{2H}{L^2 n_h} \tag{2-39}$$

2. Infinitely long pile ($z_{\max} > 4.0$)

$$\rho = \frac{0.93H}{(n_h)^{3/5}(EI)^{2/5}} \tag{2-40}$$

For the above solutions, $z_{\max}$ is defined as

$$z_{\max} = L/T \tag{2-41}$$

where

$$T = \left(\frac{EI}{n_h}\right)^{1/5} \tag{2-42}$$

$EI =$ Flexural rigidity of the pile

Solution for pile head deflection and slope are plotted in Fig. (2-22). The actual slope and deflection are given by Eqns. (2-30) and (2-31), except that $K_h d$ is now replaced by $n_h L$ in the denominator of these equations.

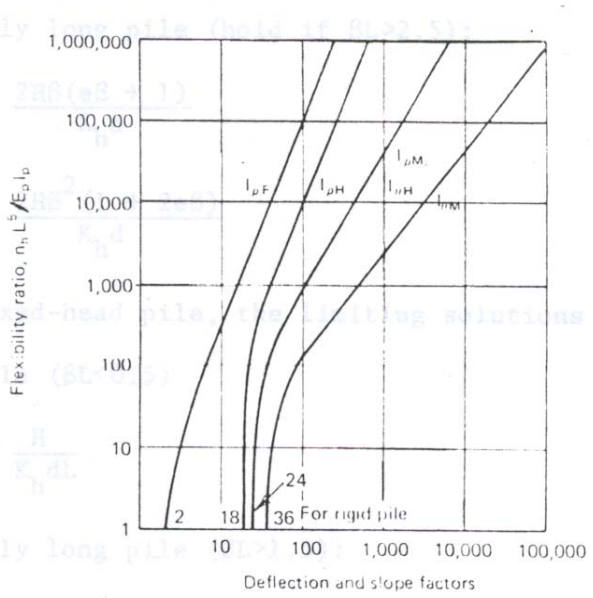

Fig. (2-22)
Top Deflection and Rotation for Lateral Loads on Vertical Piles for k_h Proportional to Depth
(Barber, 1953)

6. Correlation with Test Data

In cohesive soils the lateral deflection at workings loads can be calculated by the methods previously presented if the stiffness of the pile section, the pile diameter, the penetration depth, and the average unconfined compressive strength of the soil are known within the significant depth (Broms, 1964b).

The lateral deflections calculated from Eqns. (2-32a), (2-34), (2-33a), and (2-35) have been compared with the test data (Broms, 1964b). The measured lateral deflections at the ground surface varied between 0.5 to 3.0 times the calculated deflections. Broms noted that the calculated lateral deflections for short piles are inversely proportional to the assumed coefficient of subgrade reactions and thus to the measured average unconfined compressive strength of the supporting soil. Thus, small variations of the measured average unconfined compressive strength will have large effects on the calculated lateral deflections. Broms also noted that agreement between measured and calculated lateral deflections improves with decreasing shear strengths of the soil. The cohesive soils reported with a high unconfined compressive strength have been preloaded by desiccation and it is well known that the shear strength of such soils is erratic and may vary appreciably within short distances due to the pressure of shrinkage cracks (Broms, 1964b).

Test data (Broms, 1964a) indicates that the proposed method can be used to calculate the lateral deflection at working loads (at load levels equal to one-half to one-third the

ultimate lateral capacity of a pile) when the unconfined compressive strength of the soil is less than about 1.0 tsf. However, when the unconfined compressive strength of the soil exceeds about 1.0 tsf, it is expected that the actual deflections at the ground surface may be considerably larger than the calculated lateral deflections due to the erratic nature of the supporting soil (Broms, 1964a).

For cohesionless soils, the calculated lateral deflections have been compared with some available test data on free-headed and restrained steel, reinforced concrete, and timber piles driven or jetted into dense, medium, or loose cohesionless soils. The calculated lateral deflections depend on the stiffness of the pile sections, the relative density of the soil surrounding the test piles and on the degree of end restraint. The calculated lateral deflections in almost all cases considerably exceeded the measured lateral deflection.

However, Broms noted that only an estimate of the lateral deflection is required for most problems and that the accuracy of the proposed methods of analysis is probably sufficient for this purpose. Additional test data would be required to determine the accuracy and the limitations of the proposed methods used with cohesionless soils.

III. P-Y CURVES

The differential equation for solving the problem of laterally loaded deep foundations has been shown and analyzed before:

$$EI\frac{d^4y}{dx^4} + E_s y + P_x\frac{d^2y}{dx^2} = 0 \qquad (3\text{-}1)$$

Approximate solutions for the equation can sometimes be obtained by the use of non-dimensional relationships. A more favorable approach is to write the differential equation in difference form and to obtain solutions by the use of a computer. Some of the computer programs available for this type of analysis include L-Pile, FB-Pier, and CLM 2.02.

The numerical description of the soil modulus, E_s, in this equation is accomplished best by a set of curves that relates the soil reaction to pile deflection. If such a set of curves can be predicted, the differential equation can be solved to yield deflection, pile rotation, bending moment, shear, and soil reaction of any load capable of being sustained by the deep foundation.

Most of the recent research on laterally loaded piles has been in the development of such curves. Some of the important research was conducted to solve the problem in the design and construction of piles in many offshore installations. In such installations, cyclic loadings from wind and waves associated with hurricanes or otherwise play a

major role in the design criteria, along with the static loading.

1. Pile Deflection-Soil Reaction

The idea of p-y curves is presented in Fig. (3-1). Fig. (3-1a) shows a section through a pile at a depth below the ground surface. The behavior of a stratum of soil at a depth x_1 below the surface will be discussed. Fig. (3-1b) shows a possible earth pressure distribution around the pile after installation, but before applying a lateral load to the pile. The earth pressure distribution in Fig. (3-1b) assumes that the pile was perfectly straight prior to driving and that there was no bending of the pile during driving. While neither of these conditions is precisely met in practice, it is believed that in most instances the assumption can be made without serious error.

The deflection of the pile through a distance y_i, as shown in Fig. (3-1c), would generate unbalanced soil pressures against the pile, perhaps as indicated in the figure. Integration of the soil pressures around the pile would yield an unbalanced force p_i per unit length of the pile. The deflection of the pile could generate a soil resistance parallel to the axis of the pile, however, it is assumed that such soil resistance would be quite small and it can be ignored in the analysis. As shown in Fig. (3-1), the deflection of y_i is the distance the pile deflects laterally as being subjected to a lateral load. The soil resistance p_i is the force per unit length from the soil against the pile, which develops as a result of the pile deflection.

The set of curves shown in Fig. (3-2) would seem to imply that the behavior of

the soil at a particular depth is independent of the soil behavior at all other depths. That assumption is not strictly true. However, it has been found by experiment (Matlock, 1970) that for the patterns of pile deflections that can occur in practice, the soil

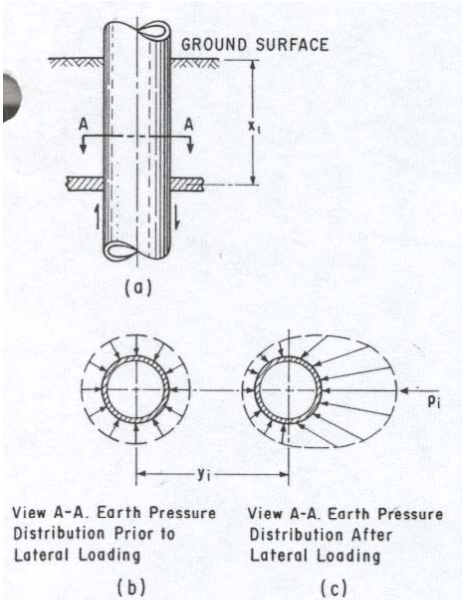

Fig. (3-1)
Graphical Definition of p and y
(Reese, 1974)

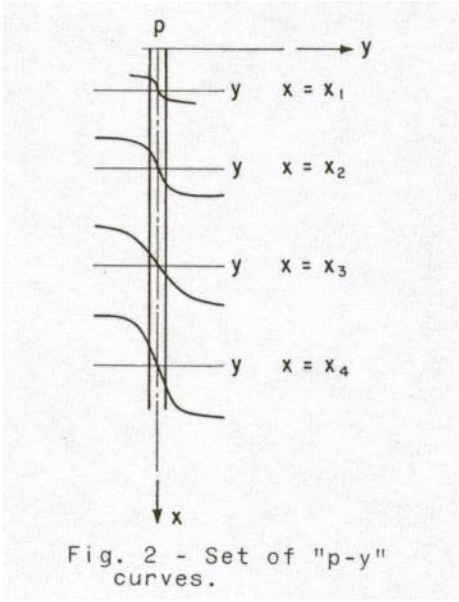

Fig. (3-2)
Set of "p-y" Curves
(Reese, 1974)

reaction at a point is dependent essentially on the pile deflection at that point and not on the pile deflection above or below. Thus, for purposes of analysis, the soil can be removed and replaced by a set of discrete mechanisms with load-deflection characteristics of a character such as shown in Fig. (3-2) (Reese, 1974).

The proper form of the p-y relation is influenced by a great many factors, including (1) natural variation of soil properties with depth, (2) the general form of the pile deflection, (3) the corresponding state of stress and strain throughout the effected soil

zone, and (4) the rate and sequence and history of cyclic loadings.

If the soil behavior at each depth can be reduced to a single p-y curve the analysis and design of complex loading can be achieved. For cyclic wave loading it would be hopeless to attempt to follow analytically the continuous path of soil response. What is needed for design will be a quasi-static approximation of the lower bound of soil resistance under an indefinitely large number of loading cycles.

In the remainder of this chapter, the recommended procedure for computing and constructing p-y curves in the cases of sand, soft clays, and stiff clays are described. The methods presented are based on results of full-scale tests of instrumented piles. Description of instrumentation, soil conditions, and procedure of testing at the different sites considered are included also.

2. P-Y Curves for Sand Deposits

A series of tests were conducted on two 24-inch diameter test piles installed at a site where the soil consisted of clean fine sand to silty fine sand (Reese, 1974). Two types of loadings were employed, static loading and cyclic loading. The data was analyzed and families of curves were developed which showed the soil behavior presented in terms of soil resistance p as a function of pile deflection y.

The experiments entailed the application of known lateral loads in the field to full-sized piles, which are instrumented for the measurement of bending moment along the length of the piles. In addition to the measurements of the load at the ground line, measurements were made of the pile head deflection and the pile head rotation. Two

types of loading were employed, static and cyclic.

Two piles were driven open-ended at the test site on Mustang Island near Corpus Christi, Texas. The water table was maintained above the ground surface during loading to simulate conditions which would exist at an offshore location. For each type of loading, a series of lateral loads were applied, beginning with a load of small magnitude. A bending moment curve was obtained for each load; thus, the experiments resulted in a set of bending moment curves along with the associated boundary conditions for each type of loading.

Soil studies were made at the site involving the use of undisturbed sampling. Laboratory studies were performed. The sand at the test site varied from clean fine sand to silty fine sand, both having relatively high densities. The sand particles by inspection through a microscope were found to be subangular with a large percentage of flaky grains. The angle of internal friction ϕ was determined to be $39°$ and the value of the submerged unit weight γ' was found to be 66 lb/ft^3 (Reese, 1974).

a. Elastic Modulus

A typical p-y curve is shown in Fig. (3-3). The initial portion of the curve is essentially a straight line, as defined by the modulus E_{si}. This portion of the curve can be thought to represent the elastic behavior of the soil. Terzaghi suggested numerical values of E_{si} as a function of the unit weight and the relative density of sand. He suggested that E_{si} is zero at the ground surface and increases linearly with depth (Terzaghi, 1955). His

suggestion was based on the fact that experiments had shown that the initial slope of a laboratory stress-strain curve for sand is a linear function of the confining pressure.

E_{si} is given by the following equation:

$$E_{si} = kx$$

where

k = a coefficient, lb/in^3

x = depth below ground surface, in

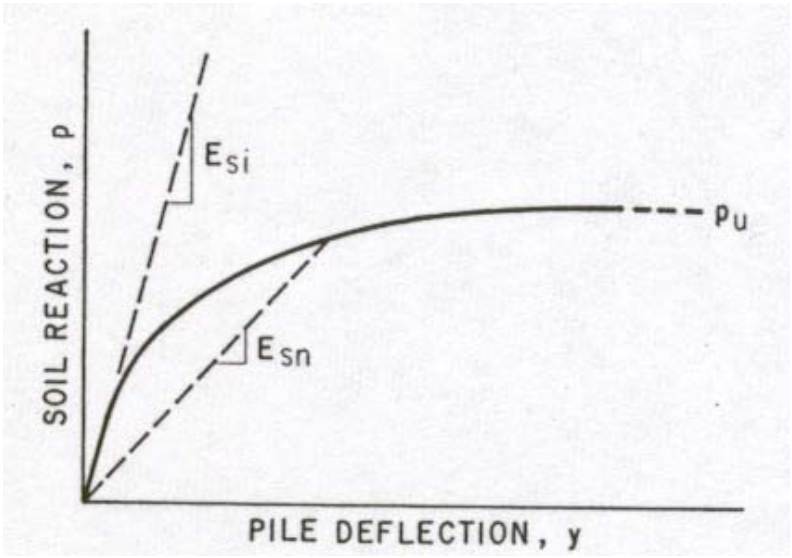

Fig. (3-3)
Typical "p-y" Curve
(Reese, 1974)

The value of k recommended by Terzaghi are shown in Table 1. The values of k obtained from the Mustang Island test for the static case were 2.5 times the highest value reported by Terzaghi. The values for the cyclic case were 3.9 times the highest value

given by Terzaghi. With regard to recommended values, it is proposed by Reese that the values of k shown in Table 2 and 3 be used. These values of k are recommended for static and cyclic loading (Reese, 1974 and Reese, 1984). An examination of the shape of the p-y curves which are recommended in Fig. (3-7) shows that the initial straight-line portions of the curves (where E_s is constant with deflection) governs for only small deflections. Therefore, the initial slope of the p-y curve influences analyses only for the

TABLE 1

Relative Density	Loose	Medium	Dense
Range of values of k (lbs/in^3)	2.6 – 7.7	7.7 – 26	26 – 51

Terzaghi's Values of k for Submerged Sand (Reese, 1974)

TABLE 2

Recommended Values of k for Submerged Sand based of Pile Tests Performed at Mustang Island for Static and Cyclic Loading (Reese, 1974)

Relative Density	Loose	Medium	Dense
Recommended values of k (lbs/in^3)	20	60	125

TABLE 3

Recommended Values of k for Sand Above the Water Table (Reese, 1984)

Relative Density	Loose	Medium	Dense
Recommended values of k (lbs/in^3)	25	90	225

very smallest loads. In more normal cases, a secant modulus, such as the one defined by E_{sn} shown in Fig. (3-3), controls the analyses. Because the initial portion of the p-y curve has little influence on most analyses and because of the relatively small amount of data on the early portions of the curves, it was thought to be undesirable to recommend different values of k for static and for cyclic loading.

b. Soil Resistance

Referring to Fig. (3-3), it may be seen that soil resistance p attains a limiting value defined as the ultimate soil resistance p_u. Soil mechanics theory can be applied to derive equations for p_u for two cases, near the ground surface and at a depth.

The ultimate soil resistance near the ground surface is computed using the free body shown in Fig. (3-4). As may be seen in the figure, the total ultimate lateral resistance F_{pt} on the pile section is equal to the passive force F_p minus the active force F_a. The force F_a may be computed from the Rankine's theory, using the minimum coefficient of active earth pressure. The passive force F_p may be computed from the geometry of the wedge, assuming the Mohr-Coulomb failure theory to be valid for sand. By referring to Fig. (3-4), it can be seen that the shape of the wedge is defined by the pile diameter b, the depth of the wedge H, and by the angles α and β. It is assumed that no frictional resistance occurs on the base of the pile; therefore, there is no tangential forces on the surface CDEF. The normal force F_n on planes ADE and BCF can be

computed using a coefficient for the lateral earth pressure at rest. If the force F_n is known, the force F_s can be computed using Mohr-Coulomb theory (Reese, 1974).

Referring to Fig. (3-4b), the direction of the force F_ϕ on the plane AEFB is known from theory; that is, the force acts at an angle ϕ from the normal to the plane,

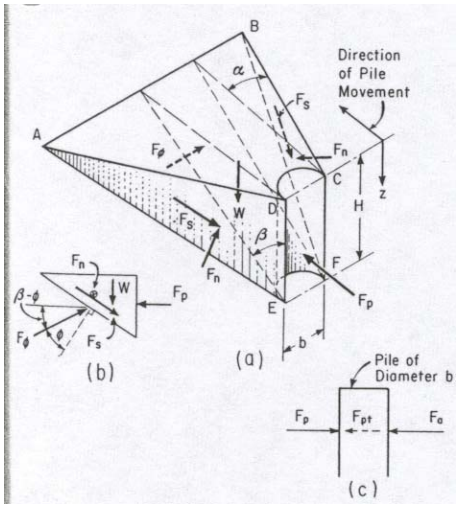

Fig. (3-4)
Assumed Passive Wedge-type Failure. (a) General shape of wedge. (b) Forces on wedge. (c) Forces on pile
(Reese, 1974)

where ϕ is the angle of internal friction of the sand. The weight of the wedge W can be computed from the unit weight of the sand γ. For sand below the water table, the submerged unit weight should be used. With the above information, the force F_t can be computed using equations of statics. Therefore, the soil resistance F_{pt} against the pile may be computed as indicated previously. The soil resistance per unit length of the pile at

any depth may be found by differentiating the force F_{pt} with respect to the depth H. The result of that differentiation is shown in eqn. (3-3).

$$P_{ct} = \gamma H \left[\begin{array}{l} \dfrac{K_0 H \tan\phi \sin\beta}{\tan(\beta-\phi)\cos\alpha} + \dfrac{\tan\beta}{\tan(\beta-\phi)}\left(b + H\tan\beta\tan\alpha\right) + \\ K_0 H \tan\beta\left(\tan\phi\sin\beta - \tan\alpha\right) - K_a b \end{array} \right] \tag{3-3}$$

The values of the parameters in this equation can be determined from theory and experimental data. The angle β is approximated by the following equation:

$$\beta = 45 + \phi/2 \tag{3-4}$$

This value for β is that which would be obtained from Rankine's Theory for the passive pressure condition and for the two-dimensional case. The Rankine conditions are not satisfied; however, some model experiments indicate that eqn. (3-4) gives a fairly good approximation of the slope of the failure surface (Reese, 1974).

Values of the angle α have been determined from results of model tests with a small flat plate in sand. From these model tests, Bowman states that α is probably a function of the void ratio of the sand, with values ranging from $\phi/3$ to $\phi/2$ for loose sand to ϕ for dense sand (Bowman, 1958).

Measurements at the soil surface around laterally loaded tubular model piles gave values for α as high as the value of ϕ for dense sand. Contours of the wedge that formed in front of the test piles at Mustang Island indicated that the value of α was equal to

about $\phi/3$ for static loading and about $3\phi/4$ for cyclic loading.

The value of the coefficient of earth pressure at rest is dependant on the void ratio or relative density of the sand and the process by which the deposit was formed. Terzaghi and Peck state that the value of the coefficient of earth pressure at rest is about 0.4 for loose sand and about 0.5 for dense sand (Terzaghi, 1948). In the absence of precise methods for determining relative density in the field, especially when soil deformations are large, a value of 0.4 for K_0 was selected in computing the ultimate soil resistance near the ground surface. The value of α selected for this computation was $\phi/2$. The angle of internal friction ϕ was taken as $39°$ as indicated previously.

The coefficient K_a in eqn. (3-3) is the Rankine coefficient of minimum active earth pressure and is given by the following equation:

$$K_a = \tan^2(45 - \phi/2) \tag{3-5}$$

With regard to the use of theory for computing the ultimate lateral resistance against the pile at a considerable depth below the ground surface, the model shown in Fig. (3-5) is employed. In this model, the soil is assumed to flow in the horizontal direction only. Referring to the model, Block 1 will fail by shearing along the dashed lines allowing the soil in that block to follow the pile. Block 2 will fail along the dashed line as shown. Block 3 will slide horizontally. Block 4 will fail as shown, and Block 5 will be in the failure condition as the pile pushes against it. In this simplified model it is assumed that

the cylindrical pile can be simulated by a rigid block of material (Reese, 1974).

With regard to the stresses σ_1 at the back of the pile, it is reasoned that this stress cannot be less than the minimum active earth pressure (Reese, 1974). Otherwise, the soil could slump from the ground surface with a vertical motion, which is expressly eliminated in the model which was selected. With a value of σ_1, the other stresses can be computed using Mohr-Coulomb Theory. Using the model shown, the ultimate soil resistance at a depth such that there is horizontal flow around the pile may be computed by

$$P_{cd} = K_a b\gamma H\left(\tan^8 \beta - 1\right) + K_0 b\gamma H \tan\phi \tan^4 \beta \qquad (3\text{-}6)$$

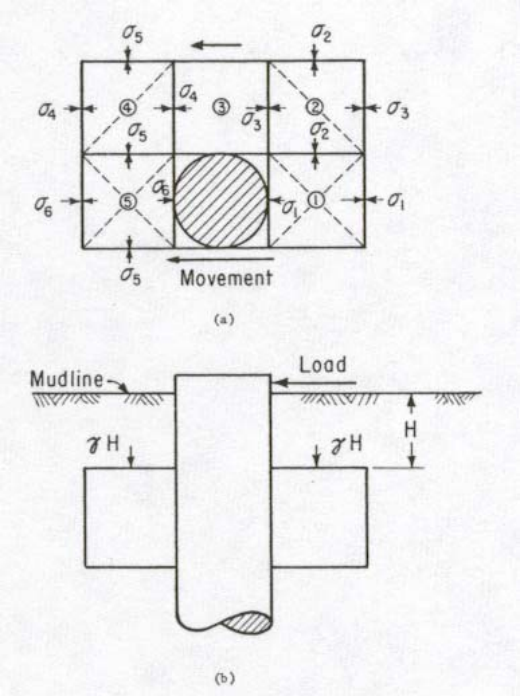

Fig. (3-5)
Assumed Mode of Soil Failure by Lateral Flow around the Pile. (a) Section through the pile. (b) Elevation of the pile.
(Reese, 1974)

For the Mustang Island test, values of P_c were computed using Eqns. (3-3) and (3-6). These values are shown plotted in Fig. (3-6). The values of the parameters used in making the computations are as follows (Reese, 1974):

$\phi = 39°$

$\alpha = \phi/2$

$K_0 = 0.4$

$\gamma = 66\, lbs/ft^3 \,(submerged)$

$\beta = 45° + \phi/2$

$b = 2\, ft$

The symbol X_t shown in Fig. (3-6) defines the intersection of Eqns. (3-3) and (3-6).

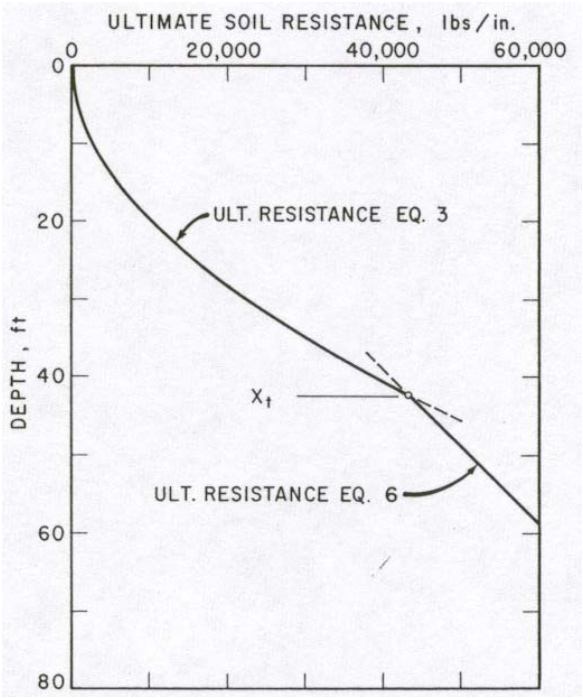

Fig. (3-6)
Ultimate Soil Resistance vs. Depth from Theory
(Reese, 1974)

c. Construction of the p-y Curve

A study of the families of p-y curves developed from the experiments for both static and cyclic loading shows that the characteristic shape of the curves may be represented by the curves shown in Fig. (3-7). The curves consist of three straight lines and a parabola. The initial straight portion of the p-y curve represents “elastic” behavior of the sand and the horizontal portion represents “plastic” behavior. These two straight lines are joined with a parabola and a sloping straight line. The parabola and the intermediate straight line were selected empirically to yield a shape consistent with the

experimental p-y curves. The slope of the initial portion of the curves may be obtained

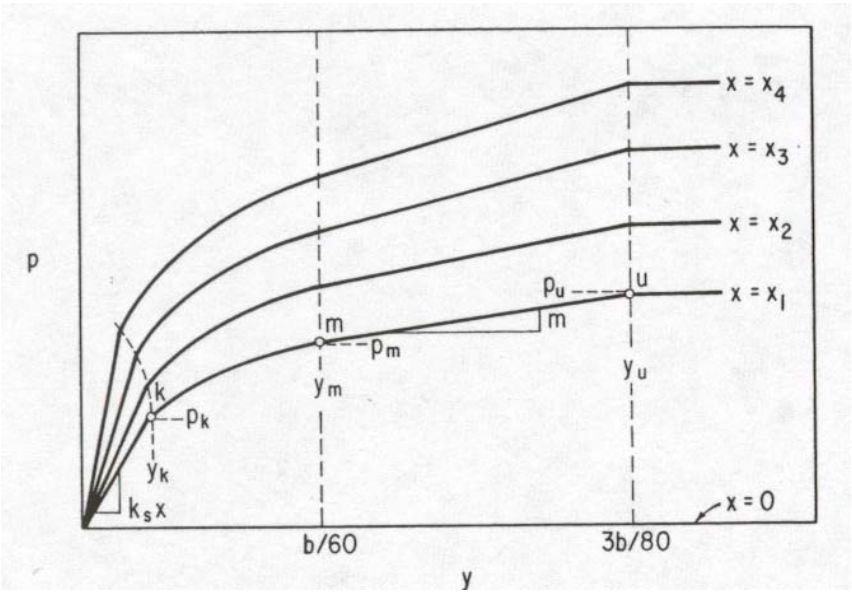

Fig. (3-7)
Typical Family of p-y Curves for proposed Criteria
(Reese, 1974)

from Table 2 or 3. The paragraphs below present the procedure for obtaining information for plotting the other portions of the curves (Reese, 1974).

When the computed values of the ultimate soil resistance were compared with the measured values, it was found that the agreement was poor. The poor agreement prevailed even though the effect of the friction against the pile wall was considered and even though other parameters were varied through a reasonable range. It was, therefore, decided to adjust the ultimate resistance according to the observed values, in the following manner (Reese, 1974):

$$P_u = AP_c \tag{3-7}$$

where

P_u = ultimate resistance in proposed criteria, lbs/in

P_c = ultimate resistance from theory, lbs/in

A = empirical adjustment factor

Values of A were obtained by dividing the observed ultimate soil resistances by the computed ultimate soil resistances for the Mustang Island tests. Values were obtained for A_s, the static case, and for A_c, the cyclic case. Plots of A_s and A_c versus the non-dimensional depth x/b are shown in Fig. (3-8). It should be noted again that observed values of ultimate resistance were obtained to a relatively shallow depth. eqn. (3-7), with values of A for either the static or the cyclic case, can be used to compute the ultimate soil resistance to be used in the development of p-y curves (Reese, 1974).

In the preceding sections, the magnitude of the ultimate soil resistance and the slope of the initial straight-line portion of the curve were obtained. It remains to establish values of p and y corresponding to points k and m as shown in Fig. (3-7) and to establish the values of y corresponding to point u. These points define the intermediate portion of the p-y curve which can be represented by a parabola connecting points k and m (Reese, 1974).

For the results of the Mustang Island, it was found that the values of y_m and y_u were 0.4 in. and 0.9 in., respectively. The respective values of y/b were $1/60$ and $3/80$. The value of p_m was obtained from the p-y curves, for both static and cyclic loading.

From these values, values of the parameter B were computed as follows (Reese, 1974):

$$B = \frac{P_m}{P_c} \tag{3-8}$$

Values of B for both static and cyclic cases are shown in Fig. (3-9). Thus, from the

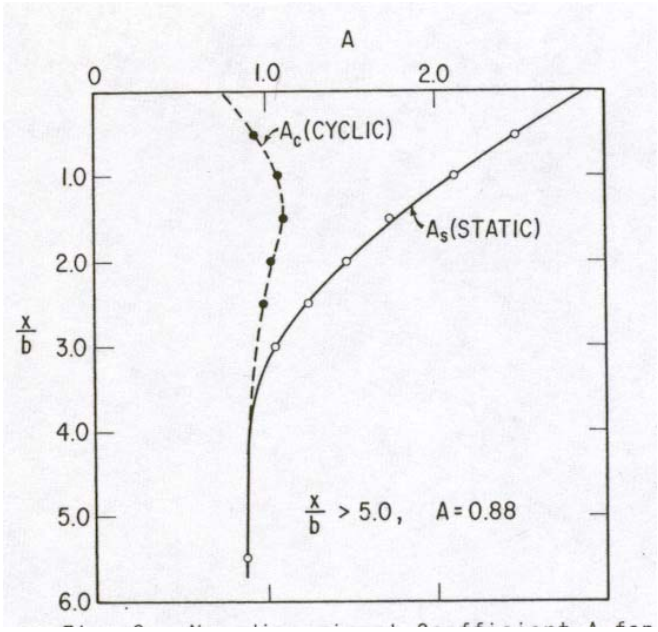

Fig. (3-8)
Non-dimensional Coefficient, A, for Ultimate Soil Resistance vs. Depth
(Reese, 1974)

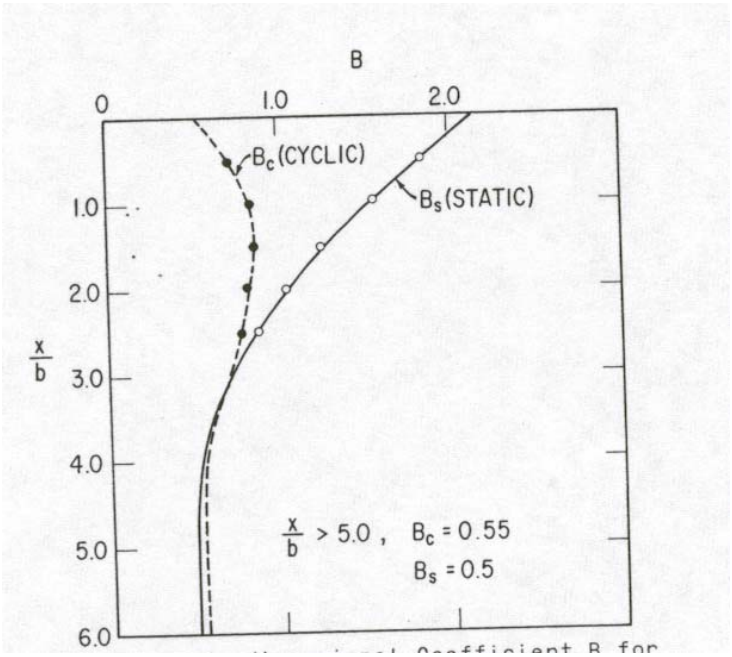

Fig. (3-9)
Non-dimensional Coefficient, B, for Ultimate Soil Resistance vs. Depth
(Reese, 1974)

values of P_c, computed by eqn. (3-3) or eqn. (3-6), values of P_m can be obtained for any pile in any soil by using the empirical relationships that are given (Reese, 1974).

The p-y curve can now be completed by constructing a parabola between points k and m. This was accomplished by constructing a parabola, passing through the origin, and connecting at point m with a slope equal to that of the straight line from m to u. The intersection of this parabola with the initial straight-line portion of the p-y curve established point k (Reese, 1974).

d. Step-by-Step Procedure

For convenience in making computations for a family of p-y curves, the following

step-by-step procedure is presented (Reese, 1984). A typical family of such curves is shown in Fig. (3-7).

1. Obtain values for significant soil properties and pile dimensions, ϕ, γ, and b.

2. Use the following for computing soil resistance: $\alpha = \phi/2$, $\beta = 45 + \phi/2$, $K_0 = 0.4$, and $K_a = \tan^2\left(45 - \phi/2\right)$.

3. Use the following equations for computing soil resistance:

   a. Ultimate resistance near ground surface.

$$P_{ct} = \gamma H \left[\begin{array}{l} \dfrac{K_0 H \tan\phi \sin\beta}{\tan(\beta-\phi)\cos\alpha} + \dfrac{\tan\beta}{\tan(\beta-\phi)}\left(b + H\tan\beta\tan\alpha\right) + \\ K_0 H \tan\beta\left(\tan\phi\sin\beta - \tan\alpha\right) - K_a b \end{array} \right] \qquad (3\text{-}9)$$

   b. Ultimate resistance well below the ground surface.

$$P_{cd} = K_a b \gamma H\left(\tan^8\beta - 1\right) + K_0 b \gamma H \tan\phi \tan^4\beta \qquad (3\text{-}10)$$

4. Find the intersection, X_t, of the equation for the ultimate soil resistance near the ground surface and the ultimate soil resistance well below the ground surface. Above this depth use eqn. (3-3), below this depth use eqn. (3-6).

5. Select one depth at which a p-y curve is desired.

6. Establish y_u at $3b/80$. Compute p_u by the following equation:

$$P_u = AP_c \tag{3-7}$$

Use the appropriate values of A from Fig. (3-8), for the particular nondimensional depth, and for either the static or cyclic case. Use the appropriate equation for P_c, eqn. (3-3) or eqn. (3-6) by referring to computation in step 4.

7. Establish y_m as $b/60$. Compute p_m by the following equation:

$$p_m = BP_c \tag{3-8}$$

Use the appropriate values of B from Fig. (3-9), for the particular nondimensional depth, and for either the static or cyclic case. Use the appropriate equation for P_c.

8. Establish the slope of the initial portion of the p-y curve by selecting the appropriate value of k from Table 2 or 3. Use the equation,

$$p = (kx)y$$

9. Select the following parabola to be fitted between points k and m:

$$p = Cy^{1/n} \tag{3-11}$$

10. Fit the parabola between points k and m as follows:

    a. Get slope of line between points m and u by,

$$k_{mu} = \frac{p_u - p_m}{y_u - y_m} \tag{3-12}$$

    b. Obtain the exponent of the parabolic section by,

$$n = \frac{p_m}{k_{mu} y_m} \tag{3-13}$$

c. Obtain the coefficient C as follows:

$$C = \frac{p_m}{y_m^{1/n}} \tag{3-14}$$

d. Determine point k on the curve as,

$$y_k = \left(\frac{C}{kx} \right)^{n/n-1} \tag{3-15}$$

where k is obtained from Table 2 or 3.

e. Compute appropriate numbers of points on the parabola by using eqn. (3-11).

This completes the development of the p-y curve for the desired depth. Repeating the steps above for each depth desired can develop any number of curves.

e. Limitations

The following limitations were taken from Reese, 1974:

1. The soil is assumed to be cohesionless sand. A soil that is predominately granular but contains a sufficient amount of clay to give some cohesion would behave entirely different than cohesionless sand.

2. The pile is assumed to have been driven so that the sand is densified rather

than loosened during installation. The proposed method does not apply to piles that have been installed by jetting.

3. The pile is assumed to be essentially vertical. However, it is believed that the method can be used to predict the behavior of batter piles if the batter is not to severe.

3. P-Y Curves in Soft Clay

A research program was performed by Matlock to solve the problems pertinent to the design of laterally loaded piles in soft, normally consolidated marine clay (Matlock, 1970). The program was oriented mainly for offshore structures and has included field tests with an instrumented pile and laboratory model testing. Three types of loading were considered: (1) short-term static loading, (2) cyclic loading, and (3) subsequent reloading after cyclic loading. The research included extensive field-testing with an instrumented pile, experiments with laboratory models and parallel development of analytical methods and correlations.

The steel test pile was 12.75 inches in diameter and 35 pairs of electric resistance strain gages were installed in the 42 foot embedded portion. The pile was calibrated to provide extremely accurate determinations of bending moment. Gage spacing varied from 6 inches near the top to 4 feet in the lowest section.

Free-headed tests were done with only lateral loads applied at the mud line. As shown in Fig. (3-10), restrained-headed loadings utilized a framework to simulate the effect of a jacket-type structure. The load from hydraulic rams was transmitted to the pile

by a walking beam and loading strut. For cyclic loadings, the peak forward and reverse loads during cycling were automatically controlled.

Precise determination of the bending moments during all static loadings allowed differentiation to obtain curves of the distribution of soil reaction along the pile to a very satisfactory degree of accuracy. Integration of the bending moment diagrams provided the deflected shape of the pile. For illustrative purposes, see Fig. (3-10b). Loads were increased by increments, and for any selected depth, the soil reaction p may be plotted as a function of pile deflection y. These experimental p-y curves are the principle basis for the development of design procedures.

The pile was driven twice and two complete series of free-headed loadings, one static and one cyclic, were performed at Lake Austin. At a site near the mouth of the Sabine River there were four primary series of test loadings, two static and two cyclic, with each type tested under both free-headed and restrained-headed conditions. In addition to these, numerous variations were tried including tests with sand, artificially softened clay, and the use of sand and pea gravel to restore the loss in resistance of the pile caused by previous cyclic loadings.

Some laboratory experiments were performed which are helpful in explaining the nature of the deterioration of resistance under cyclic loading. Fig. (3-11a) shows one of the types of laboratory loadings that were performed, the lateral displacement of a rigid rod embedded in soft clay. The cavity shown behind the rod is typical of field tests also. Fig. (3-11b) shows one recorded cycle of load versus deflection and clearly indicates the

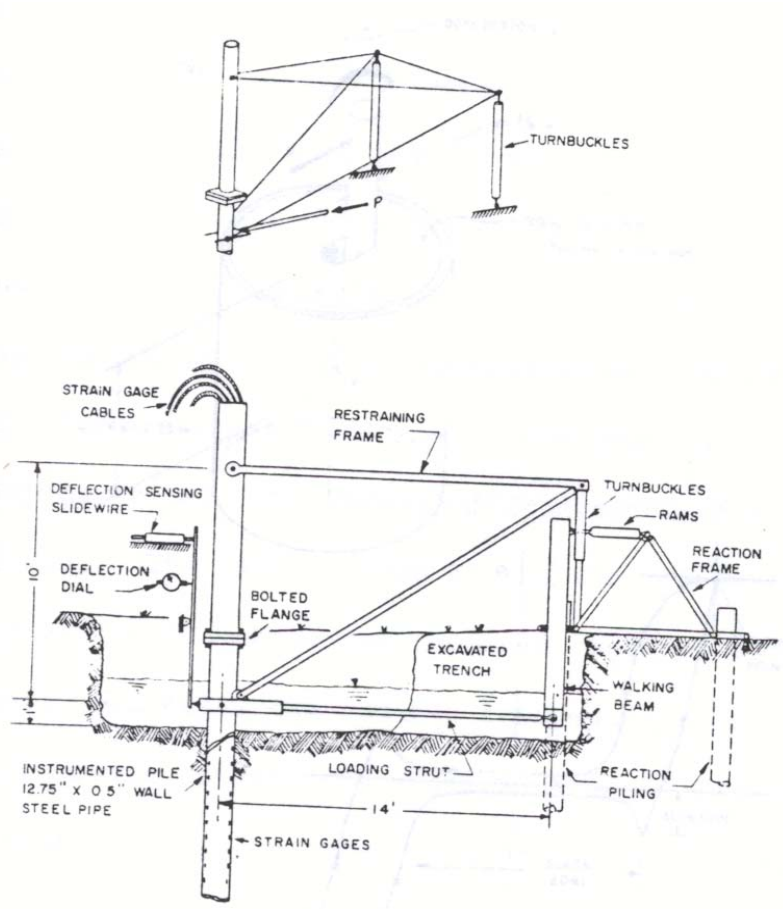

Fig. (3-10)
Arrangements for Field Tests at Sabine using Restrained-head Lateral Loading
(Matlock, 1970)

reduced resistance encountered by a segment of a pile in moving through the slack zone produced by a previous loading. As the control point is moved to larger deflections, the cavity is extended (Matlock, 1970).

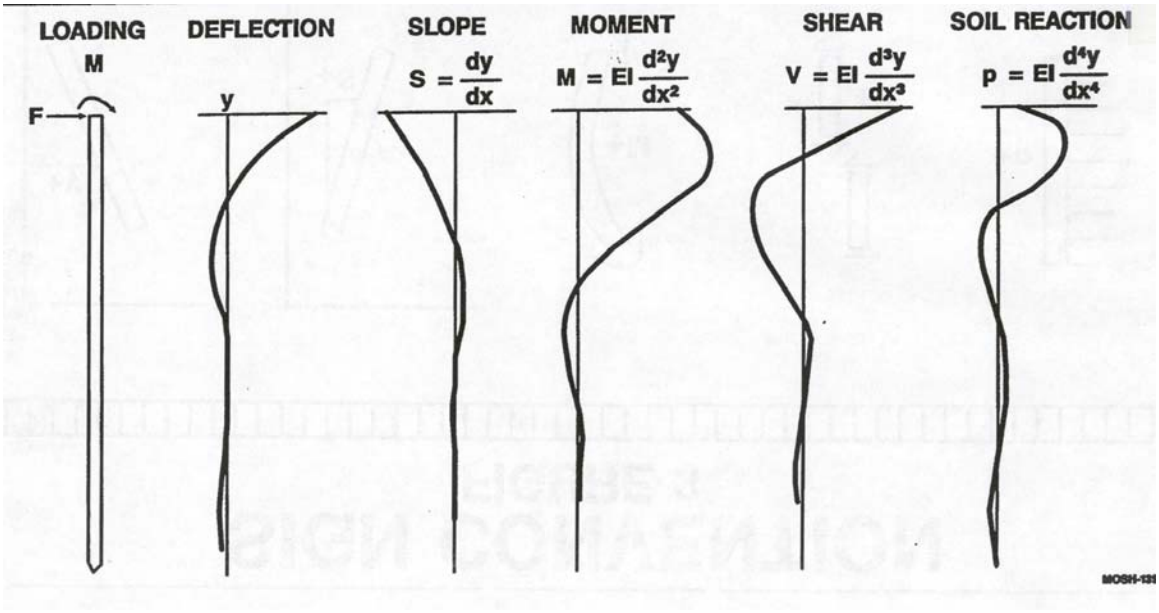

Fig. (3-10b)
Form of the Results Obtained from a Laterally Loaded Pile.
(Prospect, 2003)

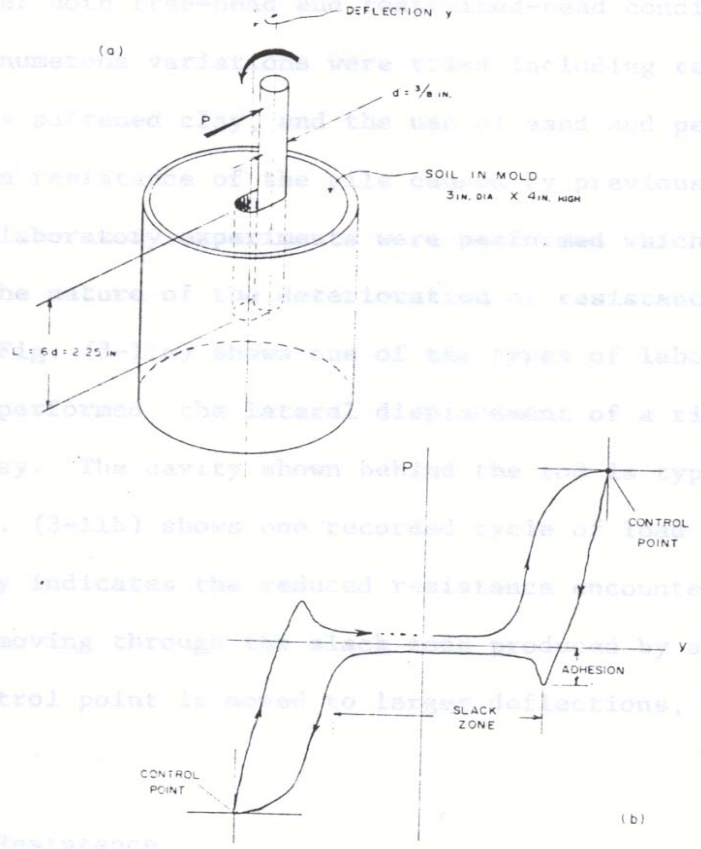

Fig. (3-11)
Laboratory Model Studies.
(a) Test specimen. (b) A typical loading cycle.
(Matlock, 1970)

a. Soil Resistance

In conventional soil mechanics, most problems involving load capacity of soils are handled by consideration only of ultimate strength characteristics. In contrast, with long piles laterally loaded, the static ultimate soil resistance is seldom achieved except very near the surface; the allowable stresses in the pile are usually reached first, with most of the soil still in a pre-plastic state of strain. Nevertheless, a rational and orderly prediction of soil deformation characteristics for various loading conditions should start with an estimate of static ultimate resistance.

In soft clay, soil is confined so that plastic flows around a pile occur only in horizontal planes. The ultimate resistance per unit length of pile may be expressed as

$$p_u = N_p c d \tag{3-16}$$

where c is the soil strength, d is the pile diameter, and N_p is a non-dimensional ultimate resistance coefficient. A consensus of the investigators appears to indicate that for soft clay soil flowing around a cylindrical pile at a considerable depth below the surface, the coefficient should be

$$N_p = 9 \tag{3-17}$$

Very near the surface, the soil in front of the pile will fail by shearing forward and upward and the corresponding value of N_p reduces to the range of 2 to 4, depending on whether the pile segment is considered as a plate with only frontal resistance or whether it is a square cross section with soil shear acting along the sides. For a cylindrical pile, a

value of 3 is believed to be appropriate. The resistance should be expected to vary from this value at the surface to the maximum indicated by eqn. (3-17) at some depth X_r, which is termed the depth of reduced resistance. Within the upper zone, resistance to vertical movement is provided by the overburden pressure σ_x from the soil itself and by resistance developed by deformation within the surrounding soil mass. This resistance increases with distance from the free soil surface. The following equation appears to describe this variation to a satisfactory degree of approximation:

$$N_p = 3 + \frac{\sigma_x}{c} + J\frac{x}{d} \tag{3-18}$$

The first term expresses the resistance at the surface, the second term gives the increase with depth due to overburden pressure, and the third term may be thought of as the geometrically related restraint that even a weightless soil around a pile would provide against upward flow of the soil. The equation corresponds closely to one developed by Reese who considered a failing prism or wedge of soil ahead of the pile. However, Reese's value of J was 2.8, which does not agree with experimental results. Therefore, the coefficient J must be determined empirically.

Fortunately, the third term in eqn. (3-18) represents only a part of the total ultimate resistance coefficient N_p, and according to Matlock, because it contains the depth x, it becomes relatively insignificant in the more important upper layers. From experimental evidence, a clear distinction cannot be made between contributions of the first and last terms in eqn. (3-18).

Studies based on the Sabine data indicate that a value of J equal to approximately 0.5 is satisfactory when used in eqn. (3-18). A lower value of about 0.25 fits the Lake Austin data somewhat better, which may be a consequence of the stiffer clay at that site.

If the soil strength and the effective unit weight γ are constant with depth, the value of the depth at which the value of N_p becomes equal to the maximum of 9 is obtained by the simultaneous solutions of Eqns. (3-17) and (3-18):

$$x_r = \frac{6d}{\frac{\gamma d}{c} + J} \tag{3-19}$$

The coefficient J and the resulting values of x_r should be thought of as rational but essentially empirical parameters by which correlations have been made between prediction methods and the available field results. Where soil properties undergo considerable variation with depth, it appears reasonable to consider the soil as a system of thin layers with x_r computed as a variable with depth according to the properties of each layer (Matlock, 1970).

b. Construction of the P-Y Curve

The following section presents a summary taken from Matlock's 1970 paper of the recommended procedure for constructing p-y curves for the three different loading conditions is given in Fig. (3-12). In a given problem, the appropriate form selected from Fig. (3-12) is applied at numerous depths to produce a family of p-y curves. The basis for

the construction will be described briefly.

The curves are in non-dimensional form with the ordinates normalized according to the static ultimate resistance p_u determined as described above for each depth. The horizontal coordinate is the pile deflection divided by the deflection at point c, where the static resistance is one-half of the ultimate static resistance. The form of the pre-plastic portions of the static resistance curve, up to point e in Fig. (3-12), is based on semi logarithmic plots of the experimental p-y curves, which fall roughly along straight lines at slopes yielding the exponent of $1/3$. Thus, the point of intersection with the plastic branch at point e will always occur at a horizontal coordinate of 8. The value of the pile deflection at point c is based on concepts given by Skempton by which he combines elasticity theory, ultimate-strength methods, and laboratory soil properties, to estimate short-term load-settlement characteristics of a buried strip footing in clay soil. The strain ε_{50} is that which occurs at one-half of the maximum stress on a laboratory stress-strain curve. It may be determined by dividing the shear strength c by an estimated secant modulus E_c or it may be taken directly from stress-strain curves. Based on Skempton's recognition that the ratio E_c/c falls between 50 and 200 for most clays, a value for ε_{50} may be assumed between 0.005 and 0.020, the smaller value being applicable to brittle or sensitive clays and the larger to distributed or remolded soil or unconsolidated sediments.

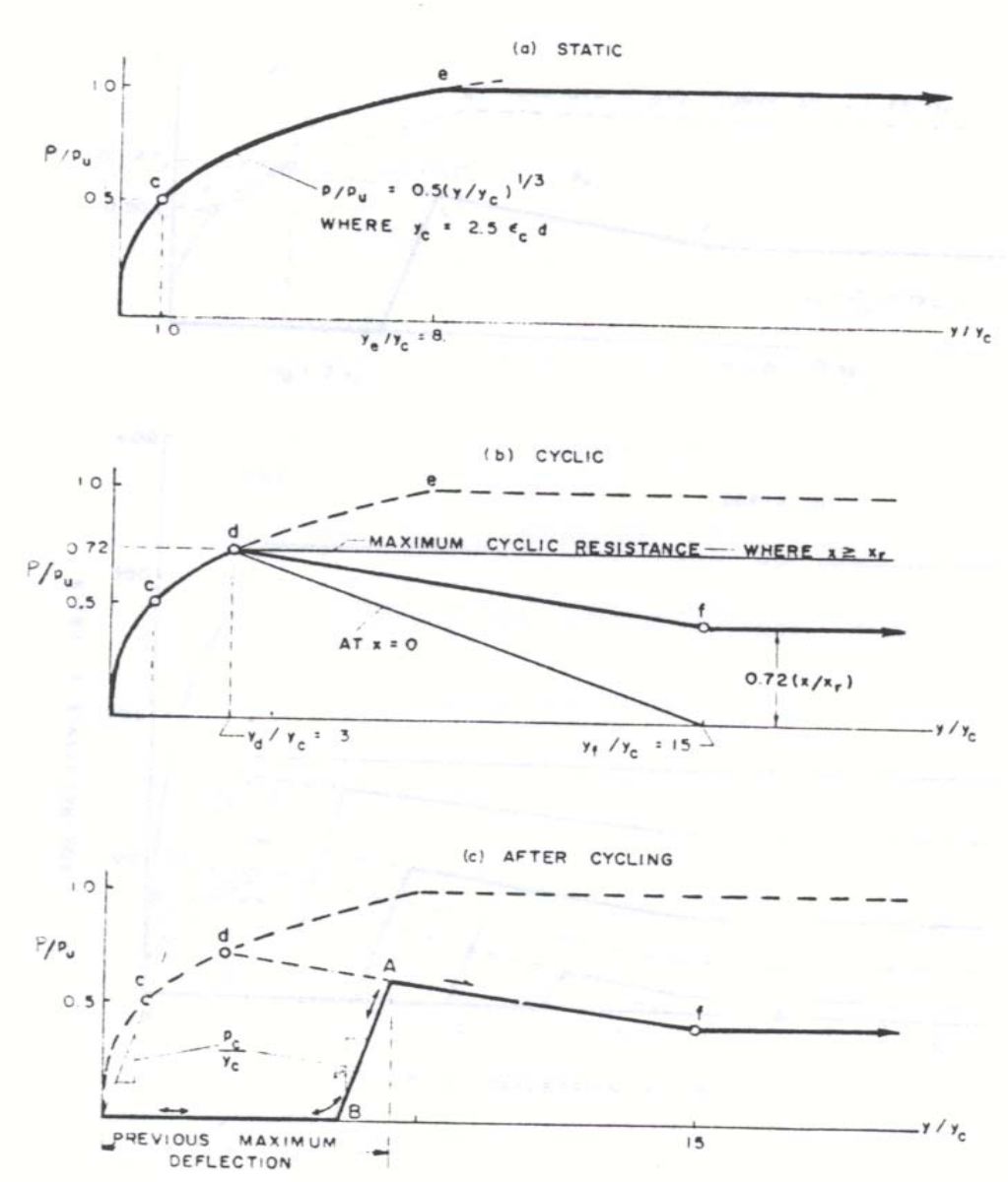

Fig. (3-12)
Criteria for Predicting p-y Curves for (a) Short-term static loading, (b) Equilibrium under initial cyclic loading, and (c) Reloading after cycling (Matlock, 1970)

An intermediate value of 0.010 is probably satisfactory for most purposes, according to Skempton (Matlock, 1970). Using Skempton's approach, the deflection sought is approximately

$$y_c = 2.5\varepsilon_{50} d \tag{3-20}$$

The modifications to the static p-y curve to express the possible deterioration due to cycling are shown in Fig. (3-12b). According to the curve, substantial deflections are possible, up to point d, without any deterioration in resistance as compared to the static curve. At this point the resistance under cyclic loading has reached a maximum even at greater depths. At shallow depths further reductions in resistance are provided which are more severe with increasing and decreasing depth. Complete loss in resistance is assumed to occur at the soil surface when deflections at that point reach $15y_c$. For deflections greater than $15y_c$, the pseudo-plastic resistance is established by

$$\frac{p}{p_u} = 0.72\frac{x}{x_r} \tag{3-21}$$

The complete effect can be seen more readily from the family of cyclic p-y curves in Fig. (3-26) (Matlock, 1970).

There are three aspects of the cyclic construction procedure, which are primarily empirical, at least from a quantitative standpoint. These are (1) the position of the cyclic deterioration threshold (point d) along the pre-plastic portion of the static p-y curve, (2) the value of the deflection y_f, and (3) the manner in which the final resistance p_f is

adjusted with depth according to eqn. (3-21). The depth x_r represents what is in reality a rather indefinite point of transition from a condition of incomplete vertical restraint to one where plastic flow is confined to horizontal planes. Furthermore, it is a quantity taken from static-loading correlations. The use of x_r in eqn. (3-21) is based primarily on intuition and judgment, but is supported as being satisfactory by comparisons of computed results versus experimental results (Matlock, 1970).

After any particular point, such as point A in fig. (3-12c), has been reached along a p-y curve, rebound to zero resistance is assumed to occur along a line parallel to a secant through point c. The resulting slack zone and reloading path are indicated in fig. (3-12c). This construction is the basis for the p-y family in fig. (3-13). The deflection for each depth must be known from a solution for the maximum loading condition in order to establish the modified return branch for each curve (Matlock, 1970).

c. Step-by-Step Procedure

A step-by-step procedure for constructing p-y curves in soft clay is given below. For short term, static loads:

1. Obtain the best possible estimate of the variation of shear strength and

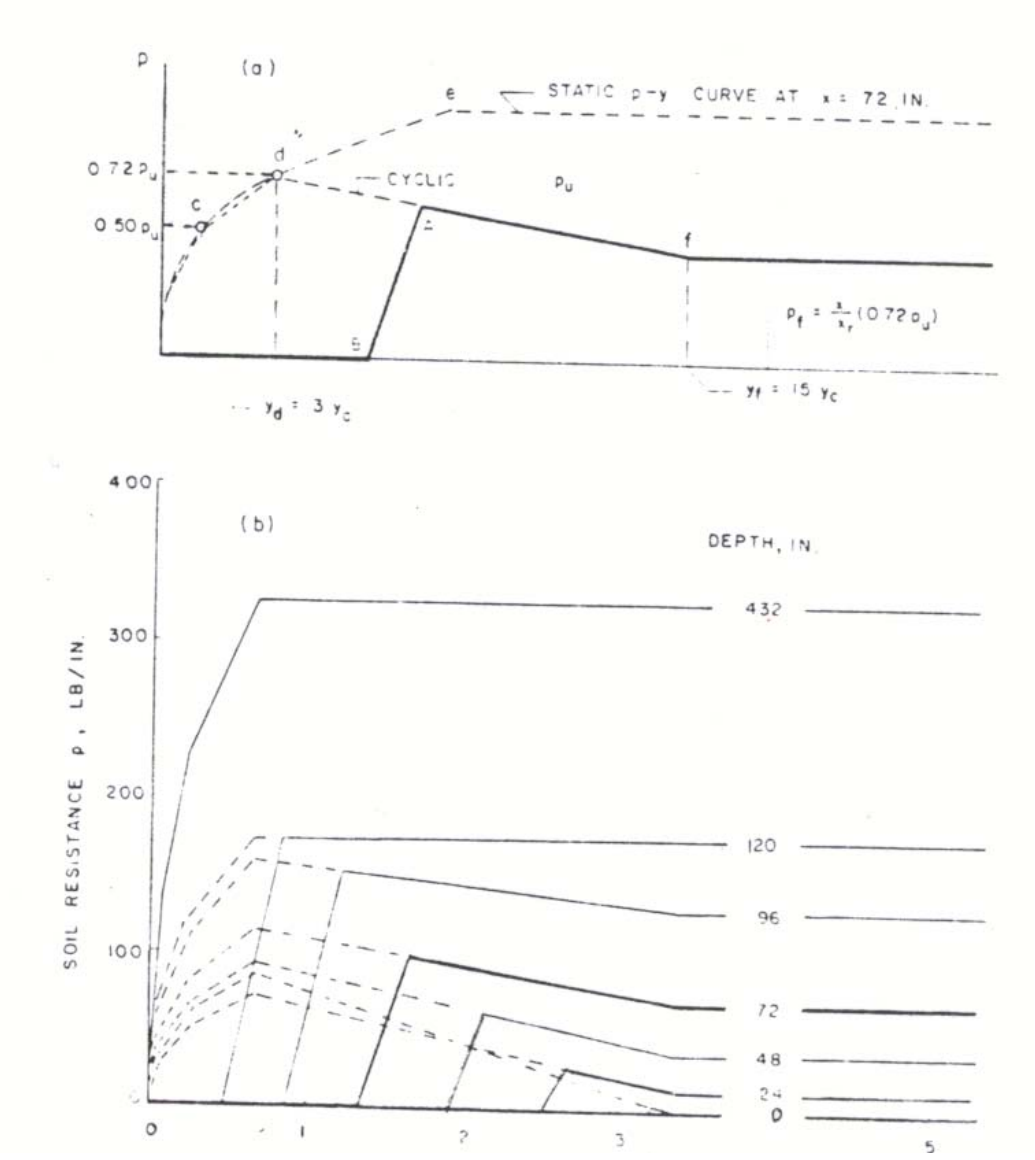

Fig. (3-13)
Force-deformation Curves Predicted for Reloading after Prior Cyclic Loading to 13.5 kips, (a) Typical construction, (b) Complete family of curves (Matlock, 1970)

effective unit weight with depth. Also obtain the value of ε_{50}, the strain corresponding to one-half the maximum principle stress difference. If no values of ε_{50} are available, typical values suggested by Skempton are given in Table 4 or Table 5.

TABLE 4

Recommended Values of ε_{50} (Desai, 1977)

Consistency of clay	ε_{50}	E_c / c
Soft	0.020	50
Medium	0.010	100
Stiff	0.005	200

TABLE 5

Shear Strength, psf	ε_{50} **, %**
250-500	2
500-1000	1
1000-2000	0.7
2000-4000	0.5
4000-8000	0.4

Representative Values of ε_{50} (Prospect, 2003)

2. Compute the ultimate soil resistance per unit length of shaft p_u, using the smaller of the values given by:

$$p_u = \left(3 + \frac{\gamma}{c}x + 0.5\frac{x}{d}\right)cd \tag{3-22}$$

and $p_u = 9cd$ (3-23)

where

$\gamma =$ average effective unit weight from ground surface to p-y curve depth

$x =$ depth from ground surface to p-y curve

$c =$ shear strength at depth x

$d =$ width of pile

3. Compute the deflection y_{50} at one-half the ultimate soil resistance from

$$y_{50} = 2.5\varepsilon_{50}d \tag{3-24}$$

4. Points describing the p-y curve are now computed from

$$\frac{p}{p_u} = 0.5\left(\frac{y}{y_{50}}\right)^{1/3} \tag{3-25}$$

For cyclic loading:

1. Construct the p-y curve in the same manner as for short-term static loading for values of p less than $0.72p_u$.

2. Solve eqn. (3-22) and eqn. (3-23) simultaneously to find the depth x_r where the transition occurs. If the unit weight and shear strength are

constant in the upper zone, then

$$x_r = \frac{6cd}{\gamma d + 0.5c} \tag{3-26}$$

3. If the depth to the p-y curve is greater than or equal to x_r, p is equal to $0.72p_u$ for all values of y greater than $3y_{50}$.

4. If the depth to the p-y curve is less than x_r, the value of p decreases from $0.72p_u$ at $y = 3y_{50}$ to the value given by the expression below at $y = 15y_{50}$:

$$p = 0.72p_u \frac{x}{x_r} \tag{3-21}$$

The value of p remains constant beyond $y = 15y_{50}$.

d. Observations from Field Testing

Matlock developed these design criteria based on the results of the Sabine tests. Matlock's observations resulted in the following principle conclusions (Matlock, 1970):

1. The resistance-deflection (p-y) characteristics of the soil are highly non-linear and inelastic.

2. Within practical ranges, the fundamental resistance-deflection characteristics of the soil appear to be independent of the degree of pile-head restraint.

3. A principle effect of cyclic loading appears to be the permanent physical

displacement of the soil away from the pile in the direction of loading. It is not clear what contribution to this effect was provided by loss in strength within the soil mass. Although no significant amount of mixing of water and soil was directly evident, the cyclic shear reversals in the soil mass may have caused some structural deterioration in the clay.

4. The permanent displacement of the soil created a slack zone in the resistance-deflection characteristics. On reloading the pile with forces less than previously attained maximum values, the slack-zone effect was manifested by much greater bending moments than obtained with similar loading during the initial cyclic series.

5. Although significant changes occurred with continued repetition of load cycles, at any given magnitude of lateral load (except the highest) the behavior of the pile-soil system tended to stabilize. Such equilibrium response was usually attained to a practical degree in less than 100 cycles.

It was demonstrated at Lake Austin and confirmed at Sabine Pass that a period of rest does not provide any restoration of soil resistance at the top of the pile. Subsequent deposition of clay or clay slurry in the cavity is not followed by any significant gain in strength because of the absence of sustained consolidating forces. Only by maintaining granular material in the cavity was the resistance improved or restored (Matlock, 1970).

4. P-Y Curves in Stiff Clay

Experiments were conducted by Lymon C. Reese and aimed at developing criteria

for predicting the behavior of stiff clay around a deep foundation subjected to lateral loads. Similar to the research conducted by Matlock, the basic concern was in short-term static and cyclic loadings. The experiments involved the loading in the field of a deep foundation that is instrumented so that bending moments can be measured along the length of the foundation (Reese, 1975).

The deep foundation that was tested was a drilled shaft, constructed by drilling an open hole with a diameter of 30 inches, to a depth of 42 feet below the surface. An instrumented column and a reinforcing steel cage were placed in the hole and the hole was then filled with a tremie-placed concrete. Using a short cylindrical form, the shaft was extended 2 feet above the ground surface, for a total length of 44 feet (Reese, 1975).

The instrumented column was a steel pipe with a wall thickness of ¼ inches, and an outside diameter of 10-¾ inches. The wall thickness was selected such that the flexural stiffness of the instrumented column was about equal to the flexural stiffness of the concrete it replaced (Reese, 1975).

To install strain gages for measuring the bending moments in the drilled shaft, the pipe for the instrumented column was split longitudinally, and two strain gages, with their axes parallel to the axis of the pipe, were mounted on each half of the pipe at each gage level. At each level, four gages were connected in a bridge circuit to give the maximum sensitivity to the bending. The strain gages were spaced at 15-inch intervals for the top 2/3 of the shaft and at 30-inch intervals in the bottom 1/3 (Reese, 1975).

The soil profile at the site consisted of 28 feet of stiff to very stiff red clay, 2 feet

of interspersed silt and clay layers, and very stiff tan silty clay to a depth of 42 feet. The water table was at a depth of 18 feet at the time of the field test (Reese, 1975).

Unconsolidated-undrained triaxial compression tests were performed on undisturbed samples taken at the test site, with the confining pressures made equal to the effective overburden pressure. The shear strength in the upper 20 feet, the zone of most importance in lateral behavior, varied widely, due in part to the slickenside structure of the sample. But, according to Reese, there was no discernable pattern of strength variation with depth. The average undrained shear strength in the upper 20 feet was 1.1 tsf. A secant modulus intersecting the stress-strain curve at ½ the maximum principle stress difference was used to describe the stiffness of the soil, E_c. The overall pattern shows a decreasing soil stiffness with depth (Reese, 1975).

To define the stress-strain relationship in nondimensional terms, the applied principle stress difference was divided by the maximum principle stress difference, and the strain was divided by the strain at ½ the maximum, ε_{50}. The values of $\frac{(\sigma_1 - \sigma_3)}{(\sigma_1 - \sigma_3)_{\max}}$ and $\frac{\varepsilon}{\varepsilon_{50}}$ were determined for all tests. These values were plotted, and the equation of the curve was found to be

$$\frac{(\sigma_1 - \sigma_3)}{(\sigma_1 - \sigma_3)_{\max}} = 0.5\left(\frac{\varepsilon}{\varepsilon_{50}}\right)^{1/2} \tag{3-27}$$

The average value of ε_{50} was 0.005 in/in (Reese, 1975).

Several of the samples were subjected to repeat loading. The additional deformation under repeated loading was dependant upon the stress level. Reese found that at high stress levels, repeated loadings would probably reduce the shear strength of the sample, thus giving an erroneous value of the stress ratio (Reese, 1975).

a. Step-by-Step Procedure

A step-by-step procedure for constructing p-y curves in stiff clay is given below (Reese, 1975).

For short term, static loads:

1. Obtain the best possible estimate of the variation of shear strength and effective unit weight with depth. Also obtain the value of ε_{50}, the strain corresponding to one-half the maximum principle stress difference. If no values of ε_{50} are available, use a value of 0.005 or 0.010, the larger value being the more conservative.
2. Compute the ultimate soil resistance per unit length of shaft p_u, using the smaller of the values given by eqn. (3-22) and (3-23). In the use of eqn. (3-22), the shear strength is taken as the average from the ground surface to the depth being considered.
3. Compute the deflection y_{50} at one-half the ultimate soil resistance from eqn. (3-24).
4. Points describing the p-y curve are computed from

$$\frac{p}{p_u} = 0.5\left(\frac{y}{y_{50}}\right)^{1/4} \tag{3-28}$$

5. Beyond $y = 16y_{50}$, p is equal to p_u for all values of y.

For cyclic loads:

1. Construct the p-y curve in the same manner as for short-term static loading as described previously.
2. Determine the number of times the design lateral load will be applied to the deep foundation.
3. For several values of $\frac{p}{p_u}$, obtain the value of C. The parameter describing the effect of repeated loading on deformation from a relationship developed by laboratory test or, in the absence of test, is given by

$$C = 9.6\left(\frac{p}{p_u}\right)^4 \tag{3-29}$$

4. At the values of p corresponding to the values of $\frac{p}{p_u}$, selected in step 3, compute new values of y for cyclic loading from

$$y_c = y_s + y_{50}C\log N \tag{3-30}$$

where

$y_c =$ deflection under N cycles of load

y_s = deflection under short-term static load

y_{50} = deflection under short-term static load at ½ ultimate resistance

N = number of cycles of load application

5. The $p - y_c$ curve defines the soil response after N cycles of load.

5. Correlation with Test Results

In this section, the close agreement between test results and analytical computations, using the previously proposed methods for relating the soil reaction to the pile deflection for various deposits of soil, is demonstrated. The correlation is done with the specific test sites described previously. Bearing in mind that deposits are distinctive, with characteristics depending on many factors, some empirical coefficients could be revised. This problem will be dealt with later.

From the sets of experimental bending moment curves described previously, values of p and y at points along the pile can be obtained by solving the following equations (Reese, 1974):

$$y = \int\int \frac{M(x)}{EI} \tag{3-31}$$

$$p = \frac{d^2}{dx^2} M(x) \tag{3-32}$$

Approximate boundary conditions must be used and the equations must be solved numerically.

According to Reese, the solution of eqn. (3-31) for values of y can normally be

accomplished with appropriate accuracy. However, analytical difficulty is encountered in the solution of eqn. (3-32). If extremely accurate values of bending moment are available, the double differentiation can be performed numerically (Reese, 1974).

The procedure employed for obtaining the soil resistance curves involved the prior assumption that the soil modulus could be described as a function of depth by a two-parameter, nonlinear curve. The two parameters were computed from the experimental data, allowing the soil reaction curve to be computed analytically (Reese, 1974).

a. Sand Deposits

Reese compared calculated values of moment, deflection and slope with the field measurements. Lateral load versus measured and computed values of maximum moment for the static tests is shown in Fig. (3-14). Lateral load versus measured and computed values of deflection at the ground line for the static tests is shown in Fig. (3-15). Lateral

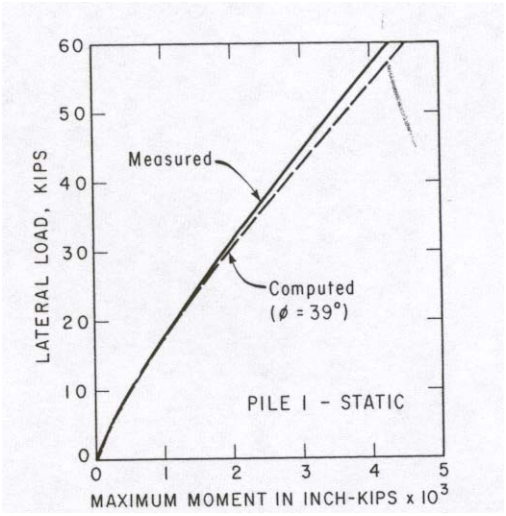

Fig. (3-14)
Comparison between Measured Results of Mustang Island Tests and Results Computed with Proposed Criteria; Pile 1 Maximum Moment
(Reese, 1974)

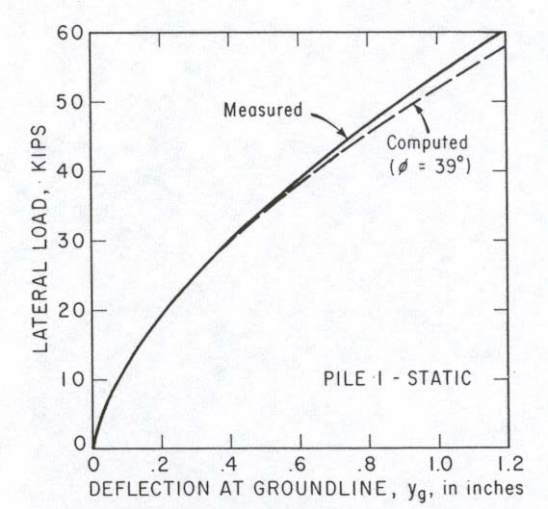

Fig. (3-15)
Comparison between Measured Results of Mustang Island Tests and Results Computed with Proposed Criteria; Pile 1 Deflection at Ground Line
(Reese, 1974)

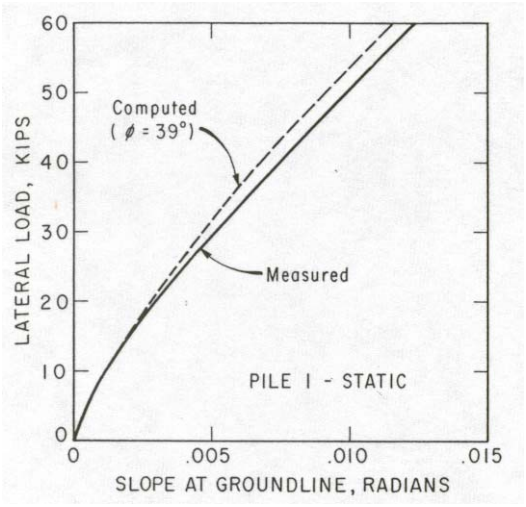

Fig. (3-16)
Comparison between Measured Results of Mustang Island Tests and Results Computed with Proposed Criteria; Pile 1 Slope at Ground Line
(Reese, 1974)

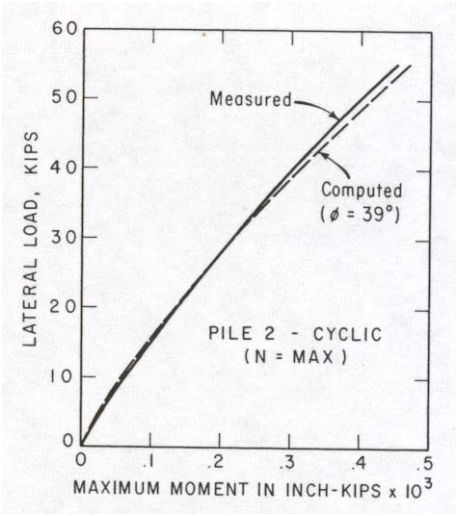

Fig. (3-17)
Comparison between Measured Results of Mustang Island Tests and Results Computed with Proposed Criteria; Pile 2 (N = max) Maximum Moment
(Reese, 1974)

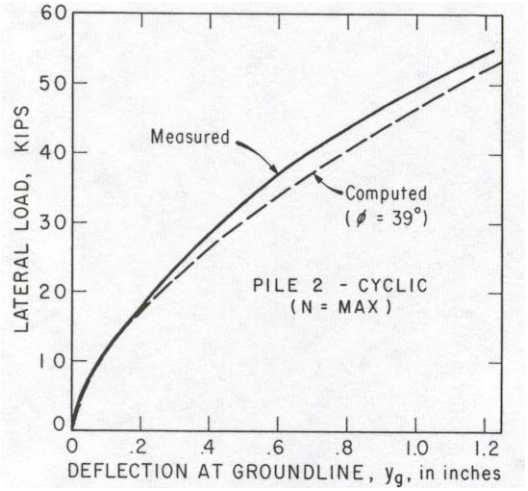

Fig. (3-18)
Comparison between Measured Results of Mustang Island Tests and Results Computed with Proposed Criteria; Pile 2 (N = max) Deflection at Ground Line
(Reese, 1974)

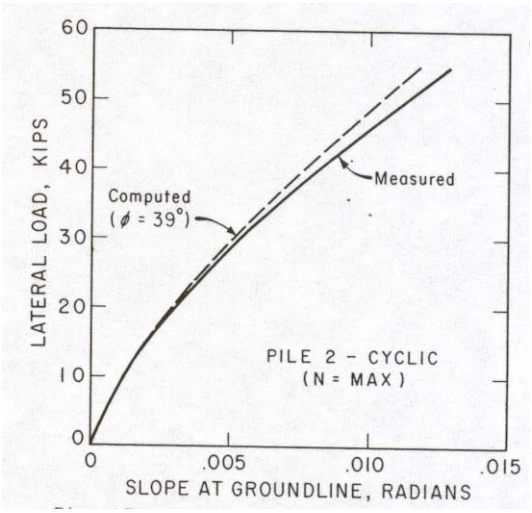

Fig. (3-19)
Comparison between Measured Results of Mustang Island Tests and Results Computed with Proposed Criteria; Pile 2 (N = max) Slope at Ground Line
(Reese, 1974)

load versus measured and computed values of slope at the ground line for the static tests is shown in Fig. (3-16). Similar plots for the cyclic loading are shown in Fig. (3-17), (3-18), and (3-19) (Reese, 1974).

In addition to the comparisons shown, measured and computed moment curves are shown for the maximum load in Fig. (3-20) for the static test on pile #1, and in Fig. (3-21) for the cyclic test on pile #2. The agreement between the measured and computed values in all cases are acceptable, indicating that Reese's recommendations for the p-y curves in sand are valid at least for the Mustang Island test. All the known parameters, which influence the problem, are included in these recommendations, allowing these recommendations to be applied to the analysis of any laterally loaded pile in sand (Reese, 1974).

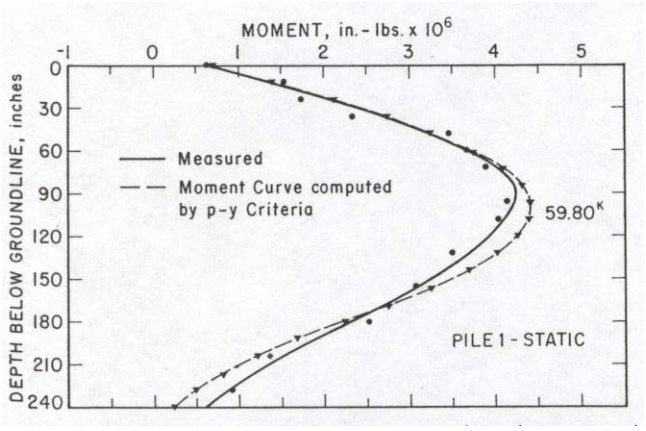

Fig. (3-20)
Comparison between Measured Maximum Moment of Mustang Island Tests and Results Computed with Proposed Criteria; Pile 1
(Reese, 1974)

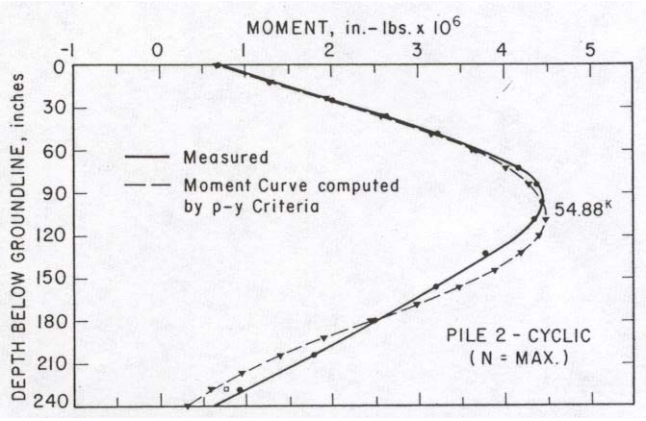

Fig. (3-21)
Comparison between Measured Maximum Moment of Mustang Island Tests and Results Computed with Proposed Criteria; Pile 2 (N = max)
(Reese, 1974)

b. Soft Clay Deposits

Fig. (3-22) shows a family of p-y curves for short-term static loading conditions, which had been developed according to the data and conditions of the Sabine test, performed by Matlock. The ultimate resistance p_u for the 432-inch depth is based on $N_p = 9$. All depths greater than 120 inches are found to have x_r values less than the depth considered. The ultimate resistance values for all shallower depths were determined using eqn. (3-18). From laboratory stress-strain data, a value of 0.007 was selected for the strain ε_{50}, or ε_c as shown in the figure. The value of y_c is therefore 0.223 inches as indicated in the figure. The pre-plastic portion of each p-y curve follows the prescribed cubic parabola form (Matlock, 1970).

Matlock used a computer program to make repeated trial and error adjustments until compatibility was achieved. The resulting solution and comparison with typical field

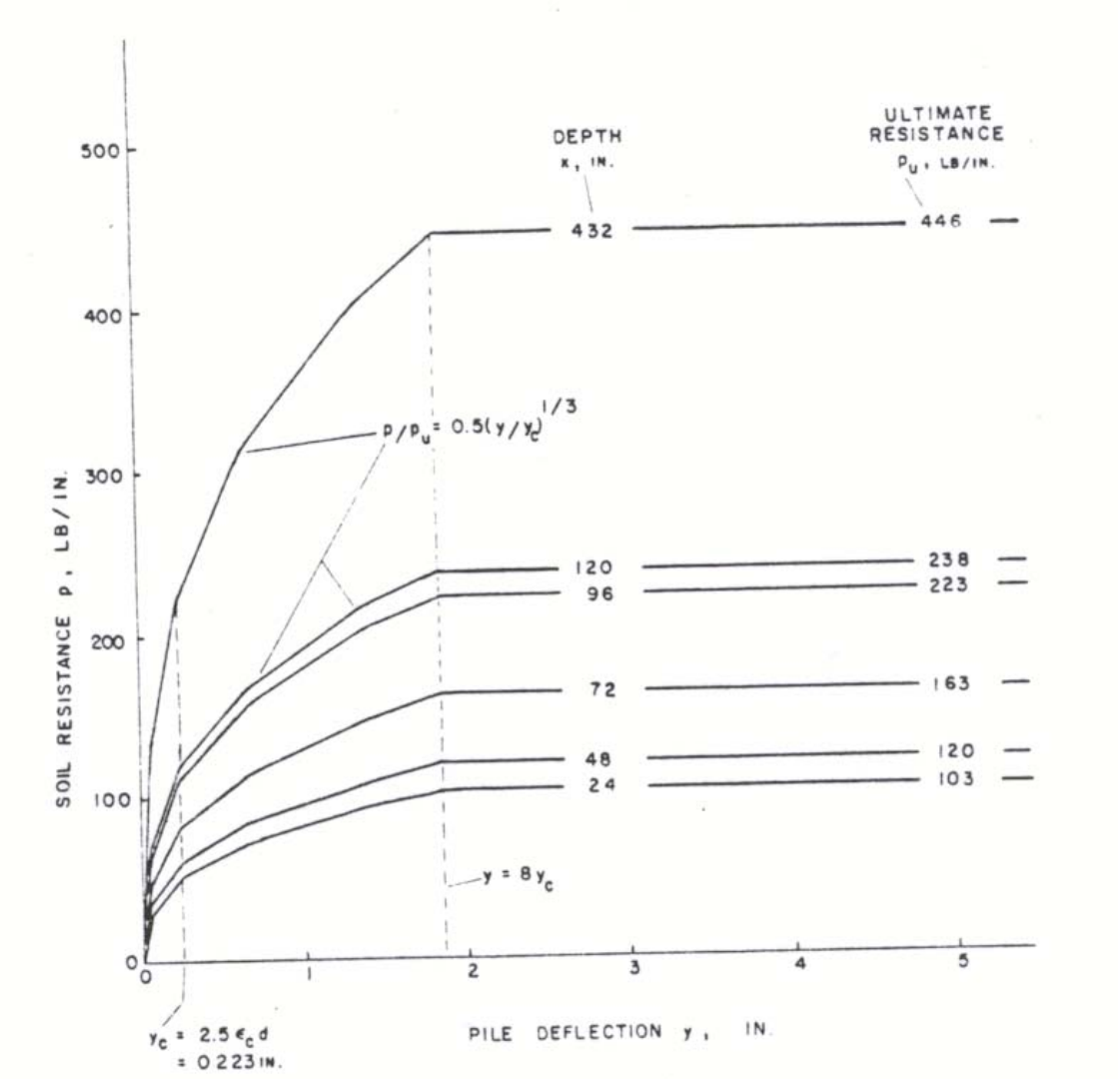

Fig. (3-22)
Predicted Family of p-y Curves for Sabine Clay for Short-term Static Loading
(Matlock, 1970)

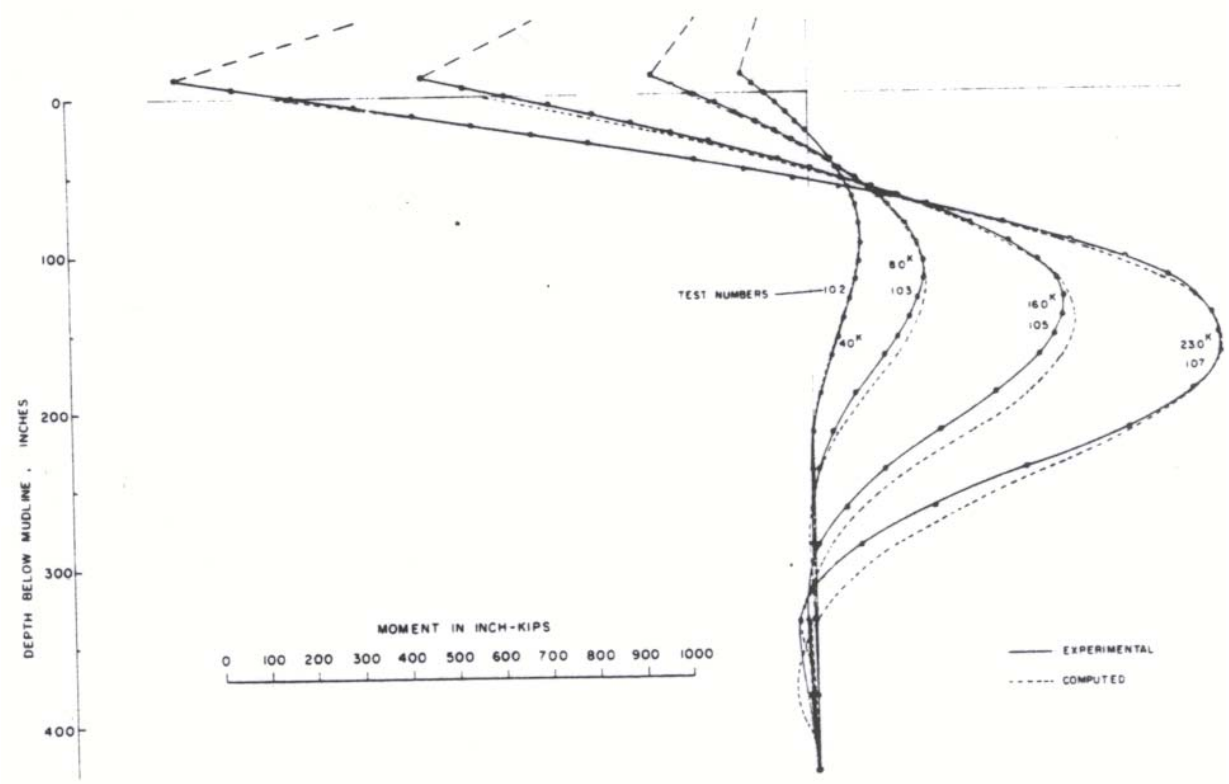

Fig. (3-23)
Predicted Bending Moments for Sabine Restrained-head Static Loadings,
Compared with Experimental Results
(Matlock, 1970)

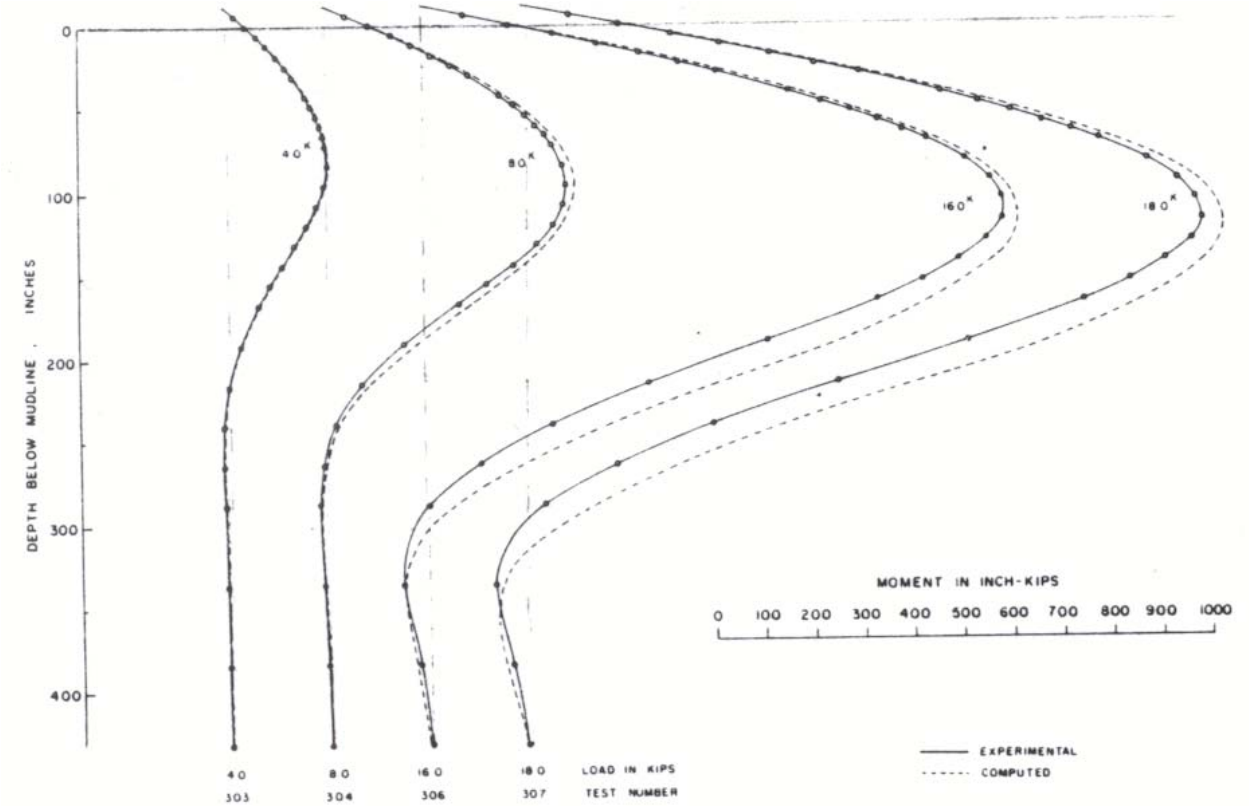

Fig. (3-24)
Predicted Bending Moments for Sabine Free-head Static Loadings, Compared with Experimental Results
(Matlock, 1970)

results are shown in Figs. (3-23) and (3-24). The figures indicate a satisfactory correlation. For the Lake Austin tests, an average value of 0.012 for ε_c was estimated from the soil stress- strain curves. The result with the ultimate resistance predicted according to eqn. (3-18) and with the vertical restraint factor J equal to 0.5, produced slightly unconservative results as shown in Fig. (3-25). This appears to be corrected by

changing J to 0.25 as shown by the second set of curves in the figure (Matlock, 1970).

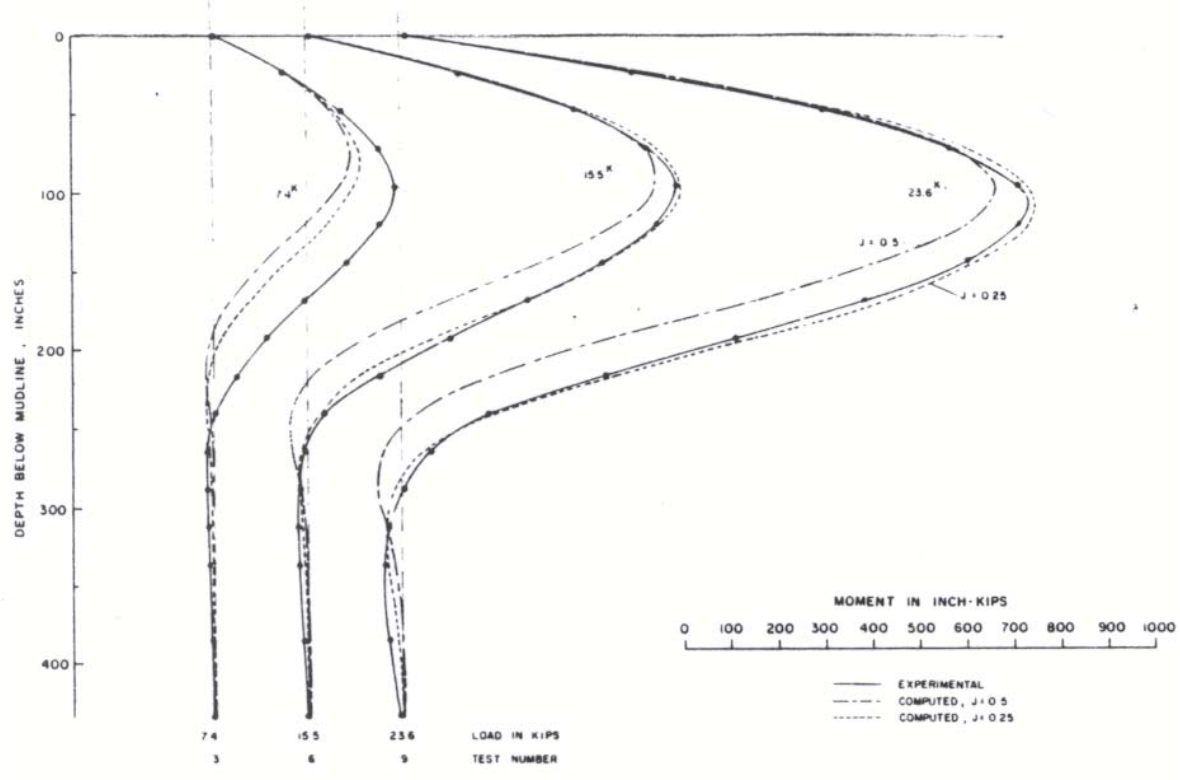

Fig. (3-25)
Comparison of Computed and Experimental Results for Lake Austin Free-head Static Tests
(Matlock, 1970)

For the cyclic loading tests, the method described in Fig. (3-12) is used to develop the p-y curves for the Sabine test conditions shown in Fig. (3-26). Comparisons are shown in Figs. (3-27) and (3-28) for the restrained head cyclic loadings and the free-head cyclic loadings, respectively. Agreement between computed and experimental results is generally good, and since these satisfactory results are obtained over a considerable range

of loadings and for two different restraint conditions gives encouragement that the correlation is a satisfactory one for similar types of clay (Matlock, 1970).

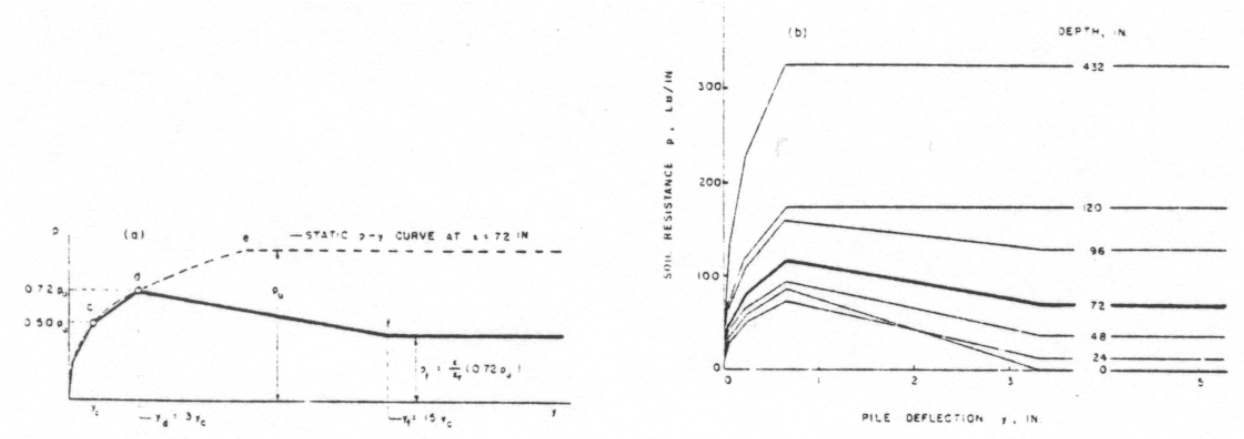

Fig. (3-26)
Predicted Cyclic p-y Curves for Sabine Clay and 12.75-inch Dia. Test Pile, based on Static p-y Curves of (a) Typical example, (b) Complete family of Curves (Matlock, 1970)

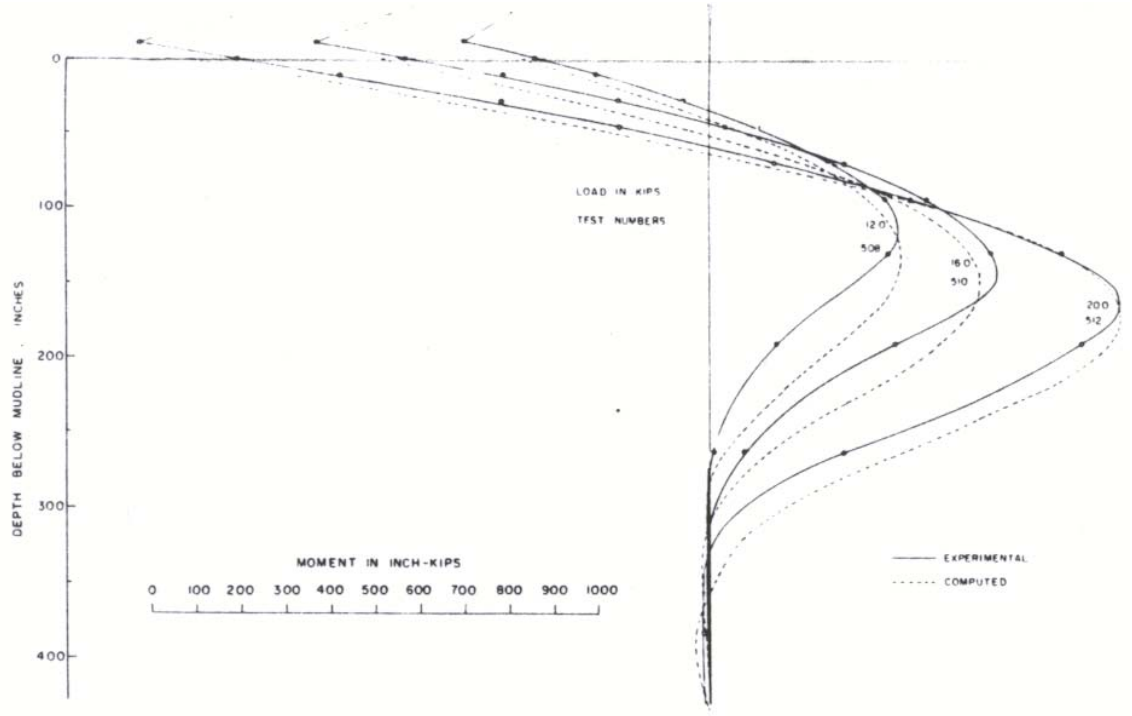

Fig. (3-27)
Comparison of Computed and Experimental Bending Moments for Sabine Restrained-head Cyclic Loadings
(Matlock, 1970)

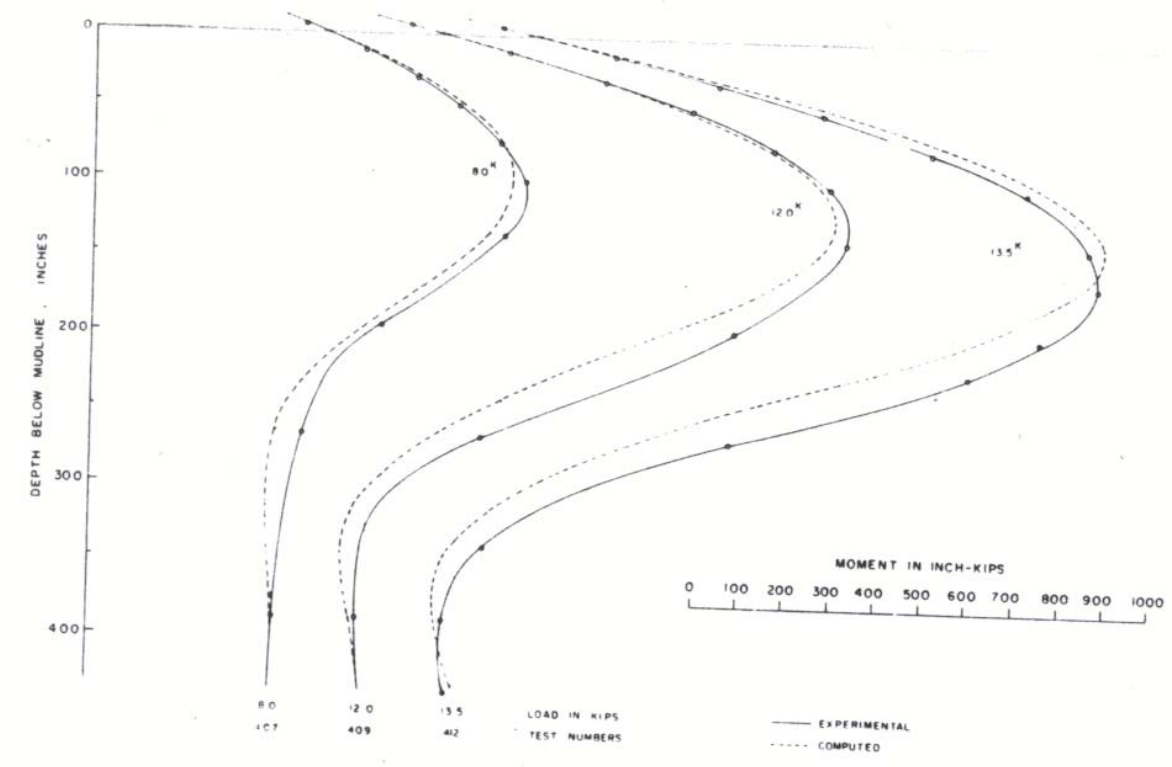

Fig. (3-28)
Comparison of Computed and Experimental Bending Moments for Sabine Free-head Cyclic Loadings
(Matlock, 1970)

At the Lake Austin site where the clay was jointed and fissured, the shear deformation and slip was highly concentrated along planes of weakness. Accordingly, it would be reasonable that cyclic deterioration would begin at considerably smaller pile deflections and that deterioration would be relatively more significant as deflections increase. Computed and experimental results are compared for three of the Lake Austin loadings in Fig. (3-29). To reach the degree of agreement that is shown, it was necessary for Matlock to modify the p-y construction procedure from that used for the Sabine

correlation. The deflection y_d was taken to equal $0.5y_c$ instead of $3y_c$ and the deflection

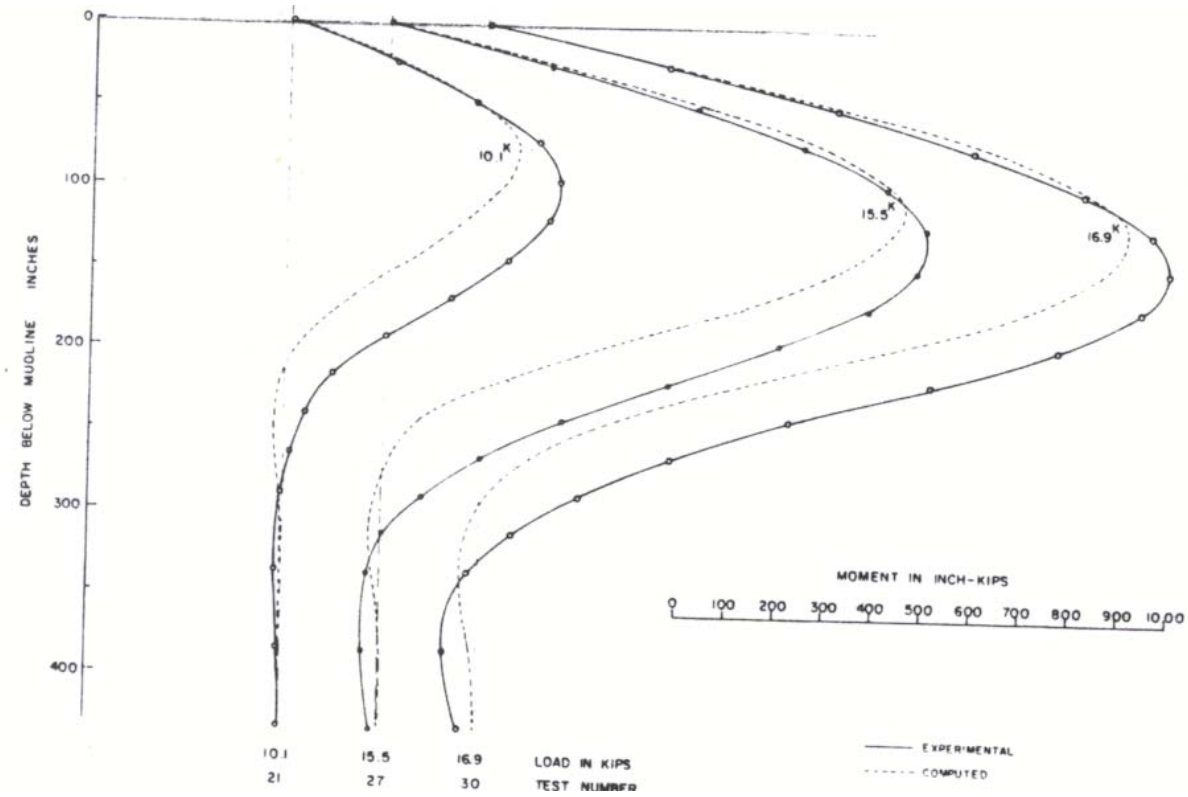

Fig. (3-29)
Comparison of Computed and Experimental Bending Moments for Lake Austin Cyclic Loadings, based on p-y Curves Adjusted for Jointed Clay
(Matlock, 1970)

y_f was taken to equal $10y_c$ instead of $15y_c$. Thus, the method for predicting minimum cyclic p-y curves is believed to be a satisfactory correlation for homogeneous marine clays. A more conservative version would be needed for jointed or fissured clays (Matlock, 1970).

For piles under reloading, a special set of p-y curves has been constructed and shown in Fig. (3-13). The curves are based on the predicted cyclic curves previously

shown for the Sabine clay in Fig. (3-26). The curves are intended to represent the modifications caused by prior free-head cyclic loading to 13.5 kips. As an example, point A in Fig. (3-13a) is established along the cyclic loading p-y curve according to the deflection at that depth which was previously computed for the 13.5 kip loading. The original cyclic curve is considered to be obliterated at all smaller deflections. Rebound and subsequent reloading are assumed to occur along line AB, which is parallel to a secant through point C. For deflections less than that at point B, a zero resistance is assumed. The curves for other depths were determined in a similar manner. No change was made for the curve at the 432-inch depth since the prior deflection did not exceed the value y_d required for cyclic deterioration (Matlock, 1970).

Static reloading after cyclic loading was performed during the Sabine tests and the results are available for comparison with computed behavior. Fig. (3-30) shows the bending moment curve computed with a lateral load of 8 kips and using the family of p-y curves of Fig. (3-13). The agreement with the corresponding experimental curve was seen to be very good (Matlock, 1970).

To illustrate the significant changes which are caused, an experimental curve from the initial cyclic loading to 8 kips is shown. The bending stresses for an 8 kip lateral load are almost doubled because of the intervening loading to 13.5 kips (Matlock, 1970).

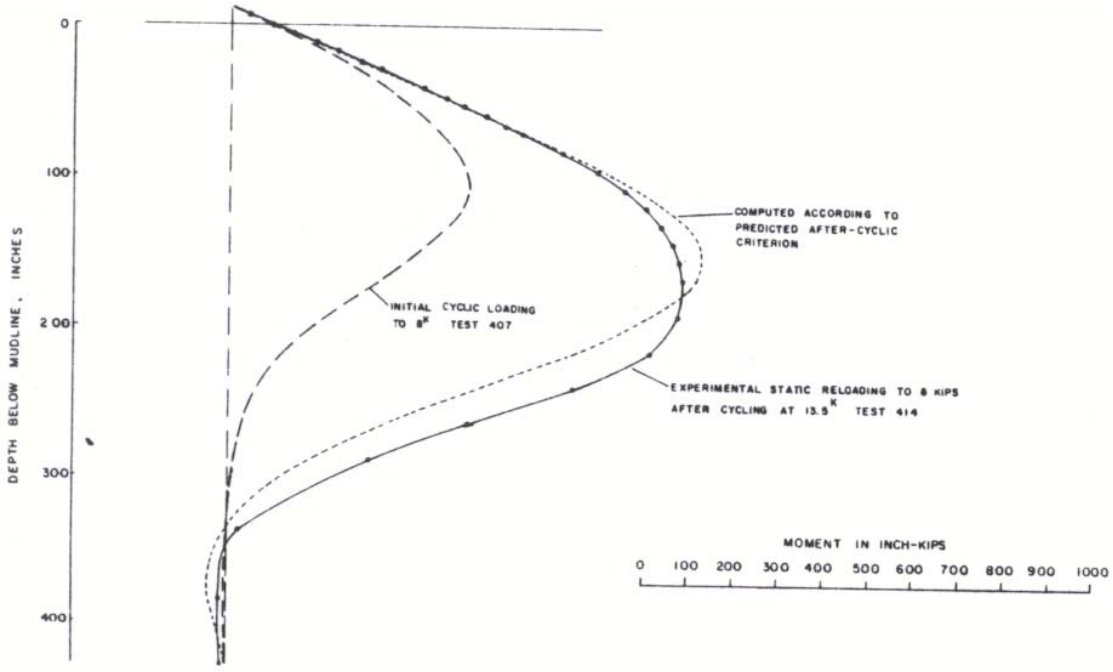

Fig. (3-30)
Comparison Between Experimental and Computed Results for Reloading to 8 kips After Prior Cycling with a 13.5-kip Lateral Load
(Matlock, 1970)

c. Stiff Clay Deposits

The proposed predictions for the p-y curve for stiff clay is based on a small amount of experimental data; therefore, the method should be used with great care until additional data allows the method to be validated.

Correlation between computed and measured values of deflection and moment, for the lateral loading test of the drilled shaft mentioned previously, was good. Table 6 and Fig. (3-31) show the comparison.

TABLE 6

Comparison of Computed and Measured Values of Top Deflection and Max Moment
(Reese, 1975)

Load, in Tons (1)	Cycle (2)	Top Deflection, in inches		Maximum Moment, in inch-pounds × 10^6	
		Measured (3)	Computed (4)	Measured (5)	Computed (6)
10	1	0.020	0.027	0.583	0.539
10	10	0.020	0.037	0.580	0.595
20	1	0.090	0.114	1.33	1.62
20	10	0.118	0.139	1.43	1.71
30	1	0.254	0.292	2.39	2.81
30	10	0.358	0.368	2.65	3.11
30	20	0.390	0.406	2.77	3.27
40	1	0.586	0.540	3.88	4.04
40	10	0.794	0.668	4.35	4.44
40	20	0.870	0.748	4.47	4.72
50	1	1.16	0.875	5.55	5.53
50	10	1.43	1.05	6.04	5.98
50	20	1.56	1.14	6.23	6.23

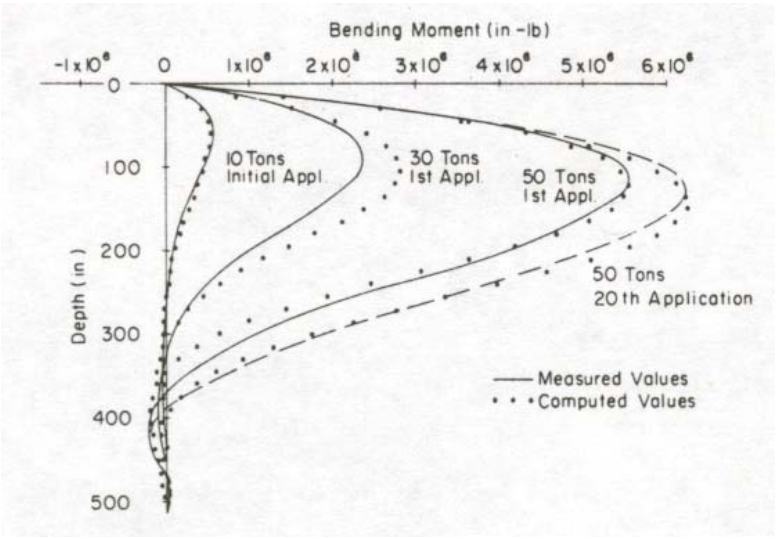

Fig. (3-31)
Computed and Measured Values of Bending Moment vs. Depth for Loading in a Stiff Clay Foundation
(Reese, 1975)

IV. DETERMINATION OF SOIL MODULUS

The determination of the soil modulus with sufficient accuracy helps in reaching a realistic result for the problem of laterally loaded piles. The soil modulus has been the subject of many researches and many recommendations have been presented.

The determination of the soil modulus, also known as the modulus of elasticity of the soil or modulus of subgrade (soil) reaction, is generally carried out by either direct means or indirect means. One direct mean would consist of having a full-scale lateral load test on a pile. This is the most direct mean but it is the most time consuming and expensive. It would only be feasible for large-scale projects.

Other direct means would be the results of in-situ tests such as a plate-loading test or a pressuremeter test. Recent advances have been made in the determination of the soil modulus by using an in-situ testing instrument known as a flat dilatometer. Each of these in-situ tests is relatively inexpensive.

Indirect means to determine the soil modulus would include empirical correlation with other soil properties, mainly the stress-strain relationship, which is most relevant.

Terzaghi, in 1955, considered that for clays, the coefficient of subgrade reaction is essentially the same both horizontally and vertically, and is independent of depth. He suggested the following conservative relationship for the coefficient of subgrade reaction, k_h for laterally loaded foundations:

$$k_h = \left(\frac{1}{1.5d}\right)\left(\bar{k}_{s1}\right) \tag{4-1}$$

where

$\bar{k}_{s1}$ = constant of vertical subgrade reaction for a square plate, 1 ft. wide

d = width or diameter of the load area in feet

Table 7 shows Terzaghi's values of $\bar{k}_{s1}$. Adaptation of the coefficient of subgrade reaction to fit the soil modulus, E_s, leads to

$$E_s = k_h d \tag{4-2}$$

E_s is by definition the ratio between the pressure at any point of the surface of contact and the pile deflection produced by the load application at that point,

$$p = -E_s y \tag{4-3}$$

The value of E_s would be constant only if the soil were a perfectly elastic material. However, it is known that E_s generally increases with depth, and at a given depth it becomes smaller as the deflection increases.

Terzaghi also showed that for a cohesionless soil, the modulus of subgrade reaction would increase approximately linearly with depth and decrease linearly with the width d of the load area, as expressed in Eqn. (2-36).

Broms related k_h for clays to the secant modulus E_{50} at half the ultimate stress in an unconsolidated-undrained test as

$$k_h = 1.67 \frac{E_{50}}{d} \tag{4-4}$$

Calculation of the modulus of subgrade reaction by these methods is only approximate and can be used only as an estimate. However, if it is required to determine the lateral deflection accurately, a field test should be performed.

TABLE 7

Terzaghi's Values of $\bar{k}_{s1}$

TERZAGHI'S THEORY ($\bar{k}_{s1}$=48q_u)			
	SOFT/MED	STIFF	VERY STIFF
q_u (psf)	200-2000	2000-4000	4000-8000
$\bar{k}_{s1}$ (pci)	5.6-56	56-111	111-222

V. COMPARISON OF THE VARIABLES OF LATERALLY LOADED FOUNDATIONS

The problem of the laterally loaded foundation involves many variables. These variables include but are certainly not limited to the unit weight of the soil, the internal angle of friction of the soil, the soil modulus, the diameter of the pile, the length of the pile, and of course the load itself. Although it is well known that many of these properties are not independent of each other, in order to study the effect of altering each variable, the variables must be treated as independent parameters. Due to the complex nature of the laterally loaded foundation, a computer program such as FB-Pier or L-Pile can be used to aid in the effort.

The appendix of this thesis presents the results of several scenarios in which one of the variables is allowed to vary, while the others remain constant. The computer program FB-Pier is used for these analyses. The first analysis presents the alteration of the p-y curve in sand as each parameter is varied. The next analysis presents an example problem in which a pile is laterally loaded in a uniform sand foundation and as each parameter is allowed to vary, the effects on the pile deflection and bending moment are observed. Finally, an example problem is presented in which a pile is laterally loaded in a soft clay foundation and as each parameter is allowed to vary, the effects on the pile deflection and bending moment are observed.

From the analysis of the impacts of the variables on the p-y curve in sand, several

conclusions can be made. By allowing the pile diameter only to vary, it is evident that the initial portion of the p-y curve is independent of the pile diameter. Also evident is that the nonlinear portion of the p-y curve will have a larger soil resistance when the pile diameter increases at a shallow depth. But at a certain greater depth, the nonlinear portion of the p-y curve will decrease in soil resistance as pile diameter increases. Allowing the soil modulus only to vary, it is apparent that this variable has little effect on Reese's Sand Model.

The next analysis compares the pile deflection and bending moment of the pile while varying each parameter independently. The scenario included a single free-headed pile of 0.5m diameter subjected to a lateral load at the ground surface. The pile was driven in uniform sand with the ground water located at the ground surface. The soil parameters, internal angle of friction, unit weight, and subgrade modulus, were each varied independently, while the other parameters remained constant. Reese's Sand Model was used in this analysis.

From the analysis, it is apparent that varying the subgrade modulus alone causes only minor, if any, changes in the pile deflection and bending moment of the pile. Also, changing the unit weight of the sand does not appear to have a significant effect on the results. The internal angle of friction of the sand proves to have a significant influence on the pile deflection and the bending moment of the pile.

It is known that these soil parameters are not independent of each other. Therefore, an analysis was made comparing the effects of a pile driven in loose sand, and

medium sand, and dense sand. The parameters of these materials were assumed based on values accepted in literature. It can be seen from this analysis, and in comparison with the previous analyses where the parameters were allowed to vary independently, that the effects of each parameter is uncertain when considered alone, and that these parameters are correlated with each other. It is evident that the pile deflection and the bending moment of the pile is interdependent on each of these soil properties.

The final analysis shown in the appendix of this thesis makes use of Matlock's Soft Clay Below the Water Table Model. This analysis is similar in that it also compares the pile deflection and bending moment of the pile while varying each parameter independently. The scenario included a single free-headed pile of 12in diameter subjected to a lateral load at the ground surface. The pile was driven in a soft clay foundation with the ground water located at the ground surface. The soil and pile parameters, shear strength, soil strain, pile diameter, and pile length, were each varied independently, while the other parameters remained constant. The final comparison shows the load condition varying, from a static load to a cyclic load.

From the analyses in which the pile properties are allowed to vary, it is evident that the pile length had very little effect on the pile deflection and the moment distribution. It can be seen that any part of the pile below a depth of 30ft is not contributing to the moment capacity. In contrast, the pile diameter is shown to have a great influence on the pile deflection and the moment distribution. It is seen that as the diameter increases, the deflection decreases and the moment distribution increases. This

is attributed to an increase in pile stiffness and also an increase in the area of resisting soil.

From the analysis allowing the shear strength to vary alone, it is evident that the shear strength has a great influence on the deflection. As the shear strength increases, deflection decreases. This is because as the soil gets stronger, its resistance to movement increases. Also note that the pile has some deflection all the way down to approx. 30 ft of the total 42 ft long pile for all shear strength values. This is because the depth of deflection is more dependent on pile diameter than shear strength. It can also be seen that as the shear strength increases, the maximum moment decreases and moves closer to the surface. The moment increases as the shear strength decreases because the pile is forced to take on more of the moment, as the soil gets weaker.

In the analysis in which the soil strain is allowed to vary independently, it is apparent that as the ε_{50} value increases, the deflection increases. This is because the ε_{50} is the strain at the midway point of the initial portion of the p-y curve; therefore as this value increases, the more deflection the pile will experience for a given load. Also evident is that as the ε_{50} value increases, the maximum moment, and the depth at which it occurs, will also increase. This is because the moment arm will increase as the strain in the soil increases because of the greater displacement in the weaker soil.

It the final comparison in which the load condition is varied, it is evident that the deflection for the cyclic loading case is about two times that of the static loading case. This is because of a gap produced during the cycled load. Due to the nature of Matlock's

soft clay model, the clay tends to stay in a deformed shape as the pile is cycled in the other direction. Therefore as the pile completes one cycle it will have to move through the gap before it is pushed against the clay again, causing the pile to gradually push the clay out of the way and allow the pile to deflect more. It is also evident that the moment produced during the cycled load is approximately twice as much as the moment produced during the static loading. This is because the moment arm in the cycled case is larger than the static case due to the gap created.

VI. COMPARISON BETWEEN P-Y CURVES AND BROMS' APPROACH

Many different methods of analysis have been proposed to solve the problem of a laterally loaded pile (or drilled shaft), where the problem can be generally defined as computing pile deflections and bending moments as a function of depth below the ground surface. Some methods are based on the theory of subgrade reaction and on simplifying assumptions such as assuming a variation of the subgrade modulus with depth and that soil is linearly elastic (Broms, 1964). These assumptions reduce the difficulty in obtaining a solution to the problem, but according to Reese (1979), errors of an unknown magnitude are introduced into the solution. A comparison is made here between the results presented earlier in the p-y curve chapter, where actual measured responses of tested piles are compared to those calculated using nonlinear variations, and those yielding from the use of Broms' assumptions.

Reese (1974) presented the results of a series of field tests that were conducted to develop criteria for the design of laterally loaded piles in sand. Two 24-inch diameter piles with 3/8 inch wall thickness and of A-53 grade B seamless steel, embedded 69 feet, were instrumented with strain gages for measuring bending moments and deflection at Mustang Island, Texas, and a complete description of it was presented by Cox and Reese (1974).

Laboratory tests were run on samples from two borings, and soil properties determined from these tests included grain size distribution, natural densities, and minimum and maximum densities. The soil was classified as medium dense sand in the top 20-foot layer, to dense sand in the rest of the formations, with an angle of internal friction, $\phi = 39°$ and a submerged unit weight of $\gamma = 66 \, lbs/ft^3$. The results for the ground line deflection are shown in Fig. (3-15) and Fig. (3-18), and compared to those computed with the proposed criteria of the p-y curve.

Table 2 gives the recommended value k_h for dense sand as $125 \, lbs/in^3$. Using this value of k_h in Eqn. (2-30a), and varying H from 10 kips to 60 kips, the comparison could be made between the p-y approach and Broms' approach. Table 8 shows this comparison. As can be seen from this table, Broms' approach gives close results for the elastic range loads. As we move to the inelastic range, errors would exceed 50%.

TABLE 8

Comparison of Ground Deflection, Using p-y and Broms' Approaches For a Sand Foundation

Horizontal Load, H (kips)	**Measured Deflection (Fig. 3-15), in**	**Computed Deflection (Fig. 3-15), in**	**Computed Deflection Broms' Approach, in**
60	1.19	1.23	0.48
50	0.89	0.93	0.40
40	0.62	0.63	0.32
30	0.40	0.40	0.24
20	0.21	0.21	0.16
10	0.07	0.07	0.08

In another test site in Houston, Texas, a drilled shaft with a diameter of 30-inches, drilled to a depth of 42 feet below the ground surface, was tested (Reese, 1975). The soil profile at the site was classified as stiff to very stiff red clay. A more detailed description of the site and instrumentation was given earlier in the section titled "P-Y Curves in Stiff Clay." The average undrained shear strength (cohesion) was found to be 1.1 tsf.

According to Reese (1979), a value of $1000 \, lbs/in^3$ for k_h is recommended for this type of clay. Calculation of the deflection using Eqn. (2-30a) would give 0.020

inches, and 0.100 inches, for a 10-ton and 50-ton loading, respectively. The measured deflection according to Table 6 gave 0.02 inches and 1.16 inches for these respective loadings. It is obvious from Table 9 that Broms' approach gave close results when the applied loading was in the range of the working load of 10 tons. As the load gets higher, results begin to conflict, especially in this type of material.

TABLE 9

Comparison of Ground Deflection, Using p-y and Broms' Approaches for a Stiff Clay Foundation

Horizontal Load, H (tons)	**Measured Deflection (Tab. 6), in**	**Computed Deflection (Tab. 6), in**	**Computed Deflection Broms' Approach, in**
50	1.16	0.875	0.100
40	0.586	0.540	0.080
30	0.254	0.292	0.060
20	0.090	0.114	0.040
10	0.020	0.027	0.020

VII. CONCLUSIONS AND RECOMMENDATIONS

The problem of a deep foundation subjected to a lateral loading involves the interaction of soil and structure. The solution to the problem usually requires the use of iterative techniques because soil response is a nonlinear function of the deflection of the foundation.

Some approximate predictions of the ultimate lateral capacity can be reached by logical and experienced assumptions of soil resistance and its distribution along the pile length. In most cases, a simplified solution of the problem, sufficiently accurate for all practical purposes, can be obtained by solving a differential equation of the fourth order.

Very often, ready-made solutions in the form of diagrams or formulas can be used to provide sufficiently accurate answers, within the "working load" range. Material constants appearing in these solutions can be determined from lateral load tests on actual piles. For some soils types, there are also established means of predicting these material constants from the laboratory or in situ measured deformation characteristics of soils.

Broms limited his method for calculating deflection to the working load range, which is normally considered to be 1/3 to 1/2 of the computed ultimate pile capacity. In the working load range, Broms assumed that the soil was linearly elastic. Even though cohesive soil is not linearly elastic in the working load range, Broms' assumption probably leads to only minor errors. However, Broms' method for cohesive soil is limited

because in many instances it is desirable to obtain the response of a pile for a full range of loads. Also, to simplify the analysis, Broms assumed that for cohesive soils, the subgrade modulus was constant with depth.

In sand soils the assumption of linearly varying soil modulus is useful in practice according to Reese and Matlock (1956), but the value of E_s will decrease substantially as the lateral load is increased. This might have contributed to the discrepancy between results when the load increased. Broms' method of solution is easy to use, and can produce a preliminary estimate of the ultimate collapse load or of the maximum bending moment for a pile in cohesionless soil. If a better estimate of the pile behavior is required, a computer program in conjunction with nonlinear soil resistance-deflection curves should be used, such as L-Pile or FB-Pier. The method of p-y curves can be improved as more information is gained on the behavior of full-scale piles under lateral loadings.

A valid solution to the problem of the laterally loaded deep foundation requires, as for other boundary-value problems, the satisfaction of the conditions of equilibrium and compatibility. It is important, however, to be able to accurately determine soil properties and predict soil response. As more knowledge is gained concerning the prediction of soil behavior, new knowledge can be incorporated into the analytical procedures.

VIII. BIBLIOGRAPHY

1. Alizadeh, M., and Davisson, M. T., 1970, "Lateral Load Tests on Piles-Arkansas River Project," J. Soils Mech. Found. Div, ASCE, Vol. 96, No. SM5, pp. 1583-1604.

2. Bowles, Joseph E., Foundation Analysis and Design, McGraw-Hill Book Co., 1968, p. 750.

3. Bowman, Elliott, R., "Investigation of the Lateral Resistance to Movement of a Plate in Cohesionless Soil," Unpublished Master's Degree Thesis, Austin, The University of Texas, January 1958.

4. Brinch-Hansen, J., "The Ultimate Resistance of Rigid Piles Against Transversal Forces," Bulletin No. 12, Danish Geotechnical Institute, Copenhagan, Denmarck 1961, pp. 5-9

5. Broms, B. B., "Lateral Resistance of Piles in Cohesionless Soils," J. Soils Mech. Found. Div, ASCE, Vol. 90, No. SM3, 1964.

6. Broms, B. B., "Design of Laterally Loaded Piles," J. Soils Mech. Found. Div, ASCE, Vol. 90, No. SM3, 1965.

7. Broms, B. B., "Lateral Resistance of Piles in Cohesive Soils," J. Soils Mech. Found. Div, ASCE, Vol. 90, No. SM2, 1964.

8. Cox, W. R., Reese, L. C., and Grubbs, B. R., "Field Testing of Laterally Loaded Piles in Sand," 6th Offshore Technical Conference," Houston, 1974.

9. Davisson, M. T., "Lateral Load Capacity of Piles," High. Res. Rec, No. 333, 1970, pp. 104-112.

10. Desai, C. S., and Christian, J. T., Numerical Methods in Geotechnical Engineering, McGraw-Hill Book Co., 1977, p. 783.

11. Fruco and Associates, "Pile Driving and Loading Tests: Lock and Dam No. 4, Arkansas River and Tributaries, Arkansas and Oklahoma," U.S. Army Corps of Engineers District, Little Rock, September 1964.

12. Garissino, A., Jamiolkowski, M., and Pasqualini, E., "Soil Modulus for Laterally Loaded Piles in Sands and N.C. Clays," 6th European Conference on Soil Mechanics & Foundation Engineering, Vienna, 1976.

13. Gill, H. L., "Lateral-Plate and Rigid-Pile Tests in Beach Sand," U.S. Naval Civil Engineering Laboratories, Rep. No. 310, California, 1964.

14. Glesser, S. M., "Lateral Load Tests on Vertical Fixed-Head and Free-Head Piles," Symposium on Lateral Pile Load Tests, ASTM Special Technical Publication 154, 1953, pp. 75-101.

15. Hetenyi, M., Beams on Elastic Foundation, University of Michigan Press, Ann Arbor, Michigan, 1942.

16. Lambe, T. W., and Whitman, R. V., Soil Mechanics, John Wiley & Sons, Inc., New York, 1969, p. 553.

17. Matlock, Hudson, and Ripperger, E. A., "Procedures and Instrumentation for Tests on a Laterally Loaded Pile," Proceedings of the Eighth Texas Conference on Soil Mechanics and Foundation Engineering, Special Publication No. 29, Bureau of Engineering Research, The University of Texas, Austin, Texas, 1956.

18. Matlock, H., and Ripperger, E. A., "Measurement of Soil Pressure on a Laterally Loaded Pile," Proc. ASTM, Vol. 58, 1958, pp. 1245-1259.

19. Matlock, H., "Correlation for Design of Laterally Loaded Piles in Soft Clay," 2nd Offshore Technology Conf., Houston, Texas, 1970.

20. Matlock, Hudson and Reese, L. C., "Generalized Solution for Laterally Loaded Piles," Transactions, ASCE, Vol. 127, Part 1, 1962, pp. 1220-1251.

21. McClelland, Bramlette and Focht, J. A., Jr., "Soil Modulus for Laterally Loaded Piles," Transactions, ASCE, Vol. 123, 1958, pp. 1071-1074.

22. Meyer, B. J., and Reese, L. C., "Analysis of Single Piles Under Lateral Loading," Federal Highway Administration, Austin, Texas, Dec. 1979.

23. Poulous, H. G., "Behavior of Laterally Loaded Piles: I-Single Piles," J. Soils Mech. Found. Div, ASCE, Vol. 97, No. SM5, May 1971.

24. Poulous, H. G., and Davis, E. H., Pile Foundation Analysis and Design, John Wiley and Sons, Inc., New York.

25. Prospect, Soil-Structure Interaction Analysis, Course Notes, U.S. Army Engineer, Waterways Experiment Station, March 2003.

26. Reese, L. C., and Welch, Robert C., "Lateral Loading of Deep Foundation in Stiff Clay," J. Geotech. Eng. Div. ASCE, Vol. 101, No. 677, July 1975.

27. Reese, L. C., Cox, W. R., "Soil Behavior from Analysis of Tests of Uninstrumented Piles Under Lateral Loading," Symposium on Performance of Deep Foundations, ASTM Special Technical Publication 444, June 1968, pp. 160-176.

28. Reese, L. C., Cox, W. R., and Koop, Francis D., "Analysis of Laterally Loaded Piles in Sand," 6th Offshore Technology Conf., Houston, Texas, 1974.

29. Reese, L. C., Cooley, L. A., and Radhakrishnan, N., "Laterally Loaded Piles and Computer Program COM624G," U.S. Army Engineer, Waterways Experiment Station, April 1984.

30. Skempton, A. W., "The Bearing Capacity of Clays," Building Research Congress, Division 1, Part 3, London, 1951, pp. 180-189.

31. Terzaghi, Karl, "Evaluation of Coefficients of Subgrade Reaction," Geotechnique, Vol. 5, December 1955, pp. 297-326.

32. Terzaghi, Karl, and Peck, Ralph B., Soil Mechanics in Engineering Practice, John Wiley and Sons, Inc., New York, 1948.

33. Valsangkar, A. J., Rao Kamenswara, N. S. V., and Basudher, P. K., "Generalized Solutions of axially and Laterally Loaded Piles in Elasto-plastic Soils," Soils and Foundations, Japanese Society of Soil Mech. And Found. Eng., Vol. 13, No. 4, Dec. 1973.

34. Yegian, M., and Wright, S. G., "Lateral Soil Resistance-Displacement Relationship for Pile Foundations in Soft Clays," 5th Offshore Technology Conf., Houston, Texas, 1973.

IX. APPENDIX

Impact of Variables

Situation:

Submerged medium dense sand

γ' = Varied

$\phi = 35^{\circ}$

k = 16300 kN/ m^3

Pile diameter = 1.0m

Depth = 2.0m

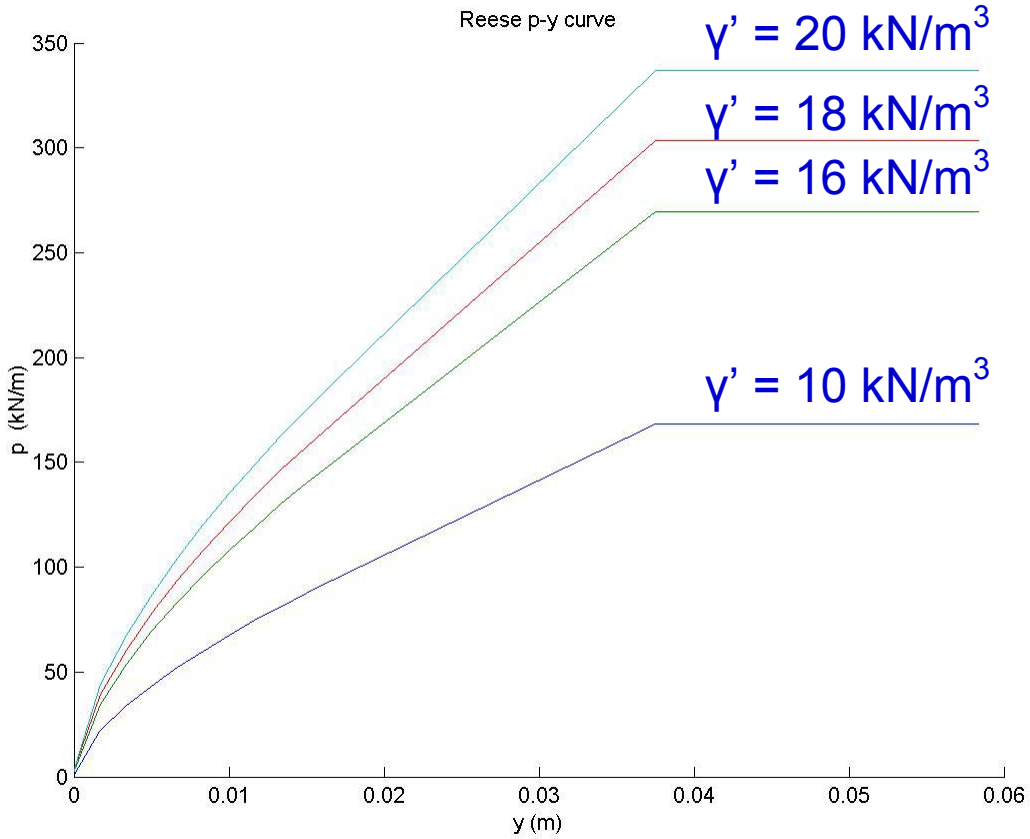

Impact of Variables

Situation:

Submerged medium dense sand

$\gamma' = 9.8$ kN/ m^3

ϕ = Varied

k = 16300 kN/ m^3

Pile diameter = 1.0m

Depth = 2.0m

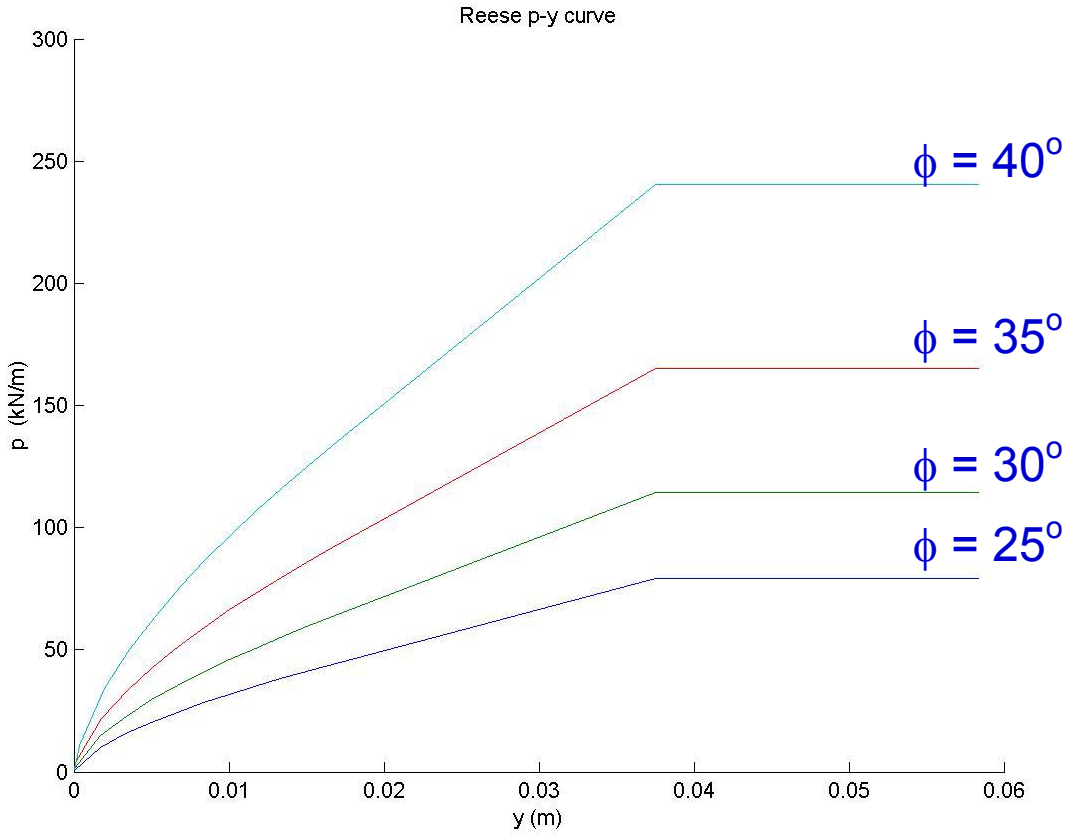

Impact of Variables

Situation:

Submerged medium dense sand

$\gamma' = 9.8$ kN/ m^3

$\phi = 35^{\circ}$

k = Varied

Pile diameter = 1.0m

Depth = 2.0m

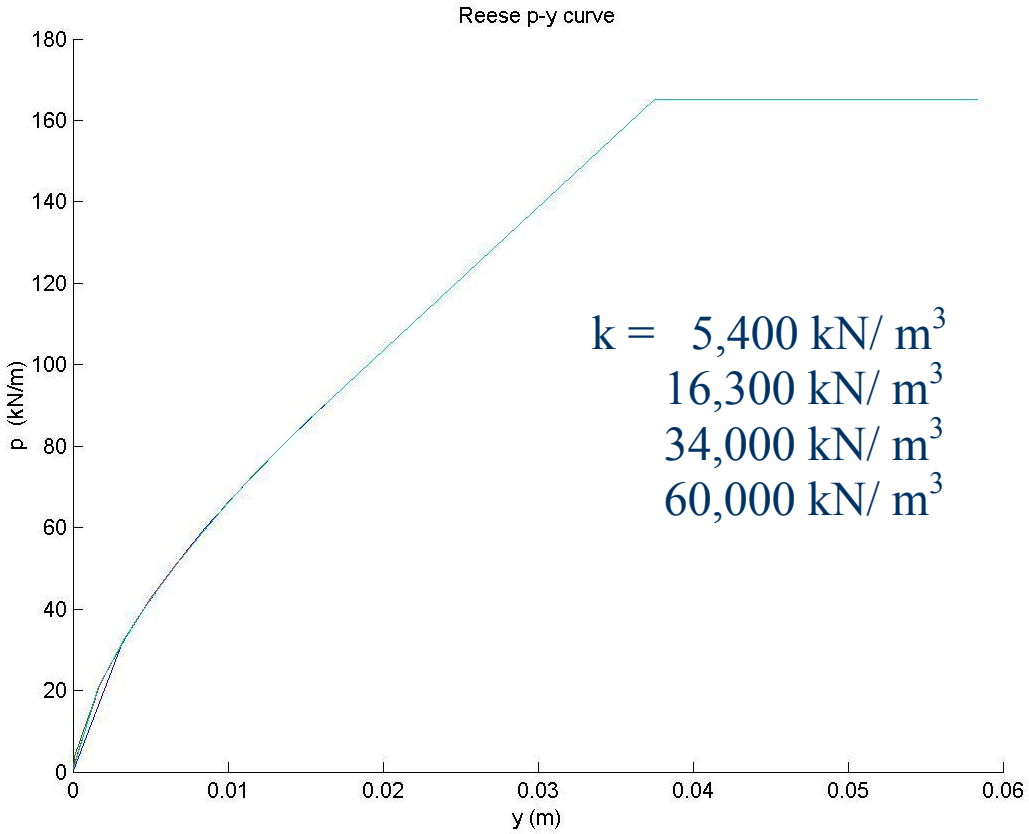

Impact of Variables

Situation:

Submerged medium dense sand

$\gamma' = 9.8$ kN/ m^3

$\phi = 35^{\circ}$

k = 16300 kN/ m^3

Pile diameter = Varied

Depth = 2.0m

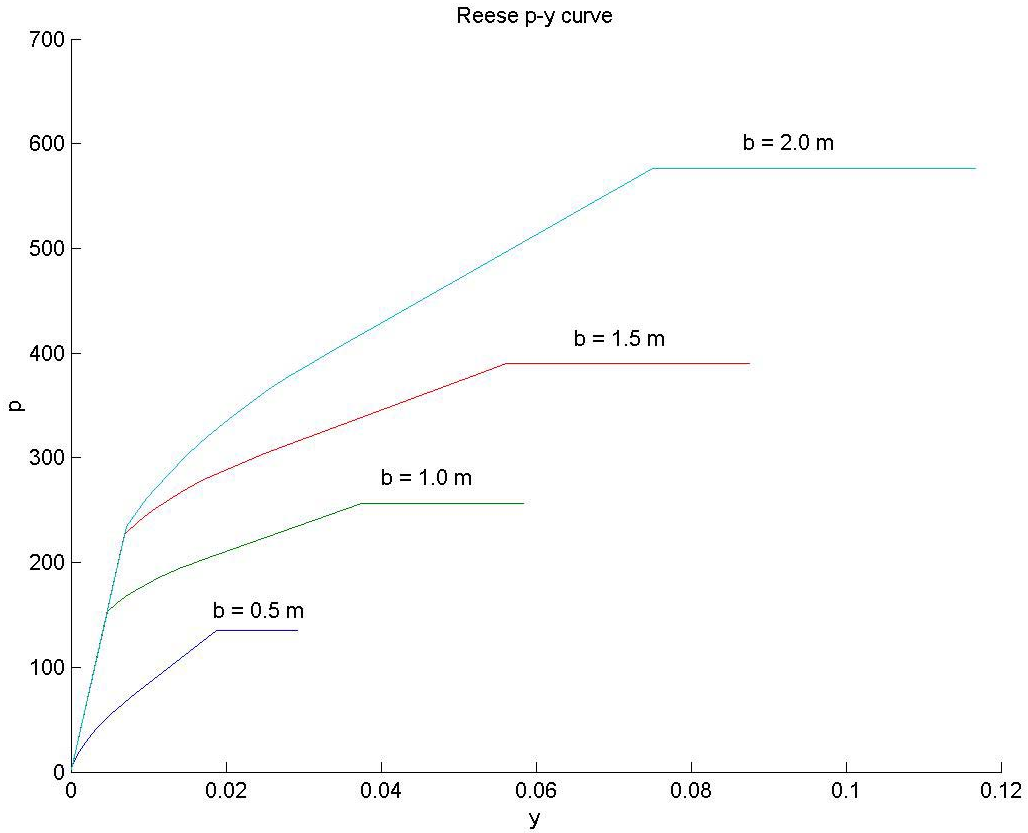

Impact of Variables

Situation:

Submerged medium dense sand

$\gamma' = 9.8$ kN/ m^3

$\phi = 35^{\circ}$

k = 16300 kN/ m^3

Pile diameter = Varied

Depth = 12.0m

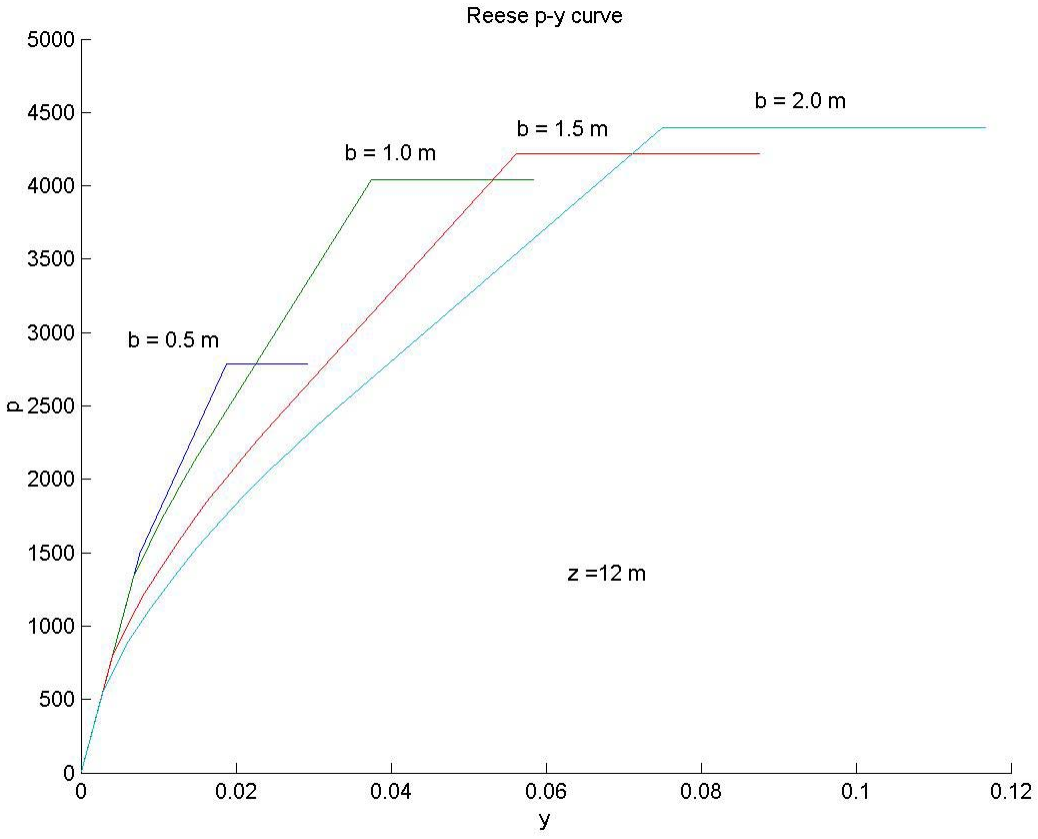

Impact of Variables

Situation:

Submerged medium dense sand

$\gamma' = 9.8$ kN/ m^3

$\phi = 35^{\circ}$

k = 16300 kN/ m^3

Pile diameter = 1.0m

Depth = Varied

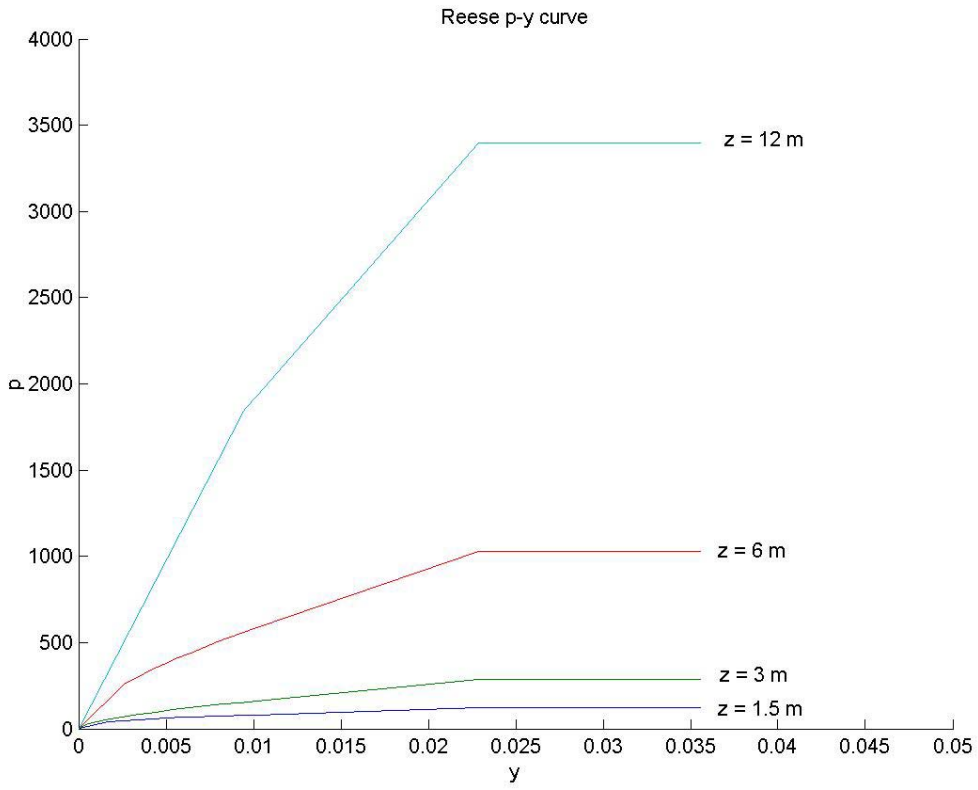

Example Problem in FB-Pier

Problem overview

- Single free head pile (Diameter = 0.5m) subjected a lateral load at the ground surface
- Uniform sand
- Water table at the ground surface

Objective

To study the effects of the soil properties (internal friction angle ϕ, subgrade modulus k, and unit weight γ) on the behavior of Reese's Sand Model

Comparison of Pile Deflection and Bending Moments with Varying Friction Angle

- Change the internal friction angle ϕ alone
- Subgrade modulus k = 16.3 MN/m^3
- Unit weight γ = 18.7 kN/m^3

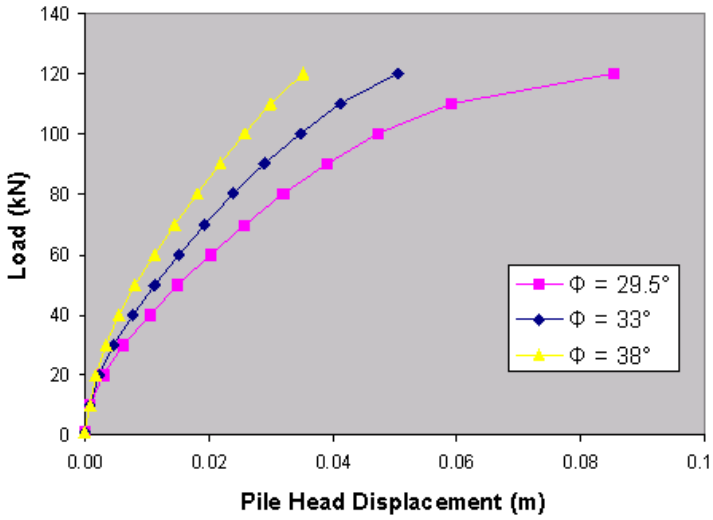

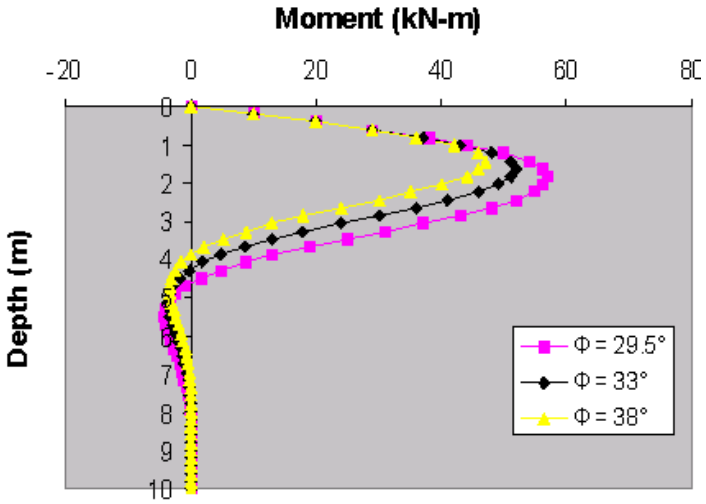

Comparison of Pile Deflection and Bending Moments with Varying Subgrade Modulus

- Change subgrade modulus k alone
- Internal friction angle $\varphi = 33°$
- Unit weight $\gamma = 18.7\ kN/m^3$

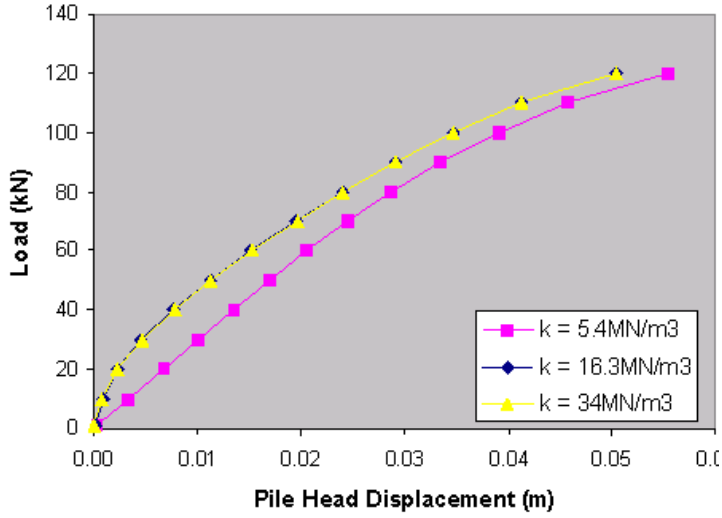

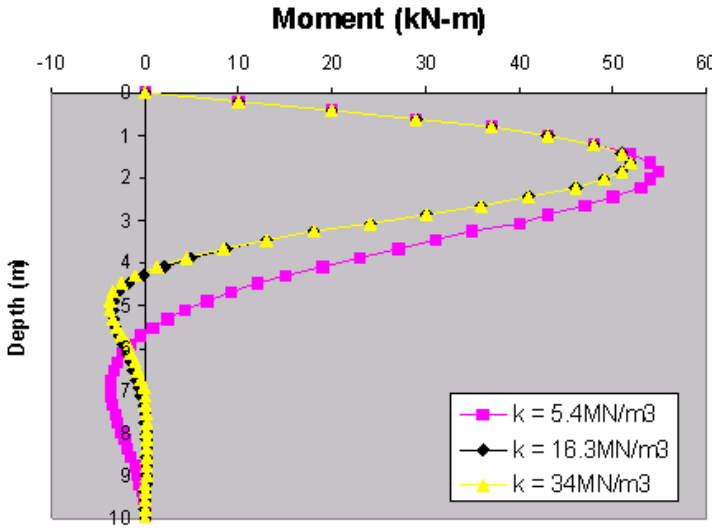

Comparison of Pile Deflection and Bending Moments with Varying Unit Weight

- Change unit weight γ alone
- Internal friction angle ϕ = 33°
- Subgrade modulus k = 16.3 MN/m³

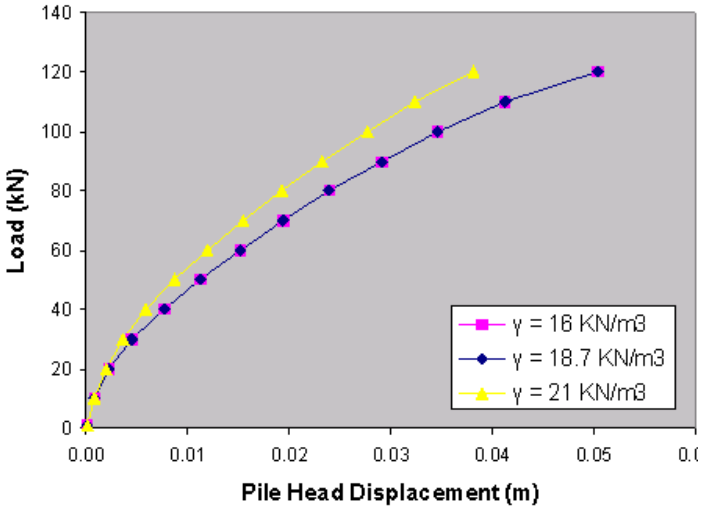

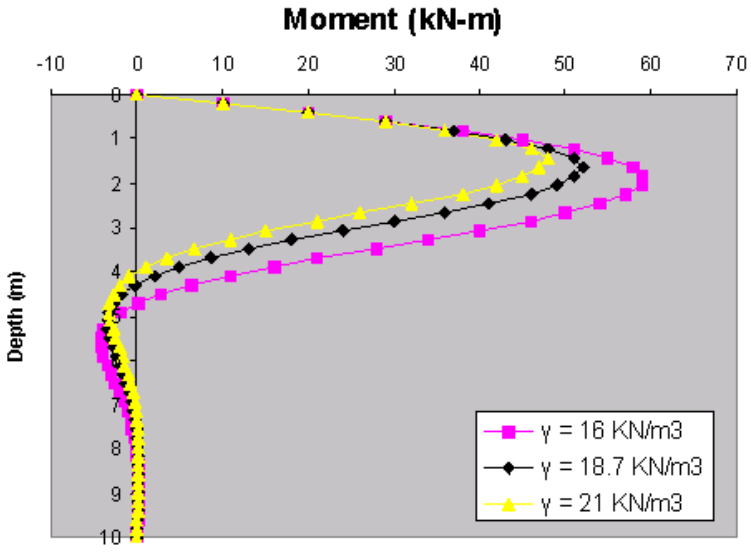

Comparison of Pile Deflection and Bending Moments with Uniform Sands

Soil properties:

	Loose sand	Medium sand	Dense sand
Internal friction angle ϕ (°)	29.5	33	38
Subgrade modulus k (MN/m³)	5.4	16.3	34
Unit weight γ (kN/m³)	16	18.7	21

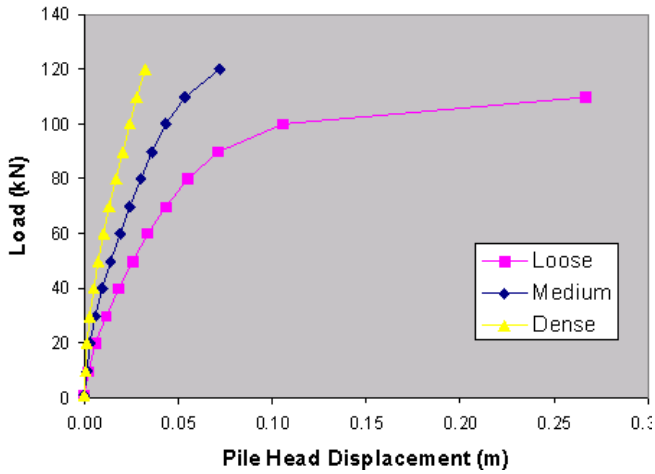

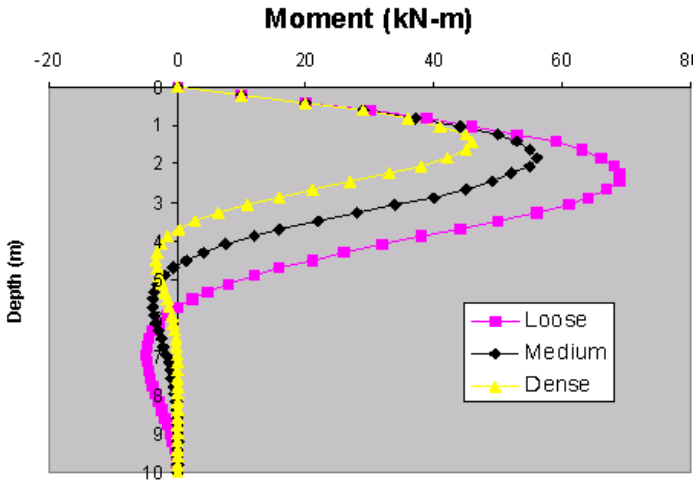

Example Problem in FB-Pier

Problem overview

•Single free head pile (Diameter = 12in) subjected a lateral load at the ground surface

•Soft clay foundation

•Water table at the ground surface

Objective

To study the effects of the soil properties and pile properties (shear strength, soil strain e_{50}, pile diameter, and pile length) on the behavior of Matlock's Soft Clay below the Water Table Model

Comparison of Pile Deflection and Moment Distribution with Varying Pile Length

- Change the pile length alone
- Shear Strength c = 300 psf
- Soil Strain ε_{50} = 1%
- Pile Diameter = 12 in

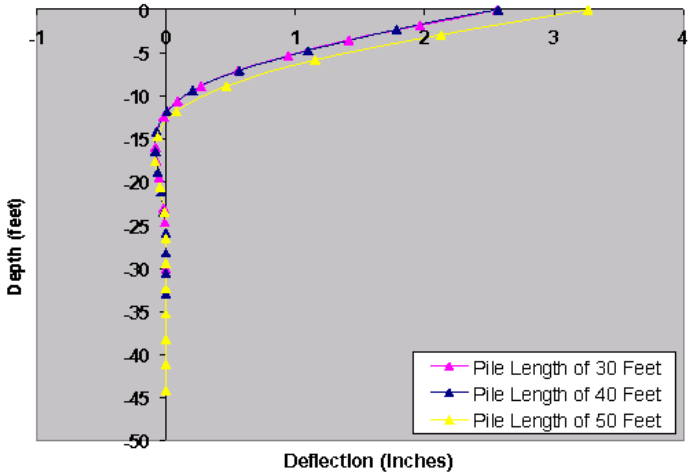

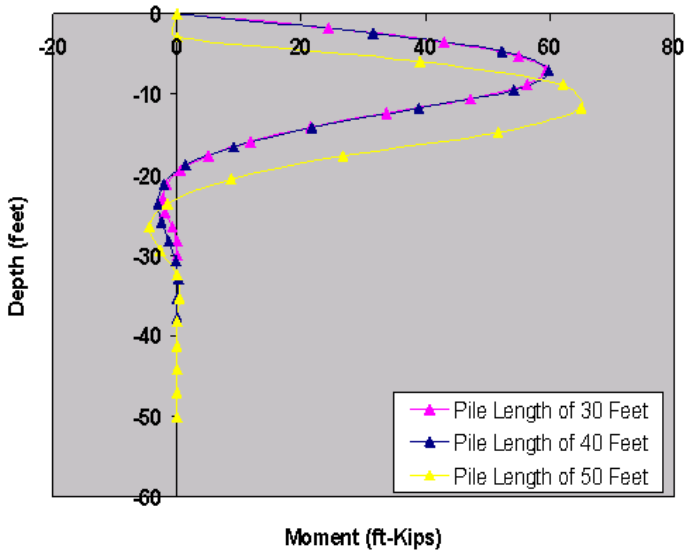

Comparison of Pile Deflection and Moment Distribution with Varying Pile Diameter

- Change the pile diameter alone
- Shear Strength c = 300 psf
- Soil Strain ε_{50} = 1%
- Pile Length = 42 ft

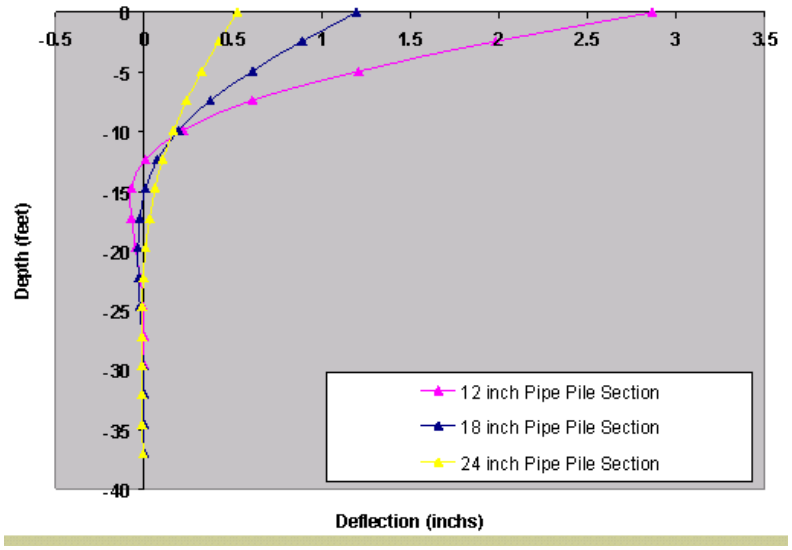

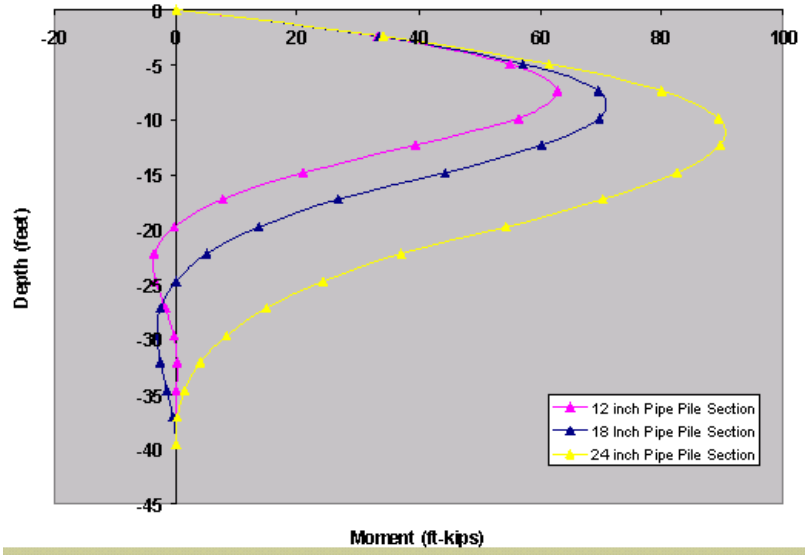

Comparison of Pile Deflection and Moment Distribution with Varying Shear Strength

- Change the shear strength alone
- Pile Diameter = 12 in
- Soil Strain ε_{50} = 1%
- Pile Length = 42 ft

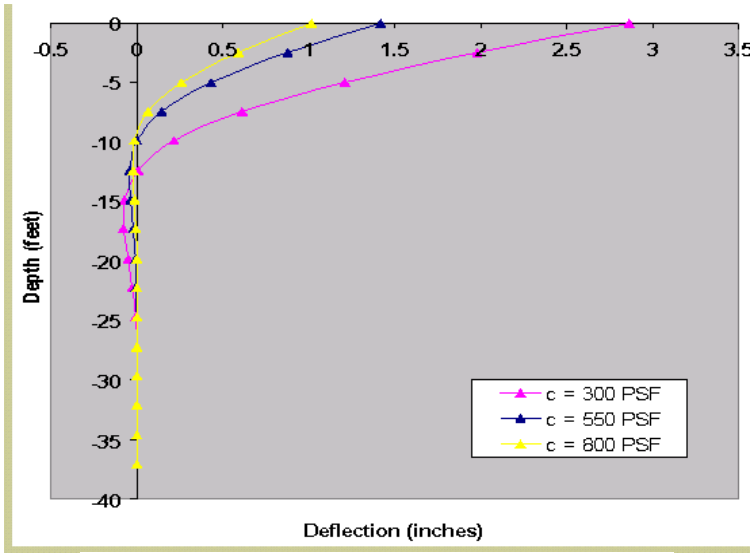

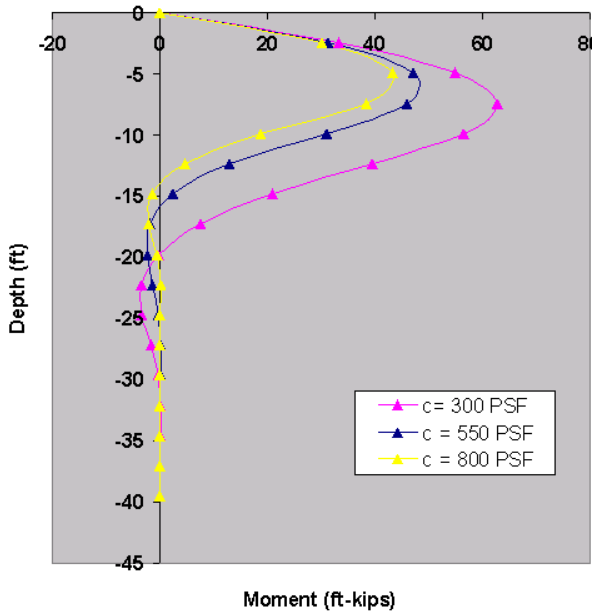

Comparison of Pile Deflection and Moment Distribution with Varying Soil Strain

- Change the soil strain alone
- Pile Diameter = 12 in
- Shear Strength c = 300 psf
- Pile Length = 42 ft

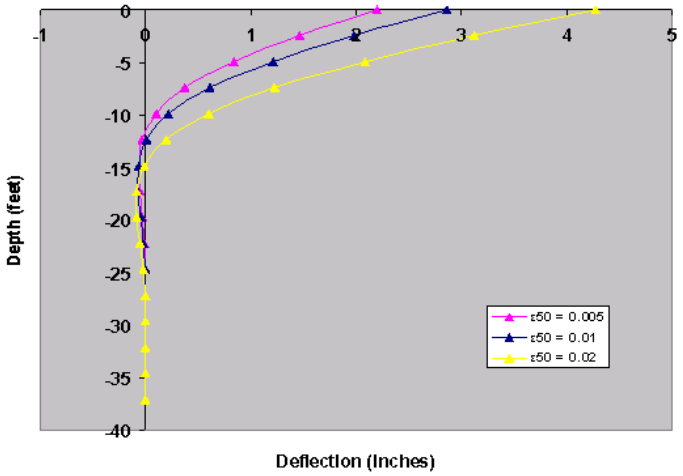

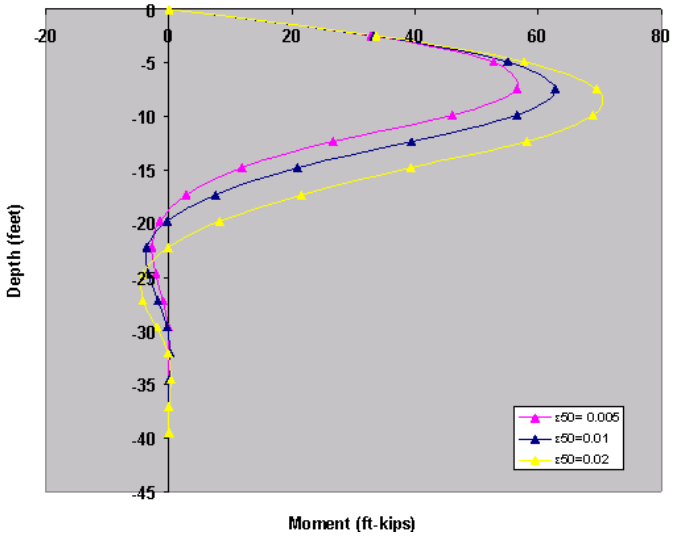

Comparison of Pile Deflection and Moment Distribution with Varying Load Conditions

- Change the load conditions alone
- Pile Diameter = 12 in
- Shear Strength c = 300 psf
- Pile Length = 42 ft
- Soil Strain ε_{50} = 1%

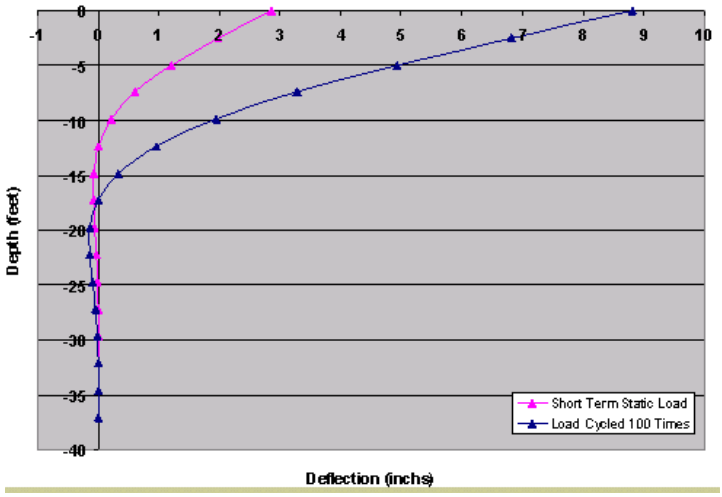

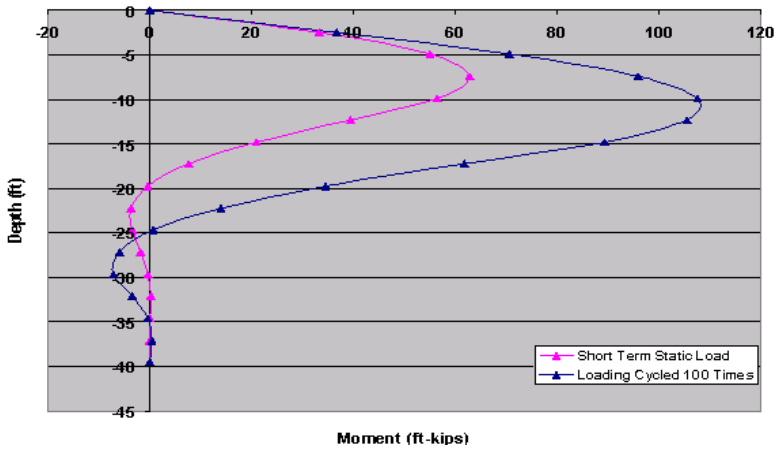

X. VITA

Chad Michael Rachel was born February 21, 1974, in Marrero, Louisiana. He received a Bachelor of Science Degree in Civil Engineering from the University of New Orleans in 2000. He currently works as a civil (geotechnical) engineer at the U.S. Army Corps of Engineers in New Orleans, Louisiana.